



**HAL**  
open science

## Recent developments of metal-based compounds against fungal pathogens

Yan Lin, Harley Betts, Sarah Keller, Kevin Cariou, Gilles Gasser

► **To cite this version:**

Yan Lin, Harley Betts, Sarah Keller, Kevin Cariou, Gilles Gasser. Recent developments of metal-based compounds against fungal pathogens. *Chemical Society Reviews*, 2021, 10.1039/D0CS00945H . hal-03312729

**HAL Id: hal-03312729**

**<https://hal.science/hal-03312729>**

Submitted on 2 Aug 2021

**HAL** is a multi-disciplinary open access archive for the deposit and dissemination of scientific research documents, whether they are published or not. The documents may come from teaching and research institutions in France or abroad, or from public or private research centers.

L'archive ouverte pluridisciplinaire **HAL**, est destinée au dépôt et à la diffusion de documents scientifiques de niveau recherche, publiés ou non, émanant des établissements d'enseignement et de recherche français ou étrangers, des laboratoires publics ou privés.

# **Recent Developments of Metal-based Compounds against Fungal Pathogens**

Yan Lin,<sup>#</sup> Harley Betts,<sup>#</sup> Sarah Keller, Kevin Cariou\* and Gilles Gasser\*

Chimie ParisTech, PSL University, CNRS, Institute of Chemistry for Life and Health Sciences,  
Laboratory for Inorganic Chemical Biology, 75005 Paris, France.

<sup>#</sup> have contributed equally to the work

## **Abstract**

This review provides insight into the rapidly expanding field of metal-based antifungal agents. In recent decades, the antibacterial resistance crisis has caused reflection on many aspects of public health where weaknesses in our medicinal arsenal may potentially be present – including in the treatment of fungal infections, particularly in the immunocompromised and those with underlying health conditions where mortality rates can exceed 50%. Combination of organic moieties with known antifungal properties and metal ions can lead to increased bioavailability, uptake and efficacy. Development of such organometallic drugs may alleviate pressure on existing antifungal medications. Prodigious antimicrobial moieties such as azoles, Schiff bases, thiosemicarbazones and others reported herein lend themselves easily to the coordination of a host of metal ions, which can vastly improve the biocidal activity of the parent ligand, thereby extending the library of antifungal drugs available to medical professionals for treatment of an increasing incidence of fungal infections. Overall, this review shows the impressive but somewhat unexploited potential of metal-based compounds to treat fungal infections.

**KEYWORDS:** bioorganometallic chemistry; fungal pathogens; medicinal inorganic chemistry; medicinal organometallic chemistry; metal complexes, antimicrobials, antimycotic activity.

## Biographies



Yan Lin obtained her MSc in organic chemistry (2018) at HangZhou Normal University in the group of Prof. Li-Wen Xu working on transition metal-catalysed asymmetric C-H activation. In 2018, she was awarded a China Scholarship Council to carry out her PhD studies under the supervision of Prof. Gilles Gasser at Chimie ParisTech, PSL University. She is currently working on the development of organometallic derivatives of antiparasitic and antifungal drugs to enhance their biological activity.



Harley Betts completed his PhD in inorganic chemistry at the University of Adelaide, Australia in 2020 under the supervision of Professors Hugh Harris, Christopher Sumby and Christopher McDevitt. During his studies he investigated the biochemical fate of silver ions in biologically relevant environments, and the development of silver-containing porous materials for use as antibacterial coatings. He is currently working as a postdoctoral research fellow at Chimie ParisTech, PSL in the Gasser Group. His work in Paris has focused on the development of organometallic adducts of existing drugs in an effort to extend and enhance their efficacies against parasitic infections.



Sarah Keller did her PhD in Chemistry at the University of Basel under the supervision of C. E. Housecroft and E. C. Constable. For her two-year postdoctoral research project in the Gasser Group at Chimie ParisTech PSL University in Paris, she was awarded a Feoder Lynen Postdoctoral Fellowship from the Alexander von Humboldt Foundation and an Early Postdoc Mobility Fellowship from the Swiss National Science Foundation. She pursued several projects in the fields of inorganic and medicinal chemistry, such as the design and synthesis of organometallic drugs, or luminophores for sustainable light-emitting devices. She recently started working at hemotune AG, a spin-off company originating out of the Functional Materials Lab at ETH Zurich, where she is responsible for the development of surface-functionalized magnetic nanoparticles for medical applications.



Kevin Cariou graduated from Chimie ParisTech in 2002, he received his PhD in 2006 from the University Pierre and Marie Curie (now Sorbonne Université) in Paris (France) under the supervision of Prof. M. Malacria and L. Fensterbank, where he studied platinum- and gold-catalysed transformations with a joint CNRS-Sanofi BDI fellowship. From 2007 to 2009, including one-year as a Lavoisier fellowship holder, he worked as a postdoctoral researcher in the group of Prof. A. J. Frontier at the University of Rochester (NY, USA) in the field of total synthesis. He was appointed as Chargé de Recherche in 2009 at the CNRS at the ICSN in the team Synthesis and Methodology Applied to Research in Therapeutics (SMART) led by Dr R. H. Dodd. He obtained his Habilitation à Diriger les Recherches (HDR) in 2015. From 2017 to 2019, he was the leader of the SMART team before moving to Chimie ParisTech in 2020. His research interest lie in the development of new synthetic methods, with a focus on I(III) reagents, nitrogen-rich building blocks and organometallic derivatives, and their application toward the synthesis of biologically active molecules, in particular anti-infectious.



Gilles Gasser obtained his PhD in 2004 at the University of Neuchâtel (Switzerland) under the guidance of Helen Stoeckli-Evans. He then undertook two post-docs, first with the late Leone Spiccia (Monash University, Australia) in bioinorganic chemistry and then as an Alexander von Humboldt fellow with Nils Metzler Nolte (Ruhr-University Bochum, Germany) in bioorganometallic chemistry. Gilles started his independent scientific career at the University of Zurich (Switzerland) in 2010 before moving to Chimie ParisTech, PSL University (Paris, France) in 2016 to take a PSL Chair of Excellence. Gilles was the recipient of several fellowships and awards including the Alfred Werner Award from the Swiss Chemical Society, an ERC Consolidator Grant, the Jucker Award for his contribution to cancer research, the European BioInorganic Chemistry (EuroBIC) medal and the Pierre Fabre Award for therapeutic innovation from the French Société de Chimie Thérapeutique. Gilles' research interests lay in the use of metal complexes in different areas of medicinal and biological chemistry.

## 1. Introduction

### 1.1 Fungal infections and antifungal drugs

The fungal kingdom comprises an estimated 1.5 million species with more than 200 species associated with humans.<sup>1</sup> Fungi are ubiquitous in the environment and exhibit many strategies to facilitate their survival in changing surroundings. They can interact with plants, animals or humans in multiple ways, including symbiotic, commensal, latent or pathogenic relationships.<sup>2</sup> Humans can be infected by various routes, which include inhalation of spores or small yeast cells. Superficial infections are the most common fungal diseases in humans and affect 1.7 billion people in the world and are primarily caused by dermatophytes such as *Epidermophyton*, *Microsporum*, and *Trichophyton*.<sup>3</sup> These pathogenic fungi specialize in the infection of keratinous substances - such as skin, hair and nails - where they utilize the keratin for nutrition. Expansion of infections in immunocompromised patients, e.g. those with HIV/AIDS, may lead to systemic fungal infections that become life-threatening. High mortality rates, which can exceed 50%, have been attributed to the difficulty of diagnosis, and shortcomings in the current antifungal arsenal.<sup>4</sup> The most significant fungal species that cause human infections, allergies and toxicosis belong to one of the five main genera: *Candida* (*C. albicans*, *C. glabrata*, *C. krusei*, *C. parapsilosis*, *C. tropicalis*, *C. glabrata*, *C. kefyr* and *C. guilliermondii*), *Aspergillus* (*A. flavus*, *A. niger* and *A. fumigatus*), *Cryptococcus* (*C. neoformans*), *Fusarium* (*F. oxysporum*, *F. moniliforme* and *F. solani*) and *Pneumocystis*.<sup>5</sup> Additionally, it is predicted that the prevalence of fungal diseases will also increase with the progression of global warming.<sup>6</sup> Although fungi were recognized as pathogens prior to bacteria, progress in the development of effective antifungals has lagged behind antibacterial research. At least two reasons can potentially explain this oversight. First, before the HIV-era, the occurrence and severity of fungal infections was believed to be too low to warrant aggressive research by the pharmaceutical industry. Second, the eukaryotic nature of fungi makes them metabolically and physiologically similar to mammalian cells (aside from the presence of a fungal cell wall) and therefore offer limited pathogen-specific targets. Numerous tests have confirmed that antibiotics have poor activities against fungi. One reason for the difference in sensitivity between fungi and bacteria can be found in different cell wall permeabilities. The fungal cell wall is a complex intertwined layer of saccharides (**Fig. 1**) and

significantly differs from mammal cells, this creates several target opportunities for the design of antifungal drugs.<sup>7</sup>

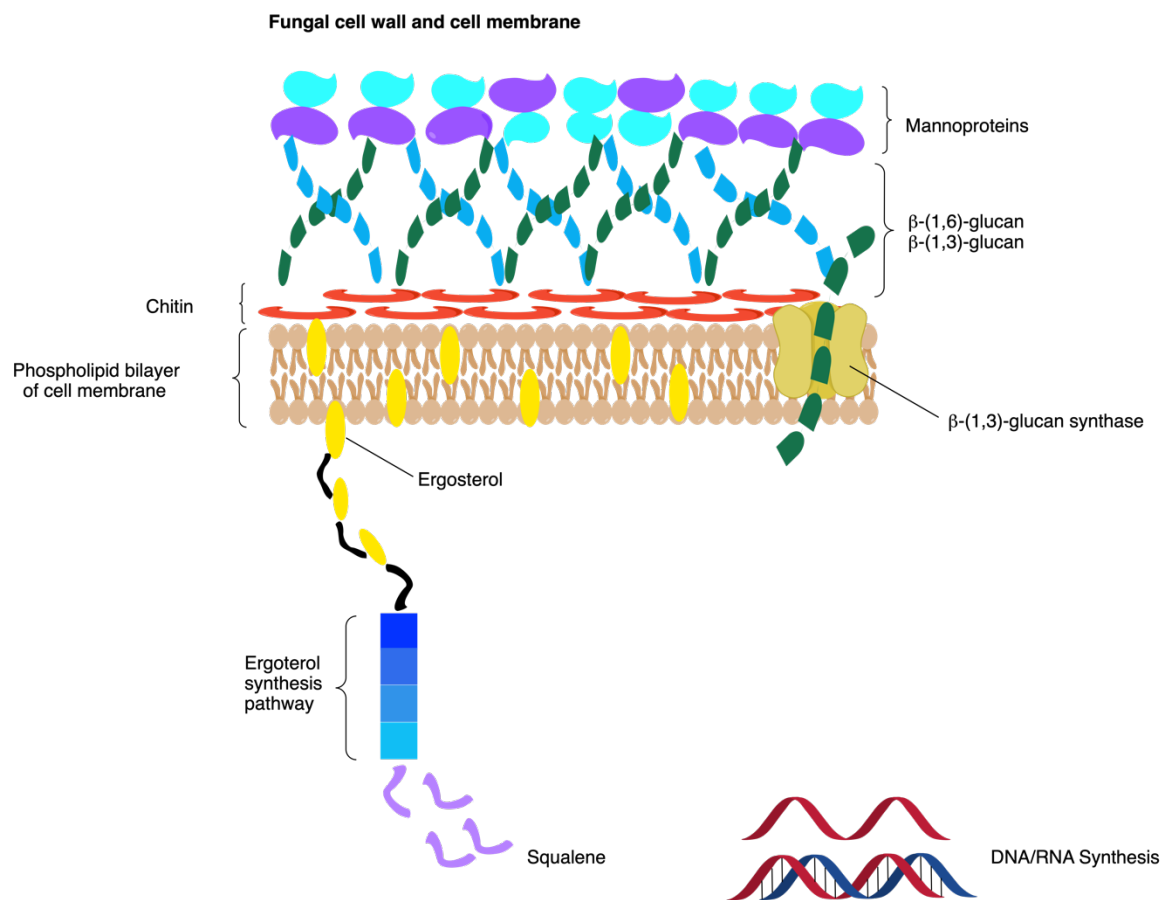


**Fig. 1:** Schematic representation of a fungal cell wall and cell membrane. Adapted from Mycoses Study Group Education and Research Consortium.<sup>8</sup>

There are five main antifungal agent classes approved for human consumption:<sup>9</sup>

1) The azoles (e.g., Fluconazole (FCZ, **Fig. 2**)) are the most commonly used antifungal drugs and target the cytochrome P-450-dependent enzyme, 14 $\alpha$ -sterol demethylase (P-450<sub>DM</sub>), preventing the synthesis of ergosterol (**Fig. 1**, bottom left), a major component of fungal plasma membranes.<sup>10</sup> Cholesterol is an analogue of ergosterol in mammals and its synthesis can also be impacted by this enzyme. However, when azole agents are used at therapeutically relevant concentrations, their affinities for fungal P-450<sub>DM</sub> are greater than for the mammalian enzyme. Exposure of fungi to azole agents results in ergosterol depletion, accumulation of lanosterol and other 14-methylated sterols and interferes with the “bulk” functions of ergosterol in fungal membranes, which alters the fluidity and integrity of the membrane. Disruption of the plasma membrane



makes the fungal organism more vulnerable to further damage associated with nutrient transport and chitin synthesis.<sup>11</sup> As azole drugs are orally administered and have few side effects, they have been used widely, however, not long after their discovery, reports of clinical failure attributed to drug resistance appeared.<sup>12</sup>

2) Polyenes, such as amphotericin B (AmB, **Fig. 2**), are naturally occurring macrolides produced by Gram-positive bacteria and are widely used as a “gold standard” for treatment of systemic infections. They bind to ergosterol, allowing holes in the fungal cell membrane to form, disruption of chemiosmotic gradients and intracellular constituent leakage. Polyenes display potent antifungal activity but high mammalian toxicity and intravenous administration limit their application.

3) Echinocandins, such as caspofungin (CFG, **Fig. 2**), inhibit the synthesis of  $\beta$ -1,3-glucan in the fungal cell wall via non-competitive inhibition of enzyme  $\beta$ -1,3-glucan synthase (**Fig. 1**, in green, right). The absence of cell walls in mammalian cells make the echinocandins minimally toxic, however, their application is limited to a narrow range of fungal pathogenic infections, including *Candidiasis* and *Aspergillosis*. Poor oral bioavailability of echinocandins require they be administered by intravenous injection, similar to AmB.<sup>13</sup>

4) Allylamines, such as terbinafine (TRB, **Fig. 2**), act by inhibiting squalene epoxidase (**Fig. 1**, bottom left) – the first enzyme in the biosynthetic pathway of ergosterol (and cholesterol) – resulting in sterol depletion and accumulation of the squalene precursor. This affects membrane structure and function, including nutrient uptake.<sup>14</sup> Although resistance to TRB has not been reported for human pathogens, observation in the corn pathogen *U. maydis* was first described in 1990.<sup>15</sup>

5) Antimetabolites such as 5-flucytosine (5-FC, **Fig. 2**). 5-FC is a fluorine analogue of cystine that is taken up by fungal cells, converted to 5-fluorouracil, phosphorylated and incorporated into RNA. The inclusion of the antimetabolite results in miscoding and halts protein synthesis. Additionally, phosphorylated fluorouracil is also converted to its deoxynucleoside which inhibits fungal DNA replication by thymidylate synthase (**Fig. 1**, bottom right). However, the use of 5-FC is limited by its bone marrow toxicity in mammals and the high rate of spontaneous mutation to resistance. Given the increasing incidence of fungal infections and the emerging resistance to existing drugs, it is important to develop structurally novel medicines.<sup>16,17</sup>

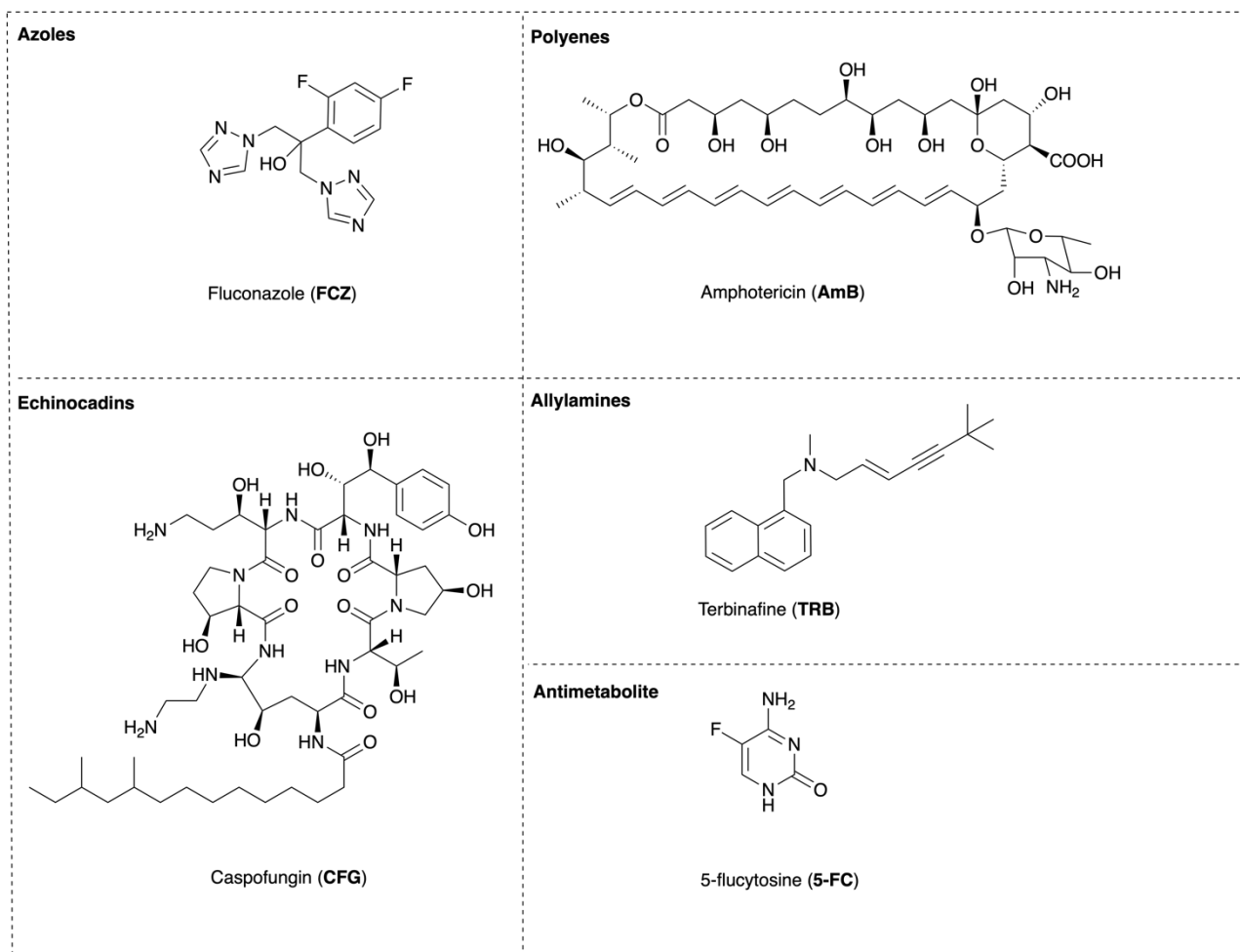


**Fig. 2:** Representative drugs of the five main antifungal agent classes approved for human clinical application.

In order to evaluate the therapeutic interest of potential new antifungals, two independent, standardised methods for susceptibility testing of fungi are generally used: 1) broth dilution testing to determine minimum inhibitory concentrations (MIC) and minimal fungicidal concentrations (MFC), which are commonly used to assess the fungicidal activities of azoles and echinocandins against *Candida* or *Aspergillus* species; and 2) disk diffusion testing/zone of inhibition assays which can quantify the inhibitory effects a compound has on the growth of an organism. These methods are convenient, economical and well suited for testing water-soluble antifungal drugs, such as 5-FC, FCZ and voriconazole (VRC), against yeasts and molds.<sup>18,19</sup>

## 1.2 Metal-based drugs

The discovery of the antitumor activity of cisplatin in 1969 stimulated significant interest in the use of metal complexes as diagnostic agents or chemotherapeutic drugs.<sup>20</sup> Metal complexes offer fantastic opportunities in the development of new agents for clinical use due to their specific, unique physicochemical properties. The wide range of thermodynamic and kinetic properties of metal complexes (e.g. redox activity, coordination number, geometry and ligand versatility as well as capacity for ligand exchange) and the intrinsic medical properties of the metal ions and ligands themselves give rise to many possibilities for the design of therapeutic agents not readily available to purely organic compounds.<sup>21</sup> Many metal compounds including arsenic, bismuth, platinum, ruthenium, gold, copper and silver have been studied in the pharmacological field as anticancer agents,<sup>22</sup> as well as antimicrobial,<sup>23</sup> antiinflammatory,<sup>24</sup> antiparasitic,<sup>25</sup> and antimalarial agents.<sup>26</sup> For instance, the organic arsenical Salvarsan ((AsR)<sub>n</sub>, where R = 3-amino-4-hydroxyphenyl and *n* = 3 or 5) which was historically used to treat syphilis and trypanosomiasis, however, in recent times it has been removed from clinical use. It is thought that the active form of the drug resulted from an *in vivo* oxidation process and Salvarsan serves as a slow-release source of RAs(OH)<sub>2</sub> with oxidation from As(I) to As(III), as demonstrated by Nicholson and co-workers.<sup>27</sup> Although the design of metal complexes with good therapeutic indices is still rather empirical, metal-based therapeutics have the potential for completely new, metal-specific modes of action that may make it difficult for fungal organisms to develop mechanisms of resistance. In this article, we provide a comprehensive overview of the developments in the design of metal complexes with antifungal activity. The particular case of metal nanoparticles will not be covered in this review.

## 2. Azole antifungal drugs

### 2.1 Overview

Azoles are a class of five-membered heterocyclic compounds that contain a nitrogen atom and at least one other non-carbon atom as part of the ring (e.g., nitrogen, sulfur, or oxygen). The first report of antifungal activity of an azole compound, benzimidazole, was described in 1944 by Woolley,<sup>28</sup> however, they were not used in clinical settings until 1958 with the release of the topical ointment, chlormidazole. In the late 1960s,

three compounds that firmly established azoles as antifungal agents were introduced: Clotrimazole (CTZ, **Fig. 3**) was developed by Bayer AG (Germany) and the first imidazole antifungal drug to enter the market; Miconazole (MCZ, **Fig. 3**) and Econazole (ECO, **Fig. 3**), both developed by Janssen Pharmaceutica (Belgium).<sup>29</sup> Ketoconazole (KTZ, **Fig. 3**) was the first orally, bioavailable, broad spectrum imidazole, representing a major advance in treatment of systemic fungal infections. However, adverse gastrointestinal side effects have been frequently reported, causing these to be replaced by triazoles.

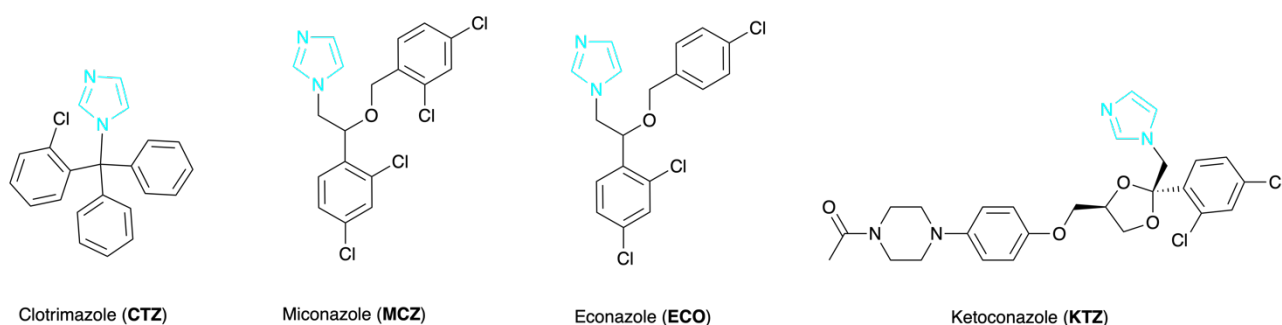


**Fig. 3:** Structures of clinically approved imidazole-based antifungal drugs.

Imidazoles and triazoles contain two or three nitrogen atoms in the five-membered heterocyclic ring, respectively. In general, triazoles have a broader spectrum of antifungal activity and reduced toxicity when compared with imidazoles. Terconazole (TER, **Fig. 4**) is a topically active drug for treatment of vaginal candidiasis and dermatomycoses and was the first triazole-based antifungal agent marketed for human use, however, the two leading triazole-based drugs are FCZ (**Fig. 4**) and Itraconazole (ITC, **Fig. 4**). FCZ was approved for use as a single-dose oral therapy for vulvovaginal candidiasis in 1994 as well as widespread use as a prophylaxis and treatment of superficial and invasive *Candida* infections and *Cryptococcus* infections. The bioavailability of FCZ is higher than other azoles, which may be attributed to its high aqueous solubility and low affinity for plasma proteins. In immuno-compromised and immuno-suppressed patients (such as those living with AIDS or bone marrow transplant recipients) ITC has become the drug of choice for the treatment of paracoccidioidomycosis, blastomycosis, histoplasmosis and sporotrichosis despite it being less effective than FCZ.<sup>30</sup> New triazoles, such as VRC (**Fig. 4**) and Posaconazole (POS, **Fig. 4**),<sup>31,32</sup> have also been approved for human use. The emergence of high-level resistance is accompanied by widespread use of azole agents.

FCZ resistance in *C. spp.* has been reported extensively and is attributed to this drug being the most widely used azole.<sup>33</sup> Furthermore, FCZ-resistant clinical isolates of *C. neoformans* and *H. capsulatum* and ITC-resistant clinical isolates of *A. fumigatus* have also been reported.<sup>34,35,36</sup> More specialized or comprehensive reviews are available for further details about cellular and molecular mechanisms of azole resistance can be referred.<sup>12,10</sup>

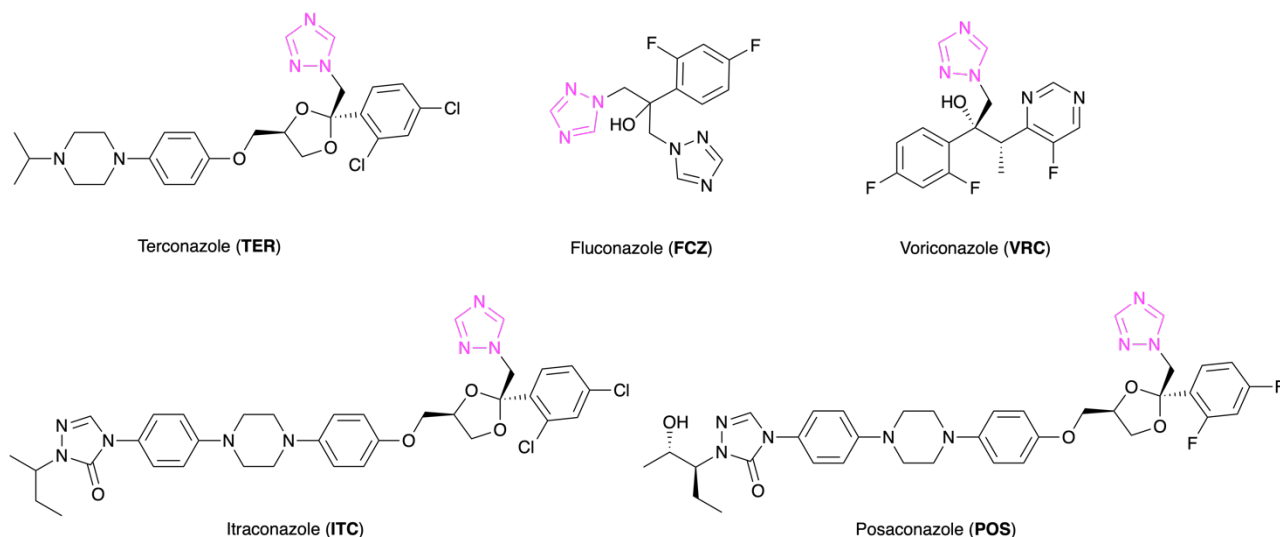


**Fig. 4:** Structures of clinically approved triazole-based antifungal drugs.

## 2.2 Metallocenyl-derivatives of azole antifungal drugs

Iron is an essential micronutrient for most living organisms as it participates in multiple metabolic processes, including synthesis of haem and iron-sulfur cluster-containing proteins, amino acids, DNA, lipids, and sterols.<sup>37,38</sup> Recently, it was also reported that high iron concentrations can alter cell wall architectures in *C. albicans*, reducing fungal cell survival upon exposure of antifungal agents.<sup>39</sup> Ferrocene is a sandwich structure consisting of two cyclopentadienyl (Cp) rings and iron atom, its discovery initiated the field of organometallic chemistry. The remarkable physicochemical properties of ferrocene have made it a very popular substituent for medicinal chemistry purposes for several reasons: 1) The general lack of toxicity of ferrocene allows it to be injected, inhaled, or taken orally without causing major health problems; 2) the stability of ferrocene in aqueous and aerobic media;<sup>40</sup> 3) the robustness of ferrocene allows for a straightforward accessibility of a large variety of derivatives; 4) the lipophilicity of ferrocene moiety makes it easier for ferrocenyl derivatives

to cross cell membranes; 5) the redox properties of ferrocene, as it can undergo a one-electron oxidation, yielding the ferrocenium cation.<sup>40,41,42</sup> Ferrocenium salts may generate DNA-damaging hydroxyl radicals *in situ* from hydrogen peroxide via Fenton-type reactions. Successful studies on ferrocenyl analogues, such as the ferrocenyl hydroxytamoxifen analogue (hydroxyferrocifen), a molecule in which a phenyl ring of tamoxifen is replaced by a ferrocene moiety, was prepared as an oestradiol receptor site-directed cytotoxic agent by Jaouen and co-workers.<sup>43,44</sup> This compound was found to be cytotoxic against breast cancer cells overexpressing the oestradiol receptor as well as those not overexpressing this receptor, contrary to tamoxifen. Using a similar synthetic strategy, Biot *et al.* obtained ferroquine (FQ) by introducing a ferrocenyl moiety into the carbon chain of chloroquine (CQ). FQ was found to be active *in vitro* against both CQ-sensitive and CQ-resistant strains of *Plasmodium falciparum* as well as *in vivo* against *P. berghei* N. and *P. yoelii* NS. FQ is currently in phase IIb trials, where the efficacy of an artemisinin-based combination therapy between artesunate and FQ in malaria patients is examined.<sup>45</sup>

The first example of implementing this strategy in antifungal research was reported in 2000 by Biot *et al.*, who replaced the 2,4-difluorophenyl ring of FCZ with a ferrocenyl moiety to give the first ferrocene-containing FCZ derivative (**1**). Unfortunately, analogue **1** showed no growth inhibition on the studied fungi (*C. albicans*, *C. glabrata*, *C. parapsilosis*, and *C. krusei*).<sup>46</sup> Fang and co-workers prepared a wide variety of ferrocene derivatives containing 1,2,4-triazole, thiazole or both, such as ferrocenyl-substituted vinyl 1,2,4-triazole derivatives (**2Z**, **2E**),<sup>47</sup> ferrocene-triadimefon analogues (**3**),<sup>48</sup> ferrocene-triadimenol analogues (**4**),<sup>49</sup> 1-ferrocenyl-3-aryl-2-(1*H*-1,2,4-triazol-1-yl)-prop-2-en-1-one derivatives (**5**, **Fig. 5**),<sup>50</sup> and *N*-substituted benzylidene-4-ferrocenyl-5-(1*H*-1,2,4-triazol-1-yl)-1,3-thiazol-2-amine derivatives (**6**, **Fig. 6**).<sup>51</sup> The fungicidal activity of complexes **2Z**, **2E** against powdery mildews and brown rusts were evaluated at concentration of 50 parts per million (ppm). For all compounds, the *E*-isomers exhibited higher inhibitory activities than the *Z*-isomers. Among them, the *E*-isomers of **2b-e**, **2g**, **2j**, and **2l** had a 20-40% increase in the efficacy compared to the *Z*-isomers against brown rusts, no positive control was given for comparison. The crystal structure of (**Z/E**)-**2d** showed the linkage (N-C-C) between the triazole ring and substituted aryl group in the *E*-isomer was linear, however, the backbone of the *Z*-isomer was distorted. The authors suggest that the *E*-isomers

might be more favourable to bind to the receptor. The antifungal activities of two series of ferrocene-triadimefon (**3**) and triadimenol (**4**) derivatives against powdery mildews and brown rusts were studied at a concentration of 50 mg·L<sup>-1</sup>. Unfortunately, all the tested compounds exhibited lower antifungal activities (~30% inhibition) than the parent compounds, triadimefon or triadimenol (~80% inhibition). The crystal structure of **3f** showed that the substituted aryl group was spatially repelled and turned toward the nearby triazole group due to the presence of the bulky ferrocene moiety. The authors proposed that the bulky ferrocene close to the triazole cycle was responsible for the decrease biological activity. The desired mechanism of action of the triazole derivatives was to target ferrous cytochrome-P450 enzymes. It was hypothesized that binding of triazole to the ferrous ions of cytochrome-P450 enzymes could be replaced by binding to the ferrous ion of ferrocene through intramolecular or intermolecular interactions. In 2006, Fang and co-workers evaluated the antifungal activity of complexes **5** against six fungal strains (*G. zea*, *A. solani*, *P. asparagi*, *P. piricola*, *C. achidicola* and *C. cucumerinum*). The crystal structure of **5I** showed that this series of complexes were in the *E*-configuration, but via a bent linkage. Most of the complexes displayed fungicidal activities within 30-50% inhibition across all the tested fungi at a concentration of 50 mg·L<sup>-1</sup>, no positive control was reported for comparison. One year later, a series of *N*-substituted benzylidene-4-ferrocenyl-5-(1*H*-1,2,4-triazol-1-yl)-1,3-thiazol-2-amine derivatives (**6**) containing thiazole and 1,2,4-triazole were prepared by Fang and co-workers. Four fungal stains (*P. zea*, *A. solani*, *P. piricola* and *C. ara*) were selected to evaluate the antifungal activities of these complexes at the same concentration. The results showed that the *P. piricola* strain was more susceptible than others reported with inhibition up to 62%. The author suggested that further structural modifications of ferrocenyl thiazole-containing derivatives would be necessary to increase the activity.

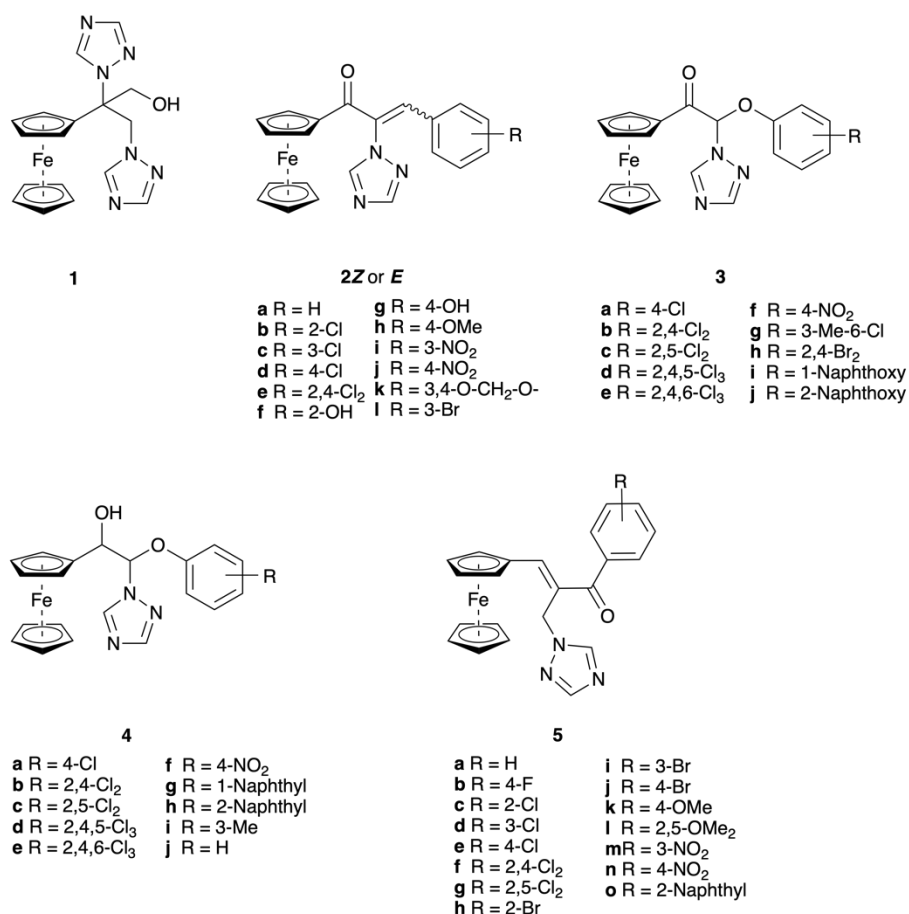


**Fig. 5:** Ferrocenyl 1,2,4-triazole-containing derivatives assessed for antifungal activity.

In 2012, Chandak *et al.* investigated the antifungal activity of ferrocene-containing thiazole derivatives **7** and **8** bearing phenyl and coumarin analogues, respectively, against *A. niger* (MTCC 282) and *A. flavus* (MTCC 871) strains (**Fig. 6**). The results were recorded as the percentage inhibition of mycelial growth. Compound **7e** showed moderate antifungal activity with >55% inhibition against both strains. By comparison, FCZ recorded inhibition of 75.3% and 74.6% against *A. niger* and *A. flavus*, respectively. All other compounds did not display any appreciable antifungal activity. Overall, it could be concluded that the activity of the phenyl analogues were higher than the coumarin analogues against both fungi.<sup>52</sup>



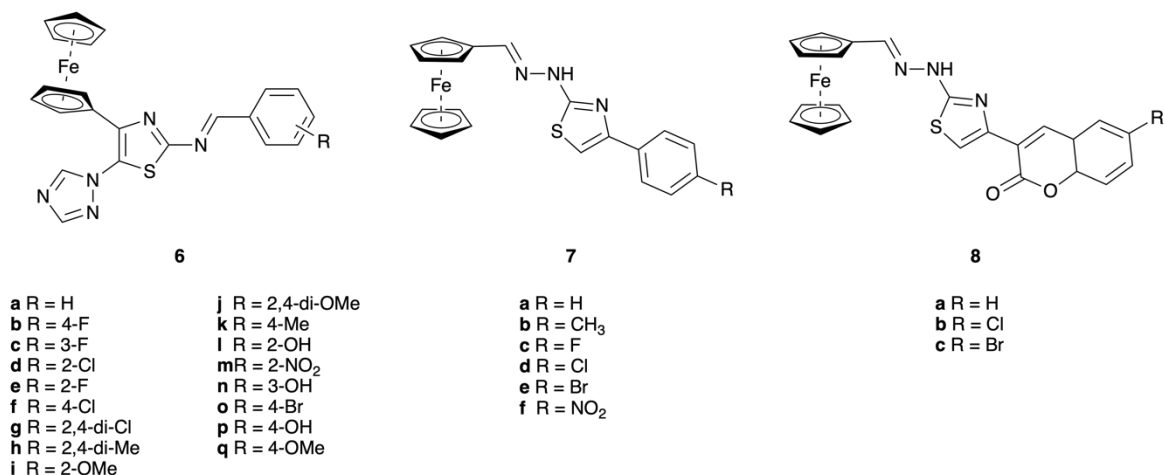


**Fig. 6:** Ferrocenyl thiazole-containing derivatives assessed for antifungal activity.

Considering the chemistry and pharmacology of thiazolidinone and pyrazole, a series of ferrocene-containing 2-pyrazolyl-1,3-thiazolidin-4-ones (**9**, **Fig. 7**) were prepared by Pejović *et al.* in 2018 and their antifungal activities evaluated against *C. albicans*. Compounds **9a** and **9j** substituted with methyl and 3-picolyl groups, respectively, displayed MIC of 1 mg·mL<sup>-1</sup>. This value was lower than other ferrocene derivatives. By comparison, the reference drug, CTZ, had an MIC value of 20 µg·mL<sup>-1</sup>.<sup>53</sup>

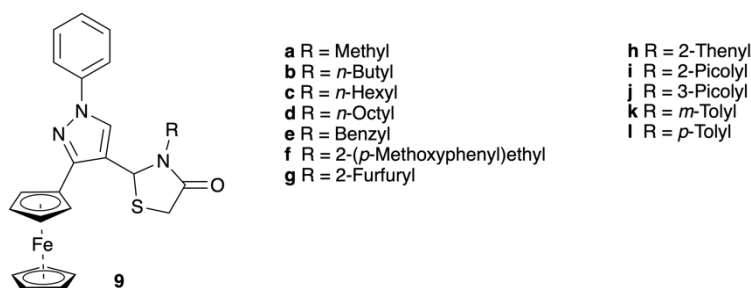


**Fig. 7:** Ferrocenyl pyrazole-containing derivatives assessed for antifungal activity.

In 2016, our group investigated the antifungal activity of ferrocenyl sedaxane derivatives against *S. cerevisiae* (**10a-d**, **Fig. 8**). Sedaxane is a potent broad-spectrum fungicide that targets succinate dehydrogenase, an enzyme involved in fungal oxidative phosphorylation.<sup>54</sup> Compound **10a** displayed impressive activity with a half maximal effective concentration (EC<sub>50</sub>) value of 43 µM, which was higher than underivatized sedaxane and its ruthenocene analogue **10b** (EC<sub>50</sub> > 100 µM). Host cytotoxicity was investigated against normal human cells, human fibroblast (MRC-5) and retinal pigment epithelial (RPE1 hTert). Compound **10a** was found to be

not toxic against both cell lines with half maximal inhibitory concentration ( $IC_{50}$ ) above 100  $\mu$ M. A 33% increase in the levels of reactive oxygen species (ROS) in the fungal culture clearly confirmed the importance of a reversible redox couple in **10a**, a property not available for the ruthenium analogue **10b** and sedaxane alone. However, compounds **10c** and **10d**, which bore phenyl or phenoxy groups on their pyrazole core, respectively, had much lower antifungal activity. This was attributed to the sterically hindered substituents that blocked the active pyrazole core. Overall, this work demonstrated that the introduction of a ferrocene moiety into known broad-spectrum drugs can produce promising fungicides (**10a**).<sup>55</sup>

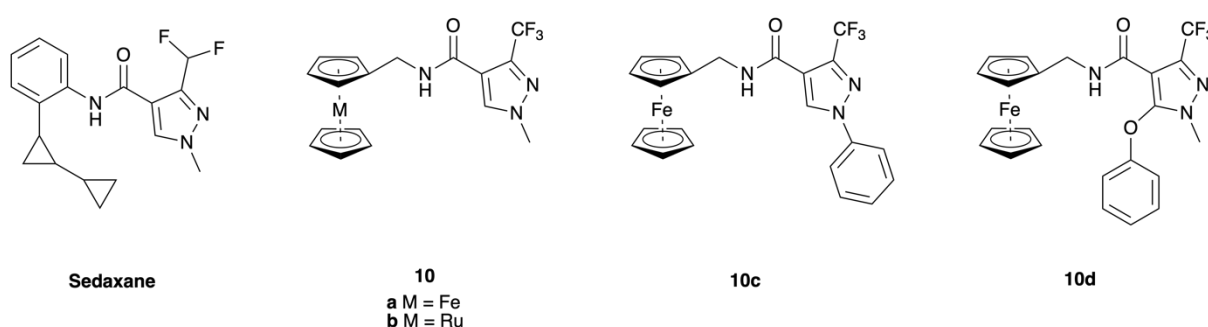


**Fig. 8:** Ferrocenyl azole-containing derivatives assessed for antifungal activity.

In 2019, Singh *et al.* reported a series of ferrocenyl chalcone derivatives containing a triazole and organosilatrane groups (**11-16**, **Fig. 9**) with the aim of merging the pharmacological actions of the constituting moieties into a single molecular scaffold. Two types of ferrocenyl chalcones were designed: Type 1 (**11-14**) in which the carbonyl group was directly linked to the ferrocene ring, and type 2 (**15-16**) with a carbonyl group directly attached to the phenyl ring. The antifungal activities of these ferrocene conjugates were evaluated against seven fungal strains. Compound **14** ( $IC_{50}$  = 31.25  $\mu$ M) was found to be the most effective against *C. albicans*, while compound **12** ( $IC_{50}$  = 31.25  $\mu$ M) exhibited the highest activity against *C. tropicalis*. Compound **11** was the most potent compound against all fungi strains with  $IC_{50}$  values ranging from 62.50 to 250  $\mu$ M. In general, type 1 compounds were more potent than type 2. Nevertheless, these ferrocene conjugates only exhibited moderate activity compared to the positive control, AmB ( $IC_{50}$  range of 0.195-1.25  $\mu$ M).<sup>56</sup>

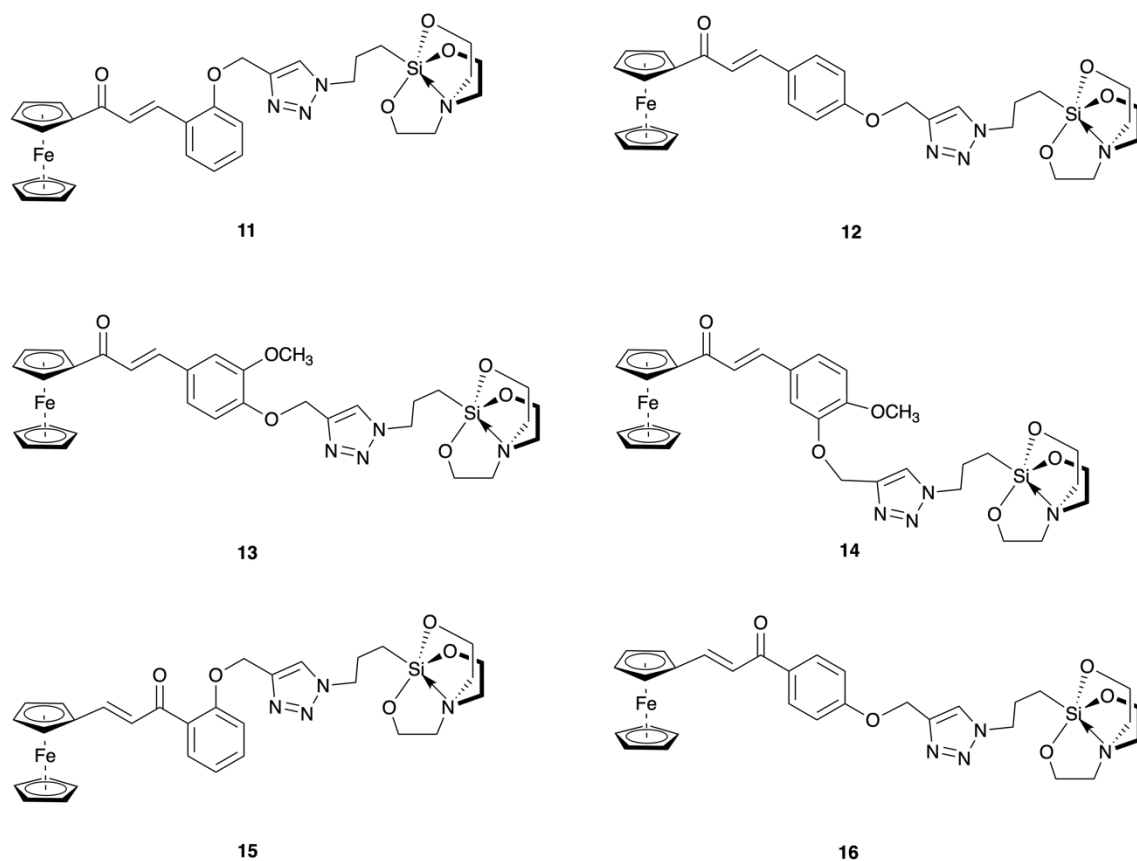


**Fig. 9:** Ferrocenyl and silatrane-containing azole derivatives assessed for antifungal activity.

A series of 3-ferrocenylidene-oxindole containing triazole conjugates **17a-n** (**Fig. 10**) substituted with benzyl, aryl, saccharide and aliphatic groups were synthesised by Yagnam *et al.* and their antifungal activities tested against *C. albicans*. Some of the ferrocenyl compounds had MIC values of  $25 \mu\text{g}\cdot\text{mL}^{-1}$  ( $43 \mu\text{M}$ ) which was greater than FCZ (MIC =  $31 \mu\text{g}\cdot\text{mL}^{-1}$  *i.e.* 10 mM).<sup>57</sup>

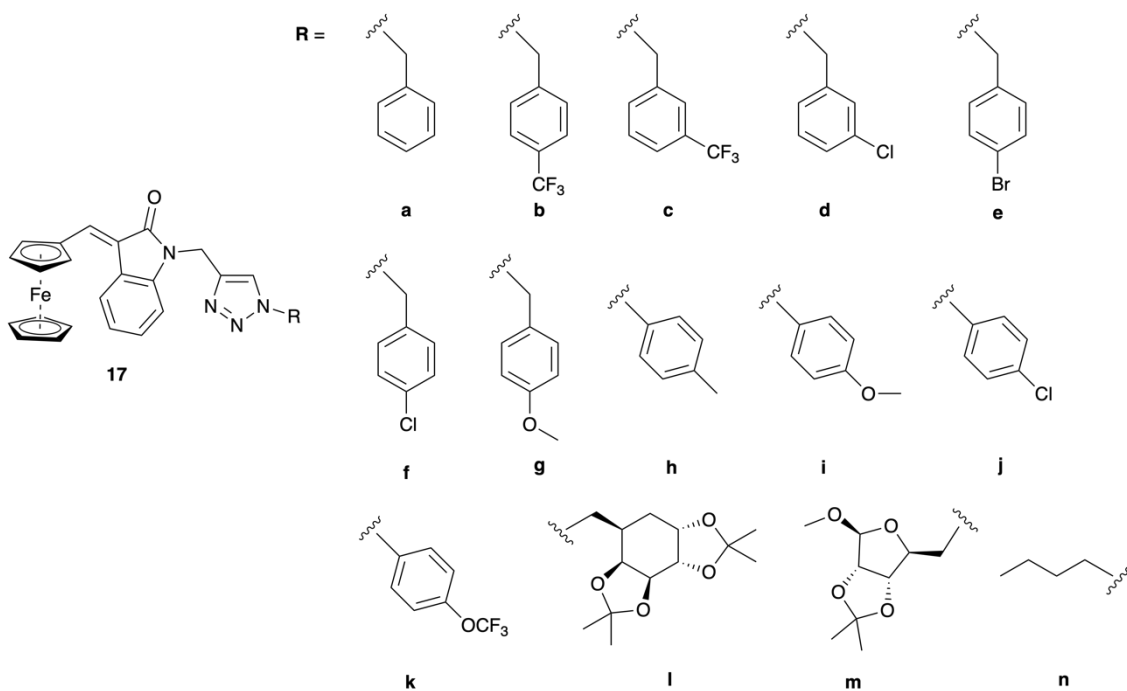


**Fig. 10:** Ferrocenyl azole-containing derivatives assessed for antifungal activity.

In 2019, Zhao and co-workers synthesised six ferrocene-containing 1,3,4-oxadiazoles **18a-f** (Fig. 11). Their antifungal activities were tested on *Gibberella nicotiancola*, *Gibberella saubinetii*, and *F. oxysporium f.sp. niveum*. Most of the compounds exhibited excellent antifungal activity, which was higher than the control compound, hymexazol. Specifically, compound **18b** had significant activities against *G. nicotiancola* ( $EC_{50} = 0.022 \mu\text{g}\cdot\text{mL}^{-1}$  i.e. 61 nM) and *G. saubinetii* ( $EC_{50} = 0.008 \mu\text{g}\cdot\text{mL}^{-1}$  i.e. 22 nM), both of which were lower than hymexazol ( $EC_{50} = 0.032 \mu\text{g}\cdot\text{mL}^{-1}$  and  $0.019 \mu\text{g}\cdot\text{mL}^{-1}$ , i.e. 323 nM and 192 nM, respectively). Similarly, compound **18e** displayed excellent activities against *G. saubinetii* and *F. oxysporium f.sp. niveum* with  $EC_{50}$  values of  $0.029 \mu\text{g}\cdot\text{mL}^{-1}$  (80 nM) and  $0.009 \mu\text{g}\cdot\text{mL}^{-1}$  (25 nM), respectively. Both **18b** and **18e** can be considered as promising drugs for further investigation.<sup>58</sup> Recently, four FCZ ferrocenyl derivatives with one triazole moiety replaced by different alkyl substituents were developed in our group. The stability of these complexes in deuterated DMSO and H<sub>2</sub>O – common media for preparation of stock solutions for biological screening – were monitored by NMR spectroscopy and showed that all tested compounds were stable for up to 24 hours in solution. *In vitro* studies against wild type *S. cerevisiae* showed that compounds **19a-d** (Fig. 11) were more active than FCZ and that compounds **19b-c** displayed 9- to 17-fold greater activities than the positive control. Additionally, the cytotoxicities of these compounds were investigated against human retinal pigment

epithelial cells (RPE-1-h Tert) and human fibroblasts (MRC-5). The results showed that **19a-d** were more selective towards microorganisms than mammalian cells with selectivity indices (SI) between 5 and 24. Compound **19b** was identified as the most promising antifungal candidate and was further screened against *C. albicans*, *P. paneum*, *A. glaucus* and *T. asahi*. The antifungal activities of **19b** were 400-fold higher than FCZ against *P. paneum* and also active against azole-resistant fungal strains. *In vivo* studies were performed on *Candida*-infected mice with drug doses of 10 mg·kg<sup>-1</sup>. Compound **19b** was found to diminish distal dissemination to the liver and brain and greatly improved inflammatory pathologies in the kidney and colon.<sup>59</sup>

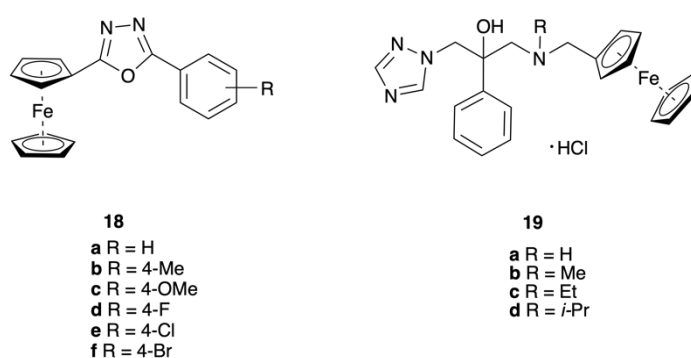


**Fig. 11:** Ferrocenyl azole-containing derivatives assessed for antifungal activity.

### 2.3 Azole-based metal complexes

In 2012, Kumar *et al.* introduced thiadiazoles into tetra-azamacrocycles to coordinate metal centres such as Ni(II), Co(II) and Cu(II). The Ni(II) and Co(II) complexes (**20** and **21**, **Fig 12**) adopted octahedral geometries while the Cu(II) complex (**22**, **Fig 12**) adopted a square planar geometry. The DNA binding modes of these metal complexes were also studied. Hypochromicity and increases in viscosity and melting temperature indicated that the bonding mode of macrocyclic metal complexes with calf thymus DNA (CT-DNA) was driven by intercalation. DNA intercalation is the insertion of a planar, chromophoric region of a molecule between two stacked base pairs. In this process, DNA primary and secondary structures still remain intact while the DNA tertiary structure (helix) is partially lengthened and thus somewhat unwound compared to the original structure.<sup>60</sup> Furthermore, the DNA photocleavage ability of metal complexes **20-22** were studied in the presence of H<sub>2</sub>O<sub>2</sub> and upon irradiation with 360 nm light. The cleavage efficiency of the Cu(II) complex was found to be higher than those of the Ni(II) and Co(II) complexes. This could be explained by the redox activity of the Cu(I)/Cu(II) couple, which can facilitate the formation of ROS that cause DNA damage via Fenton-type reactions.<sup>61</sup> The antifungal activities of these metal complexes against *C. albicans* and *C. parasilosis* ranged from 2.5 to 5 mg·mL<sup>-1</sup>, as determined by MIC measurements. The Cu(II) and Co(II) complexes exhibited better activity than the Ni(II) complex against *C. albicans* with MIC values of 2.5 mg·mL<sup>-1</sup>, no positive controls were reported.<sup>62</sup>

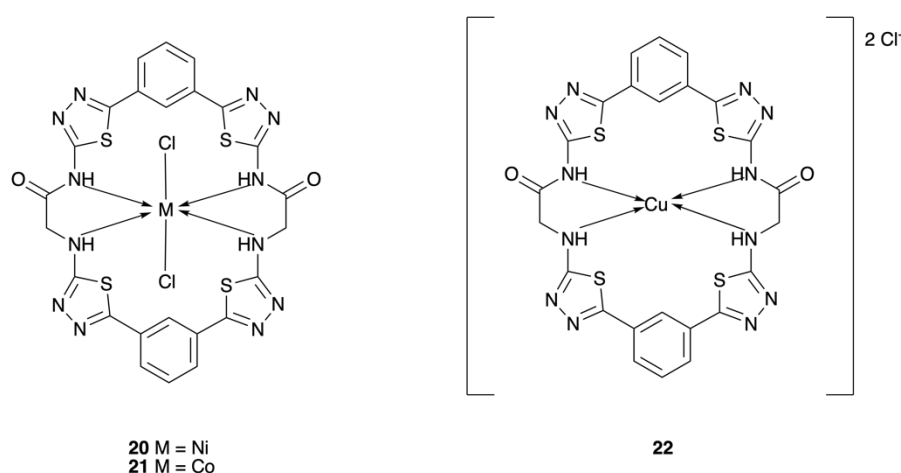


**Fig. 12:** Metal-based thiadiazole-containing complexes assessed for antifungal activity.

In 2014, Kljun *et al.* assessed the antifungal activity of nine organoruthenium complexes conjugated with three different imidazoles (L = CTZ, Tioconazole (TCZ), or MCZ) with the general formula  $[(\eta^6\text{-}p\text{-cymene})\text{-RuCl}_2(\text{L})]$  (**23**),  $[(\eta^6\text{-}p\text{-cymene})\text{-RuCl}(\text{L})_2]\text{Cl}$  (**24**), and  $[(\eta^6\text{-}p\text{-cymene})\text{-RuCl}(\text{L})_3](\text{PF}_6)_2$  (**25**) (**Fig. 13**). Of note among these compounds were complex  $[(\eta^6\text{-}p\text{-cymene})\text{-RuCl}_2(\text{CTZ})]$  reported by Sanchez-Delgado and co-workers,<sup>63</sup> and complex  $[(\eta^6\text{-}p\text{-cymene})\text{-RuCl}_2(\text{MCZ})]$  by our group.<sup>64</sup> The stability of these metal-azole complexes in deuterated DMSO was monitored by NMR spectroscopy. Partial DMSO-mediated ligand dissociation was observed in the monoazole complexes, resulting in a mixture of monoazole-ruthenium and DMSO-ruthenium species. However, the bis- and tris-azole complexes were found to be stable in DMSO and aqueous solution with a small amount of decomposition evident after 12 h (<3%). These mono-, bis-, and tris-azoles complexes inhibited the growth of *Culvularia lunata* at low millimolar concentrations, however, the efficiency decreased with increasing number of coordinating ligands. Since these complexes cannot bind to the haem iron within the active site of lanosterol 14 $\alpha$ -demethylase – due to blocking of the N3 atom through ruthenium coordination – the authors suggested that the complexes must operate via different modes of action.<sup>65</sup>

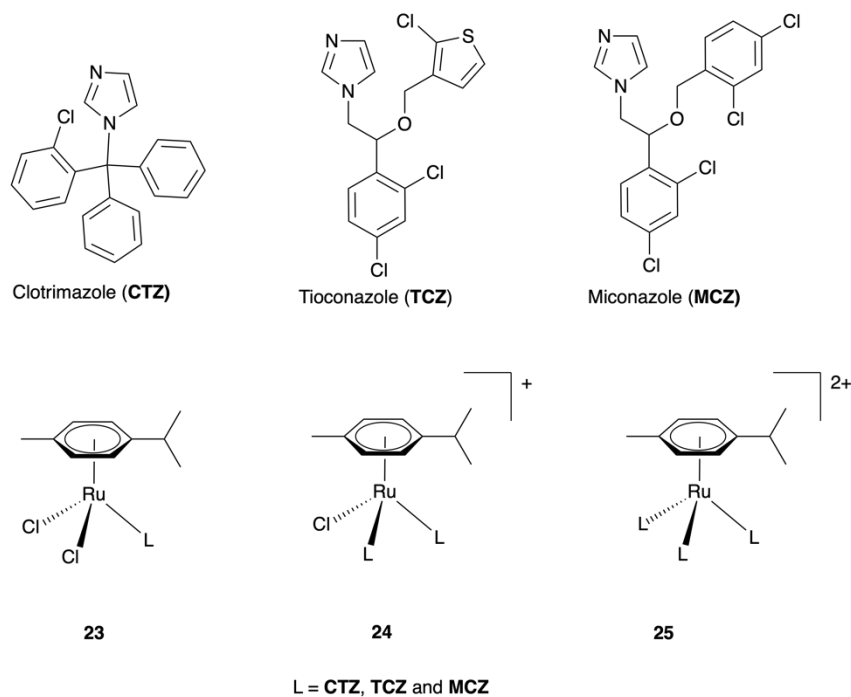


**Fig. 13:** Organoruthenium complexes containing CTZ, TCZ and MCZ assessed for antifungal activity.

Navarro *et al.* reported a series of metal-based KTZ and CTZ derivatives (M = Au, Cu and Ru),<sup>66,67,68</sup> these metal complexes displayed excellent activity against the epimastigote form of *T. cruzi*. Hence, in 2018 the same authors explored the inhibitory effects of five new metal-azole complexes [Cu(PPh<sub>3</sub>)<sub>2</sub>(KTZ)<sub>2</sub>]NO<sub>3</sub> (**26a**), [Cu(PPh<sub>3</sub>)<sub>2</sub>(CTZ)<sub>2</sub>]NO<sub>3</sub> (**26b**), [Au(KTZ)<sub>2</sub>]Cl (**27a**), [Au(CTZ)<sub>2</sub>]Cl (**27b**), and [Pt(KTZ)<sub>2</sub>Cl<sub>2</sub>] (**28a**) and three previously reported metal-azole complexes, namely, [Pt(CTZ)<sub>2</sub>Cl<sub>2</sub>] (**28b**), [Au(PPh<sub>3</sub>)(KTZ)]PF<sub>6</sub> (**29a**) and [Au(PPh<sub>3</sub>)(CTZ)]PF<sub>6</sub> (**29b**) (**Fig. 14**) against *Sporothrix* strains (*S. schenckii*, *S. brasiliensis* and *S. globose*). The coordination geometries of these complexes (**26a-b**, **27a-b** and **28a**) were deduced via use of a range of techniques (<sup>1</sup>H NMR, 2D NMR, UV-vis and IR spectroscopies, conductivity studies, etc.). Data collected for compounds **26a** and **26b** corresponded to an 18-electron Cu(I) complex with tetrahedral geometry, while the structures of cationic complexes **27a** and **27b** corresponded to 14-electron Au(I) complexes that most likely adopted linear coordination geometries. Compound **28a** corresponded to a 16-electron Pt(II) square planar complex with a *trans* configuration, which was supported by density functional theory (DFT). Complexes **26a/b** and **29a/b**, which contained phosphine as an auxiliary ligand, displayed excellent activity with MIC values less than 2 nM against all tested isolates and more active than the parent drugs KTZ and CTZ. In the case of complexes **29a** and **29b**, both compounds displayed significant fungicidal activity with MFC values ranging from 0.4 to 8 nM against the six tested fungi. The effect of the most active complexes (**26a**, **26b**, **29a** and **29b**) on the morphology of *Sporothrix spp.* was analysed by scanning electron microscopy (SEM). Furthermore, the cytotoxicity tests on mouse fibroblast cells and human red blood cells indicated that these metal complexes were more selective towards fungi than mammalian cells with high SIs (>2536). Metal complexes **26a**, **26b** and **29b** proved to be promising fungistatic drug candidates, while complex **29a** was excluded due to its haemolytic effect.<sup>69</sup>



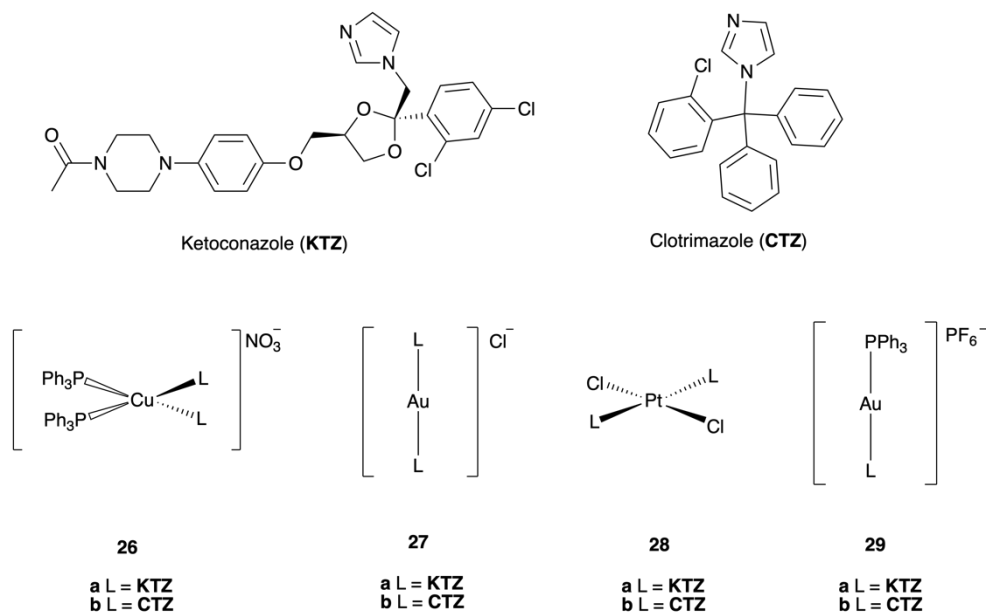


**Fig. 14:** KTZ- and CTZ-based metal complexes assessed for antifungal activity.

In 2021, Cu(II) and Zn(II) complexes derived from FCZ with the general formulas  $\{[\text{CuCl}_2(\text{FCZ})_2] \cdot 5\text{H}_2\text{O}\}_n$  and  $\{[\text{ZnCl}_2(\text{FCZ})_2] \cdot 2\text{C}_2\text{H}_5\text{OH}\}_n$  were prepared by Stevanović *et al.* The metal complexes were shown to be stable up for up to 48h in solution, as determined by molar conductance, UV-Vis, and NMR measurements. The antifungal activities of the complexes were assessed against *C. albicans*, *C. krusei*, and *C. parapsilosi* with comparisons between the parent drug, FCZ. Both showed 2.7-fold higher activities than FCZ against *C. albicans* clinical isolates. The Zn(II) complex showed 5.4- and 11-fold higher activity than FCZ against *C. krusei*, and *C. parapsilosis*. The cytotoxicities of the complexes were tested against human fibroblast cells (MRC-5) and it was found that the metal complexes had increased toxicities when compared to FCZ (11.4 to 12.7 times higher). However, the SI values of the Cu(II) and Zn(II) complexes were 41 and 73, respectively. Considering the yeast-to-hyphae transition is one of the main pathogenic properties of *Candida* spp, the metal complexes (and FCZ) were exposed to *C. albicans* ATCC 10231 at subinhibitory concentrations. The results showed that the metal complexes were able to completely inhibit hyphae formation. Additionally, metal complexes showed moderate to good inhibition against biofilm formation of *C. albicans* ATCC 10231 and *C. parapsilosis* ATCC 22019. The studies of FCZ and its metal complexes on fluorescent *Candida* species adhesion to A549 cells (an initial step to invade the host cells) indicated that the Zn(II) complex reduced the adhesive properties of fungal cells, while the Cu(II) complex and FCZ had no effect. Furthermore, the exposure of these

compounds at subinhibitory concentration reduced the amount of ergosterol in *C. albicans*. The Zn(II) complex and uncoordinated FCZ had comparable decreases in ergosterol depletion, however, the Cu(II) complex was found to be more effective. It was postulated that the mode of action could be similar to FCZ itself and that the Cu(II) complexes could be interacting with other active sites to further reduce the amount of ergosterol. Molecular docking studies of the metal complexes with CYP51 showed that Zn(II) complex had higher binding strength to the target enzyme, via electrostatic, steric and internal energy interactions.<sup>70</sup>

Navarro and co-workers reported another series of Zn(II) and Cu(II) KTZ- and CTZ-containing complexes, namely,  $[\text{Zn}(\text{KTZ})_2(\text{Ac})_2] \cdot \text{H}_2\text{O}$  (**30a**),  $[\text{Zn}(\text{KTZ})_2\text{Cl}_2] \cdot 0.4\text{CH}_3\text{OH}$  (**31a**),  $[\text{Zn}(\text{KTZ})_2(\text{H}_2\text{O})(\text{NO}_3)](\text{NO}_3)$  (**32a**),  $[\text{Cu}(\text{KTZ})_2(\text{Ac})_2] \cdot \text{H}_2\text{O}$  (**33a**),  $[\text{Cu}(\text{KTZ})_2\text{Cl}_2] \cdot 3.2\text{H}_2\text{O}$  (**34a**),  $[\text{Cu}(\text{KTZ})_2(\text{H}_2\text{O})(\text{NO}_3)](\text{NO}_3) \cdot \text{H}_2\text{O}$  (**35a**),  $[\text{Zn}(\text{CTZ})_2(\text{Ac})_2] \cdot 4\text{H}_2\text{O}$  (**30b**),  $[\text{Zn}(\text{CTZ})_2\text{Cl}_2]$  (**31b**),  $[\text{Zn}(\text{CTZ})_2(\text{H}_2\text{O})(\text{NO}_3)](\text{NO}_3) \cdot 4\text{H}_2\text{O}$  (**32b**),  $[\text{Cu}(\text{CTZ})_2(\text{Ac})_2] \cdot \text{H}_2\text{O}$  (**33b**),  $[\text{Cu}(\text{CTZ})_2\text{Cl}_2] \cdot 2\text{H}_2\text{O}$  (**34b**) and  $[\text{Cu}(\text{CTZ})_2(\text{H}_2\text{O})(\text{NO}_3)](\text{NO}_3) \cdot 2\text{H}_2\text{O}$  (**35b**) (**Fig. 15**). The antifungal activity of these metal complexes was screened against three fungi species, *C. albicans*, *C. neoformans*, and *S. brasiliensis*. Against one or more species, all metal complexes were found to be more active than the parent drugs. Amongst all tested compounds, complexes **30a** and **32a** were the most active against the three fungal species with MIC values ranging from 0.03-0.25  $\mu\text{M}$ . These values were lower than those of KTZ (MIC = 0.125-0.5  $\mu\text{M}$ ). Further studies were performed on complexes **30a** and **32a**. The superficial alterations in *S. brasiliensis* morphology after exposure to sublethal concentrations of complexes **30a** and **32a** were characterised by SEM. Treatment with complexes **30a** and **32a** resulted in pronounced changes, such as increased cell size, compromised cell walls, and loss of cellular structure when compared to untreated cells. Cytotoxic studies showed that compounds **30a** and **32a** were more toxic than KTZ against mammalian cells. Nevertheless, compounds **30a** and **32a** displayed similar SI values (>60) towards fungus over LLC-MK2 cells when compared to KTZ.<sup>71</sup>

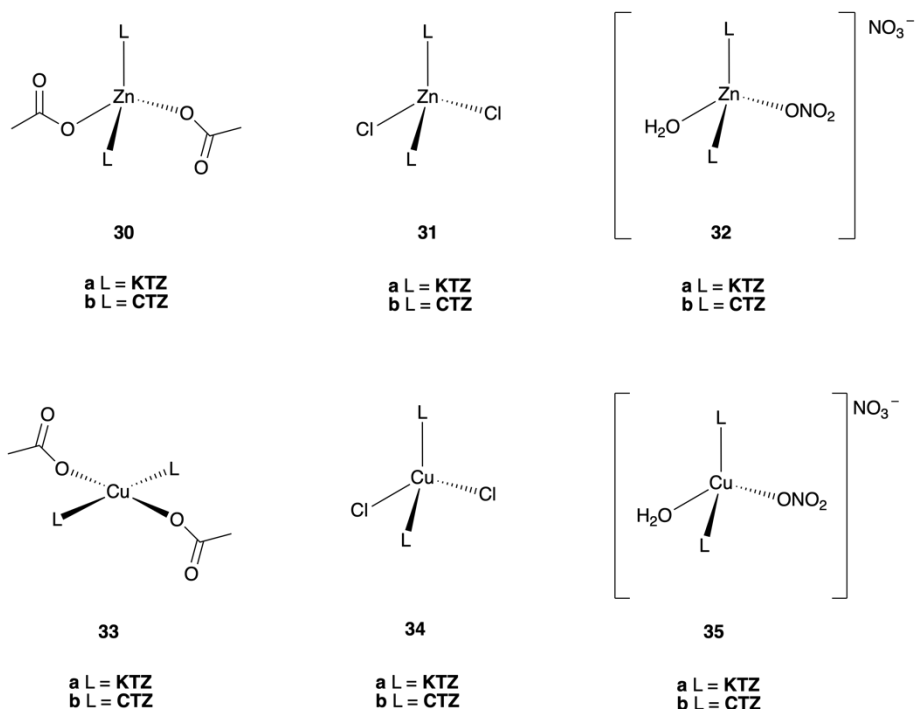


**Fig. 15:** KTZ- and CTZ-based metal complexes assessed for antifungal activity.

Recently, Castonguay and co-workers reported the antifungal activities of three Ru-cyclopentadienyl complexes, including one neutral Ru-Cl compound (**36**), and two cationic compounds, [Ru-ACN]<sup>+</sup> (**37**) and [Ru-ATZ]<sup>+</sup> (**38**, Fig. 16) against five *Candida* species (*C. albicans*, *glabrata*, *tropicalis*, *krusei* and *lusitanae*) and one *Cryptococcus* species (*C. neoformans*). Anastrozole (ATZ) is a triazole-containing aromatase inhibitor that works by blocking the production of oestrogen in the treatment and prevention of breast cancer in women. UV-Vis spectra of the metal complexes in solution with DMSO showed that they were stable up to at least 30 minutes. At 20 μM, the neutral Ru-Cl complex (**36**), ATZ and NaBF<sub>4</sub> displayed no antifungal activities, while, conversely, the [Ru-ACN]<sup>+</sup> (**37**) and [Ru-ATZ]<sup>+</sup> (**38**) complexes displayed significant inhibition on the growth of all tested strains with MIC values ranging from 2.4 to 9.3 μM. The MIC values of both cationic species were found to be lower than FCZ against *C. glabrata* and *C. krusei*, which are known to be FCZ-resistant. It was found that when *C. glabrata* cells were treated with [Ru-ATZ]<sup>+</sup>, the compound was taken up in a dose-dependent manner and generated significant amounts of intracellular ROS. By comparison, the Ru-Cl complex (**36**) had ROS levels comparable to the non-treated cells. These findings were consistent with the compounds reported antifungal activities and potentially indicated the importance of the cationic nature of

the complex. Molecular docking studies of  $[\text{Ru-ATZ}]^+$  (**38**) with the CYP51 showed that more energetically favourable interactions occurred between CYP51 and  $[\text{Ru-ATZ}]^+$  (**38**) than FCZ.<sup>72</sup>

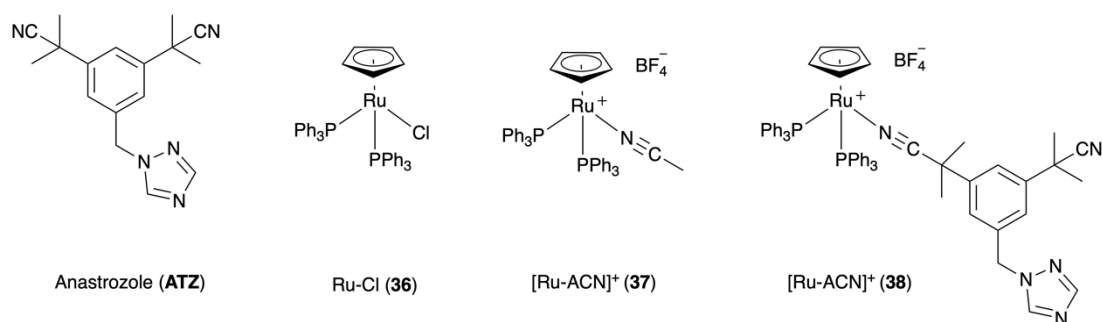


**Fig. 16:** Ruthenium-cyclopentadienyl complexes assessed for antifungal activity.

### 3. Polypyridine based metal complexes

Polypyridyl ligands, such as 1,10-phenanthroline (phen) and 2,2'-bipyridine (bipy), have played an important role in the development of coordination chemistry (**Fig. 17**).<sup>73</sup> As powerful chelating ligands, these ligands coordinate with a variety of transition metal ions to form thermodynamically stable metal complexes. Both the metal complex and the free polypyridyl ligands can possess potent bioactivity and disturb biological systems. When the ligands are active alone, it is usually assumed that the sequestration of trace metals *in situ* is involved and that the resulting metal complexes are the active species.<sup>74,75</sup>

In 2000, McCann *et al.* prepared a series of metal complexes (Mn(II), Co(II), Ni(II), Cu(II), Zn(II) and Ag(I)) of malonic acid (mal) chelated with the phen ligand, namely,  $[\text{Mn}(\text{phen})_2](\text{mal})_2 \cdot 2\text{H}_2\text{O}$ ,  $[\text{Co}(\text{phen})_3](\text{mal})_2 \cdot 2\text{H}_2\text{O}$ ,  $[\text{Cu}(\text{phen})(\text{mal})_2] \cdot 2\text{H}_2\text{O}$ ,  $[\text{Ni}(\text{phen})_2](\text{mal})_2 \cdot 2\text{H}_2\text{O}$ ,  $[\text{Zn}(\text{phen})(\text{mal})_2] \cdot 2\text{H}_2\text{O}$ , and  $[\text{Ag}_2(\text{phen})_3(\text{mal})] \cdot 2\text{H}_2\text{O}$ . The Mn(II), Cu(II) and Ag(I) complexes displayed remarkable inhibition of *C. albicans* with MIC values ranging from 1.25 to 2.5  $\mu\text{g} \cdot \text{cm}^{-3}$ . By comparison, the MIC values increased progressively from the Zn(II) complexes (>5  $\mu\text{g} \cdot \text{cm}^{-3}$ ) and the Co(II), Ni(II) complexes (20  $\mu\text{g} \cdot \text{cm}^{-3}$ ). The MIC values of the different Ag(I) complexes,  $\text{Ag}(\text{CH}_3\text{COO})$ ,  $[\text{Ag}_2(\text{mal})]$  and  $[\text{Ag}_2(\text{phen})_3(\text{mal})] \cdot 2\text{H}_2\text{O}$  were similar, indicating that the active species was likely the Ag(I) cation itself. To understand the difference between the effective complexes (Mn(II), Cu(II) and Ag(I)) and ineffective complexes (Zn(II), Co(II) and Ni(II)),  $[\text{Cu}(\text{phen})(\text{mal})_2] \cdot 2\text{H}_2\text{O}$  and  $[\text{Zn}(\text{phen})(\text{mal})_2] \cdot 2\text{H}_2\text{O}$  were

chosen to represent each group in oxidative stress studies. Reduced glutathione (GSH) is known to be an important antioxidant molecule in yeast cells, and the ratio to oxidized glutathione (GSSG) can give valuable insights into the ability of a compound to induce oxidative stress. The Cu(II) complex induced significant cellular oxidative stress, as shown by decreased ratios of reduced and oxidized glutathione (GSH/GSSG) = 5:1 and increased lipid peroxidation (7:1). By contrast, the same measurements conducted for the Zn(II) complex remained largely unchanged relative to the negative control (GSH/GSSG ratio = 22:1 and lipid peroxides = 1:1 vs. 17:1 and 1:1, respectively, for the control). These observations would appear to substantiate the hypothesis that the significant anti-*Candida* activity of the Cu(II) and Mn(II) complexes may be attributed to their redox activity and potential action as Fenton reagents.<sup>76</sup>

On the basis of previous work in their laboratory, Coyle *et al.* further investigated the modes of action of complexes [Cu(phen)(mal)<sub>2</sub>] $\cdot$ 2H<sub>2</sub>O, [Mn(phen)<sub>2</sub>](mal)<sub>2</sub> $\cdot$ 2H<sub>2</sub>O and [Ag<sub>2</sub>(phen)<sub>3</sub>(mal)] $\cdot$ 2H<sub>2</sub>O, which are highly toxic against *C. albicans*. Cells exposed to either phen or metal-phen complexes resulted in significant reductions in cellular respiration, however, despite the drug-treated cells being metabolically hindered, their oxygen-uptake was found to increase, with the exception of the Ag(I) complex. This result could be explained by the fact that cells were using oxygen for processes other than respiration (e.g., formation of ROS). Furthermore, all compounds appeared to inhibit cytochrome biosynthesis, leading to a reduction in cellular ergosterol content, with the exception of [Mn(phen)<sub>2</sub>](mal)<sub>2</sub> $\cdot$ 2H<sub>2</sub>O which increased ergosterol content. The mode action of phen and its metal complexes have been related to mitochondrial function, reduction of cytochrome *b* and *c* synthesis, induction of respiratory uncoupling and increase of cell wall permeability in fungal cells. These are distinct modes of action compared to conventional azole antifungal drugs targeting ergosterol in the fungal cell membrane. Hence these compounds can be considered as a novel group of antifungal agents to be used alone or in combination with existing antifungal drugs.<sup>77</sup> Further studies on the effect of these drugs on the morphology of fungal and mammalian cells, as well as the integrity of cellular DNA were also carried out by Coyle *et al.*<sup>78</sup>

A phen derivative, namely 1,10-phenanthroline-5,6-dione (phendio) and its Cu(II) and Ag(I) complexes – [Cu(phendio)<sub>3</sub>](ClO<sub>4</sub>)<sub>2</sub>·4H<sub>2</sub>O (**39**) and [Ag(phendio)<sub>2</sub>]ClO<sub>4</sub> (**40**) (**Fig. 17**). The X-ray crystal structure of **40** was obtained, which showed that the Ag(I) adopted a pseudo tetrahedral environment and was chelated by four nitrogens from two phendio ligands. Both of the phendio ligand and its metal complexes showed higher activity than underivatized phen against *C. albicans*. It was envisioned that the two carbonyl oxygens on the phendio play an important role in its bioactivity. Extensive and non-specific DNA cleavage was found after *C. albicans* was exposed to phendio alone, simple Ag(I) salts and the [Ag(phendio)<sub>2</sub>]ClO<sub>4</sub> complex (**40**). Moreover, phendio alone and in complex with Ag(I) (**40**) caused severe morphological alterations to *C. albicans* as well as disruption of cell division.<sup>79</sup> In continuation of this work, the antifungal activity of phendio and its Cu(II) and Ag(I) complexes (**39** and **40**) against *Phialophora verrucosa* was also assessed. The inhibition of these compounds on conidial growth followed the order (based on IC<sub>50</sub> values): [Cu(phendio)<sub>3</sub>]<sup>2+</sup> > [Ag(phendio)<sub>2</sub>]<sup>+</sup> > phendio. In addition, fungicidal effect was only determined on [Cu(phendio)<sub>3</sub>](ClO<sub>4</sub>)<sub>2</sub>·4H<sub>2</sub>O (**39**) at a concentration of 20 μM. The MIC values obtained against *P. verrucosa* showed that phendione and its Ag(I) and Cu(II) complexes were more active than their corresponding metal salts. Complex [Ag(phendio)<sub>2</sub>]ClO<sub>4</sub> (**40**) (MIC = 4 μM) had 6-fold higher activity than AgClO<sub>4</sub> (MIC = 24 μM). Complex [Cu(phendio)<sub>3</sub>](ClO<sub>4</sub>)<sub>2</sub>·4H<sub>2</sub>O (**39**) inhibited the growth of *P. verrucosa* with an MIC value of 5 μM, whereas Cu(ClO<sub>4</sub>)<sub>2</sub>·6H<sub>2</sub>O was inactive even at 54 μM. It was been speculated that such observations may result from the metal complexes having higher lipophilicities than the simple metal salts. This property was attributed to a reduction in total electron density on the free ligand by coordination with a metal ion and sharing of the positive charge of metal cation with N-donor atoms, inducing electron delocalization over the chelate ring. The inhibitory modes of action of antifungal agents against the growth of *P. verrucosa* such as ultrastructure alternations, metallopeptidase activity, sterol synthesis and morphological transitions (conidia-into-mycelial transformation) were further evidenced by the inhibitory effect of phendio and its Ag(I) and Cu(II) complexes.<sup>80</sup> Recently, Granato *et al.* reported additional mechanisms of action of phendio and its metal complexes (**39** and **40**) against *P. verrucosa*, focusing on (i) combination therapy with AmB, (ii) biofilm formation and disarticulation, (iii) interaction with

human macrophages, and (iv) *in vivo* studies on infected *G. mellonella* larvae. Overall, complex **40** was found to be a promising for the treatment of *P. verrucosa*-infected larvae due to its lower toxicity against mice.<sup>81</sup>

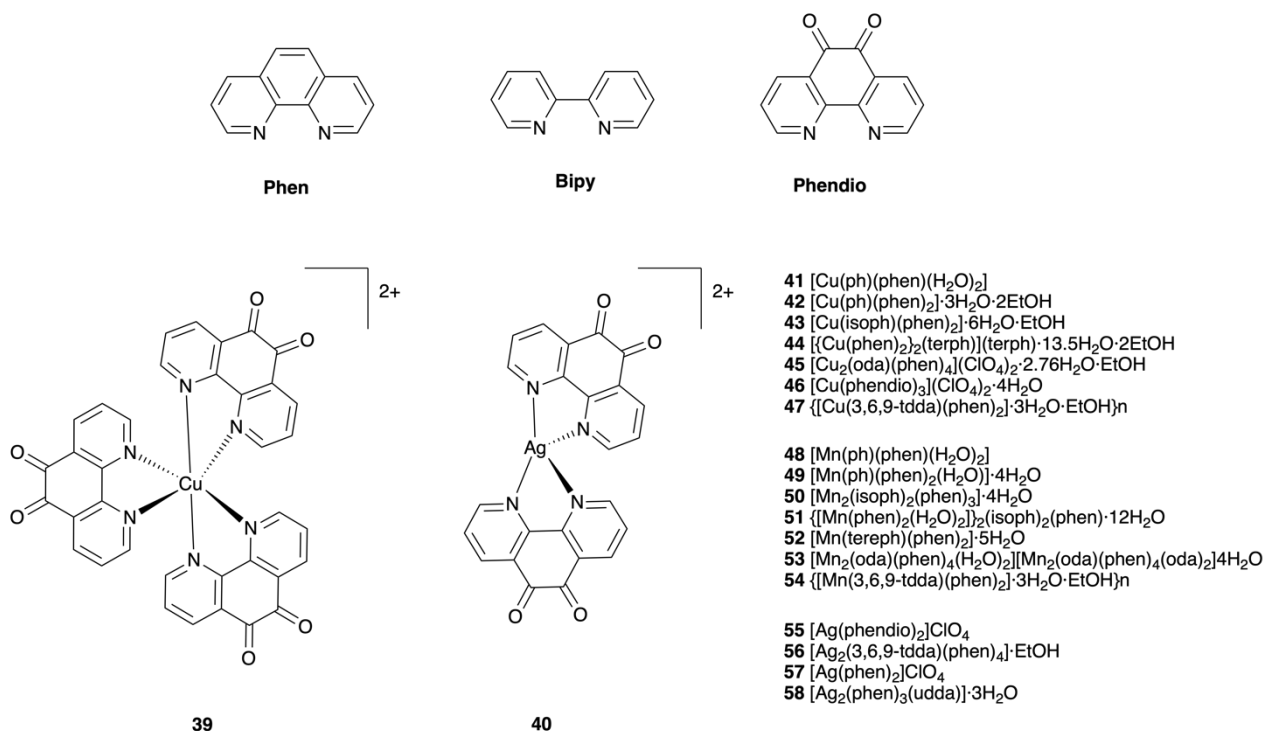


**Fig. 17:** Polypyridine metal complexes assessed for antifungal activity.

Considering the well-established antifungal activity of metal-containing phen or phendio complexes, Gandra *et al.* investigated the inhibitory effect of eighteen metal chelates (Mn(II), Cu(II) and Ag(I)) containing phen or phendio (**41-58**, **Fig. 17**) on the growth of *Candida haemulonii* complex, including *C. haemulonii*, *C. hamulonii var. vulnera* and *C. duobushaemulonii*, which are known to be more resistant to commonly used antifungal agents. The capacities of these complexes to inhibit planktonic growth and biofilm of the *C. haemulonii* complex were recorded by overall geometric mean of the MIC values (GM-MIC). Among all tested metal complexes, complexes **43** and **45-58** showed significant inhibitory effect on the viability of planktonic-growing cells of all fungus isolates with GM-MICs less than 10  $\mu$ M, however, still less effective than the positive control, CFG (0.18  $\mu$ M). Simple metal salts such as CuCl<sub>2</sub> and MnCl<sub>2</sub> were found to have no appreciable effect on fungal growth. Conversely, inorganic Ag(I) salts (such as silver nitrate) and the free ligands (phen and phendione) significantly inhibited fungal growth. The inhibitory activity of the silver salts was likely attributed to the Ag(I) ion which is known to have significant biocidal activity. However, the Ag(I)

complex with phen or phendio induced a more pronounced inhibitory effect compared to the metal ion or parent ligands alone. A similar effect was observed for Cu(II) complex (**47**) and Mn(II) complexes (**49-51** and **53-54**), indicating that the metal complexes were superior antifungal agents than the ligands themselves. Cytotoxicity studies demonstrated that Mn(II) complexes were more selective towards lung epithelial cells (A549) than fungal cells with the highest SI values (>236.40 to 48.19). Additionally, water-soluble  $[\text{Ag}_2(\text{phen})_3(\text{udda})]\cdot 3\text{H}_2\text{O}$  (**58**) (uddaH<sub>2</sub> = undecanedioic acid) displayed a relatively high SI value of 56.11. Since biofilm formation is an important virulence factor for pathogenic fungi, as it can protect the organism from the host's immune response, further examination on potent metal complexes (GM-MIC values <10  $\mu\text{M}$ ) on biofilm-growing cells were carried out. The Cu(II) complex (**47**), Mn(II) complexes **51**, **53** and **54** and Ag(I) complex **56** also exhibited significant inhibition on the growth of biofilm-growing cells with GM-MIC values less than 10  $\mu\text{M}$ , the remaining metal complexes exhibited GM-MIC values ranging from 12.04 to 28.42  $\mu\text{M}$ . Similar inhibition trends were observed for the planktonic-growing cells, however, the biofilm cells were generally more resistant.<sup>82</sup> Gandra *et al.* further investigated the *in vivo* activities of compounds **47-57** against *G. mellonella* larvae – a commonly used *in vivo* infection model to understand *C. haemulonii* infection. The results showed that the metal chelates were capable of: 1) Inhibiting fungal proliferation during *in vivo* infection; 2) inducing an immune response in the *G. mellonella* host; and 3) affecting the fungal burden of infected larvae and the virulence of *C. haemulonii* in a dose-dependent manner. Among the tested compounds, the Mn(II) complex (**54**) was the most promising antifungal agent for further investigation.<sup>83</sup>

In 2010, Raman and co-workers reported mixed-ligand Cu(II) and Zn(II) complexes with an isatin-based Schiff base (L) as a primary ligand, phen/bipy as auxiliary ligands and the general formula  $[\text{ML}(\text{phen})_2]\text{Cl}_2$  (**59**)/ $[\text{ML}(\text{bipy})_2]\text{Cl}_2$  (**60**) (**Fig. 18**). The DNA binding modes of these complexes were verified by absorption hypochromicity and viscosity measurements. The studies of cyclic voltammetry showed that in the absence of DNA the copper complexes had quasi-reversible redox properties. On the addition of DNA, the anodic and cathodic peak currents decreased with increasing DNA concentration indicating slow diffusion of the Cu(II) complex upon complexation with the DNA macromolecules. These results might be attributed to  $[\text{CuL}(\text{phen})_2]\text{Cl}_2$ , which stabilizes the duplex (GC pairs) through intercalation. No reversible redox process was



found in the Zn(II) complex. The DNA cleavage abilities of these metal complexes in the presence of H<sub>2</sub>O<sub>2</sub> were determined by the conversion of supercoiled DNA to nicked DNA and linear DNA. These observations were likely the result of ROS production. The antifungal activities of the isatin-based ligand and its metal complexes were screened against five fungal strains (*A. niger*, *F. solani*, *C. lunata*, *R. bataticola*, *C. albicans*). The MIC values of the metal complexes were lower than the free ligand (L), but higher than the reference drug, nystatin. Moreover, the Cu(II) complexes were more active than the Zn(II) complexes against all tested organisms.<sup>84</sup> In 2018, Oliveira and co-workers synthesised two octahedral Cu(II) complexes with bipy and thiouracil as co-ligands (**61-62**, **Fig. 18**). The stability of the metal complexes in H<sub>2</sub>O/DMSO (95/5% v/v) solution were assessed via UV-Vis spectroscopy and showed that these compounds were stable for up to 36 h of incubation. Complex **61** displayed significant fungistatic and fungicidal activities against 21 clinical isolates of *Candida*, with MIC values ranging from 31.25 to 125 µg·mL<sup>-1</sup> and MFC values ranging from 31.25 to 250 µg·mL<sup>-1</sup>. Conversely, complex **62** and the free ligands (2-thiouracil and 6-methyl-2-thiouracil) were found to be inactive. In addition, CuCl<sub>2</sub> displayed MIC values of 1000 µg·mL<sup>-1</sup> on all tested isolates, suggesting that the antifungal activity of complex **61** could be attributed to the synergistic effect of the metal-ligand complex. Further studies showed that complex **61** had no mutagenic potential and slightly inhibited biofilm formation, making it a promising antifungal agent for further study.<sup>85</sup>

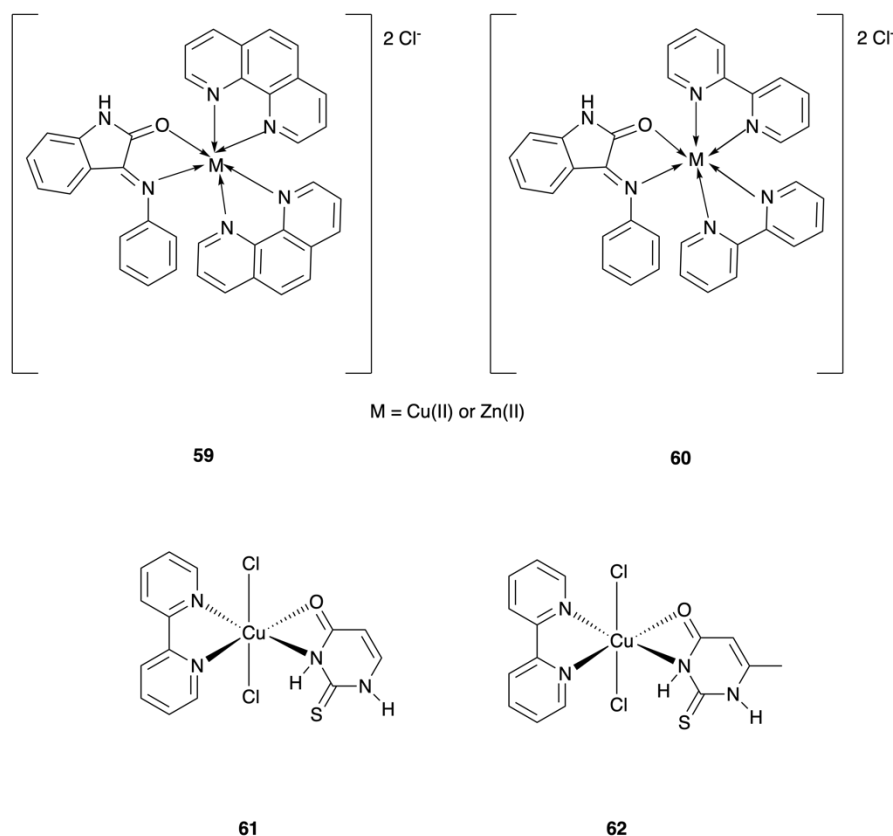
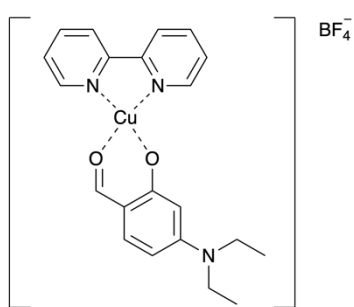


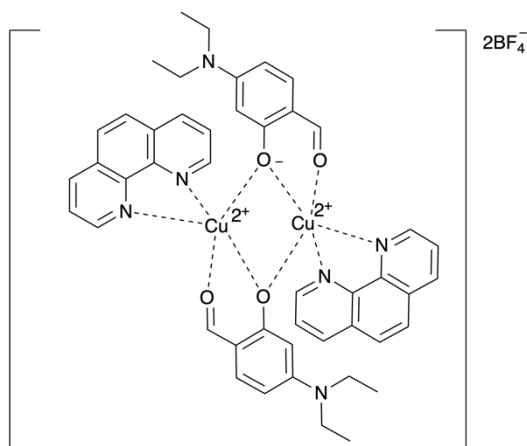
**Fig. 18:** Polypyridyl metal complexes assessed for antifungal activity.

In 2020, two Cu(II) complexes with 4-(diethylamino)salicylaldehyde (L) and  $\alpha$ -diimine (bipy or phen) ligands, namely [Cu(L)(bipy)]BF<sub>4</sub>·0.5H<sub>2</sub>O (**63**) and [Cu<sub>2</sub>(L)<sub>2</sub>(phen)<sub>2</sub>](BF<sub>4</sub>)<sub>2</sub> (**64**, **Fig. 19**), were prepared by Dimitrijević *et al.*<sup>86</sup> The dinuclear Cu(II) complex (**64**) was found to exist in a monomeric form in DMSO solution, as determined by ESI-MS. The antifungal activities of two Cu(II) complexes (as well as the Cu(II) salt source, phen, bipy, and free ligand) were screened against three fungal strains (*A. brasiliensis*, *C. albicans*, and *S. cerevisiae*). The Cu(II) complexes were found to be more active than FCZ but less so than free bipy or phen. Both the Cu(II) salt and free ligand displayed low antifungal activities, indicating the importance of the bidentate  $\alpha$ -diimine ligands and resultant complexes in promoting the inhibitory effect of the metals. The cytotoxicities of these compounds were quantified by brine shrimp lethality bioassays. The Cu(II) salt and bipy/phen displayed moderate toxicities while the free ligand and compounds **63** and **64** had lower cytotoxicities. Nagashri and co-workers examined the antifungal activities of metal chelates of phen derivatives (M = Cu(II), Co(II), Ni(II), and Zn(II)) (**65**, **Fig. 19**) against *C. albicans*, *A. niger*, and *A. flavus*. Among the tested complexes, the Cu(II)

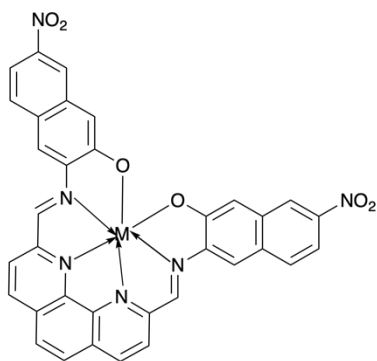
compound was found to be the most active with MIC values ranging from 18 to 25  $\mu\text{g}\cdot\text{mL}^{-1}$ ; less than nystatin (10-15  $\mu\text{g}\cdot\text{mL}^{-1}$ ). The stabilities of the complexes in DMSO and PBS buffer were monitored by UV-visible spectrophotometry and were found to be stable for up to 24 h with only minor degradation, likely due to ligand hydrolysis under physiological conditions. The inherent binding constants of the complexes with DNA were obtained based on molar extinction coefficients ( $K_b$ ): 4.11, 3.62, 3.85 and  $2.9 \times 10^5$  for Cu(II), Ni(II), Co(II), and Zn(II), respectively, indicating that Cu(II) chelate had the highest affinity.<sup>87</sup> In 2021, three Cu(II) complexes containing phen and bio-essential amino acid, L-tryptophan, (**66a-c**, **Fig. 19**) were synthesized by Arumugham and co-workers. The antifungal activities of the metal chelates against *A. niger*, *Rhizopus* spp., and *Penicillium* spp. showed that **66a** and **66c** were inactive and that only **66b** had antifungal activity, which was comparable to positive control, AmB.



**63**

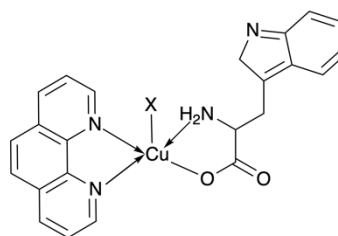


**64**



M = Co(II), Ni(II), Cu(II) and Zn(II)

**65**



X = I (a), Cl (b), and SCN (c)

**66**

Fig. 19: Polypyridyl metal complexes assessed for antifungal activity.

Recently, the activities of five complexes of Cu(II) with pyridine-4,5-dicarboxylate esters against *Candida* were evaluated by Glišić and co-workers (67-71, Fig. 20). Complex 67 adopted an elongated octahedral geometry while the geometries of complexes 68-71 were distorted square-pyramids. These metal complexes were also found to be stable in DMSO after 24 and 48 h of incubation and the partition coefficients ( $\text{Log}P$ ) of these compounds were within the ideal range,  $0 \leq \text{Log}P \leq 2.3$ . Complexes 68 and 71 both showed significant inhibition of *C. albicans* (ATCC 10231) with MIC values of  $31.25 \mu\text{g}\cdot\text{mL}^{-1}$ . Additionally, complex 71 was also found to be relatively non-toxic against human fibroblasts MRC-5 ( $\text{IC}_{50} = 70 \mu\text{g}\cdot\text{mL}^{-1}$ ). *C. albicans* filamentation and biofilm formation in the presence of complexes 67-71 at subinhibitory concentrations were also investigated. Complexes 67 and 70 almost completely inhibited the formation of fungal hyphae and efficiently inhibited biofilm formation. The affinities of these complexes with bovine serum albumin and CT-DNA were confirmed by fluorescence spectrophoresis or gel electrophoresis.<sup>88</sup>

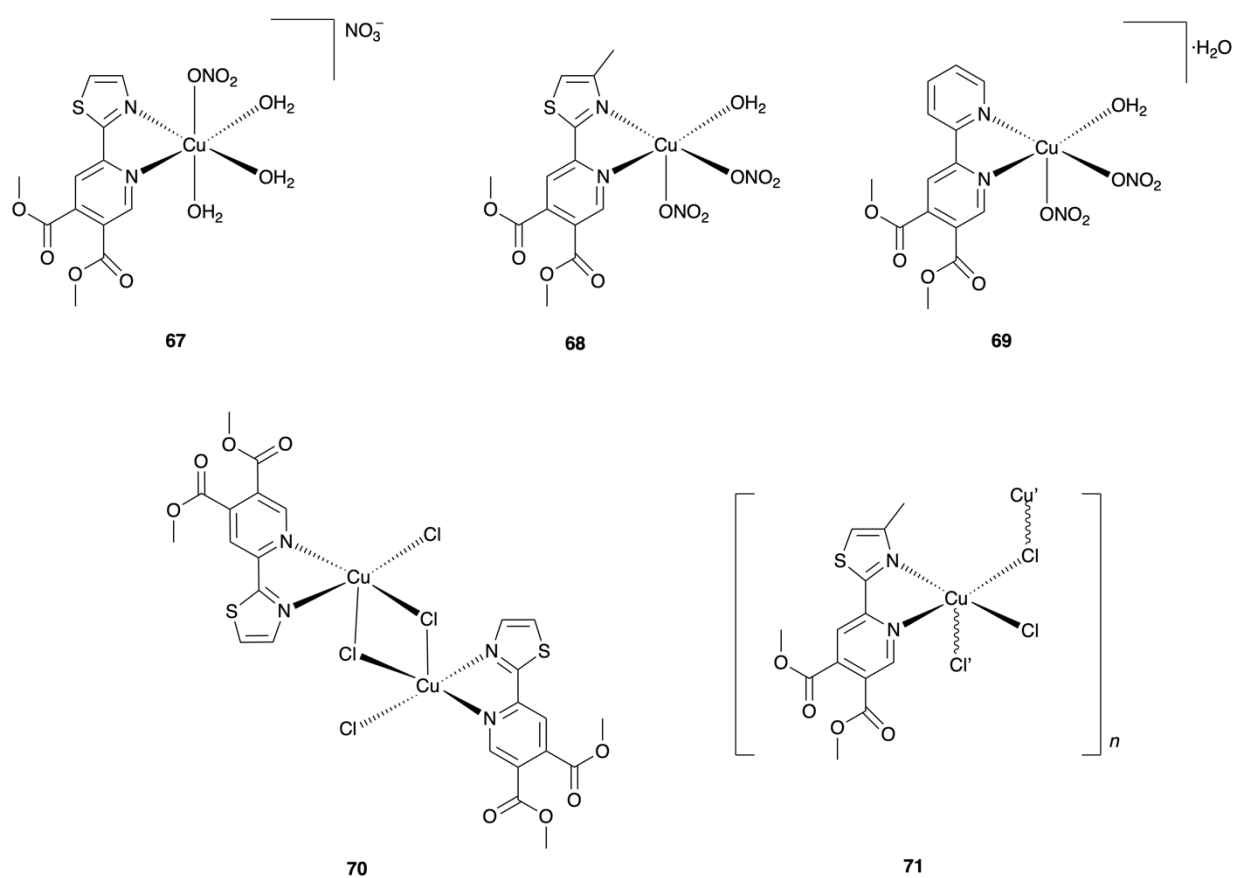
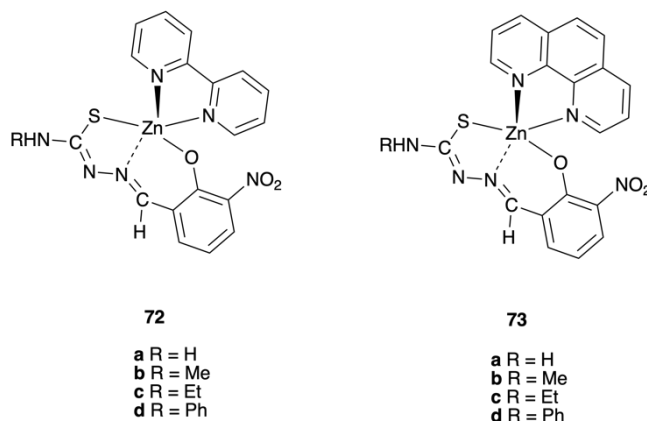


Fig. 20: Polypyridyl metal complexes assessed for antifungal activity.

In 2021, Lobana and co-workers investigated the antifungal activities of Zn(II) complexes with 3-nitro-salicylaldehyde-*N*-substituted thiosemicarbazones and bipy or phen as co-ligands. Compound **72a-b**, **73a**, and **73c** (**Fig. 21**) displayed significant inhibitory effects against *C. albicans* growth. The recorded MIC values ranged from 5 to 7  $\mu\text{g}\cdot\text{mL}^{-1}$ , which were less than AmB (MIC = 0.1  $\mu\text{g}\cdot\text{mL}^{-1}$ ).<sup>89</sup>



**Fig. 21:** Polypyridyl metal complexes assessed for antifungal activity.

#### 4. Amino acid-based metal complexes

In 2006, Chohan *et al.* reported a series of amino acid-derived ligands (**L<sub>1</sub>-L<sub>5</sub>**) and their Co(II), Cu(II), Ni(II), and Zn(II) metal complexes with the general formula  $[\text{M}(\text{L})_2(\text{H}_2\text{O})_2]$  (**74**) and  $[\text{M}(\text{L})(\text{H}_2\text{O})_4]\text{Cl}$  (**75**, **Fig. 22**). Ligands (**L<sub>1</sub>-L<sub>5</sub>**) were synthesised by condensation of  $\beta$ -diketones with the respective amino acid (e.g., glycine, phenylalanine, valine and histidine). The bidentate ligands complexed the metal ion via the azomethine nitrogen and deprotonated oxygen, adopting octahedral geometries. Remarkable increases in antifungal activities upon metal ion coordination against one or more tested fungal strains (*M. longifusus*, *C. albicans*, *A. flavus*, *M. canis*, *F. solani* and *C. glaberata*) were reported. The increase in the activity of the metal complexes was explained on the basis of increased lipophilicity of the metal complexes relative to the metal ions or ligands alone, possibly allowing for increased cellular uptake. The cytotoxicities of these complexes were determined using a brine shrimp bioassay with all metal complexes being less cytotoxic than the metal-free ligands.<sup>90</sup>

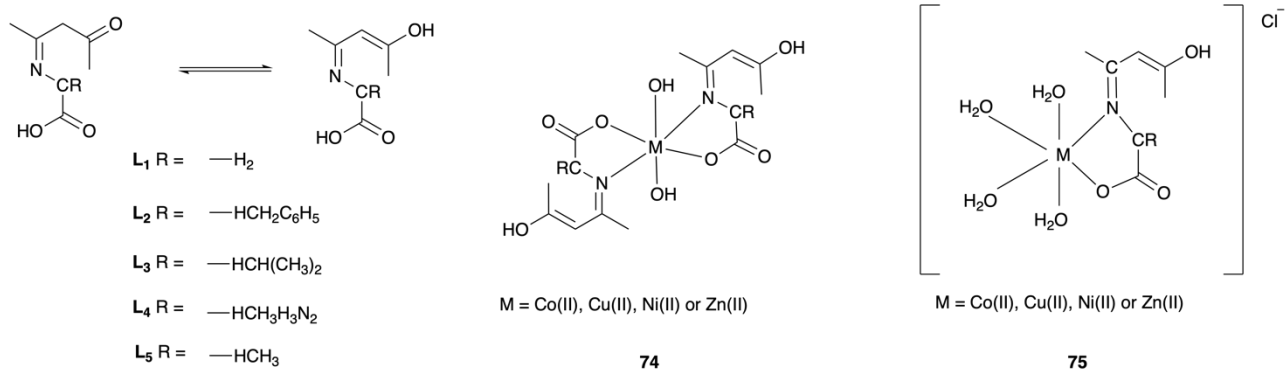


**Fig. 22:** Amino acid-based metal complexes assessed for antifungal activity.

In 2007, Arunachalam and co-workers synthesised water-soluble polymeric Cu(II) complexes,  $[Cu(\text{phen})(L\text{-thr})(\text{BPEI})]ClO_4 \cdot 2H_2O$  (L-thr = L-threonine and BPEI = branched polyethyleneimine), with varying degrees of Cu(II) complex inclusion in the polymer chains. The antifungal activities of the Cu(II)-polymer chelates against *C. albicans* were determined using the disk diffusion method with CTZ as a reference drug. Inclusion of the BPEI polymer in the metal complex,  $[Cu(\text{phen})(L\text{-thr})(\text{BPEI})]ClO_4 \cdot 2H_2O$ , was found to appreciably increase the recorded zone of inhibition diameter (10 mm) relative to either BPEI alone (6 mm) or the polymer-free copper complex  $[Cu(\text{phen})(L\text{-thr})(H_2O)]ClO_4$  (3 mm). The DNA binding properties of these complexes were studied by electronic absorption spectroscopy, fluorescence spectroscopy and gel electrophoresis. The authors suggested that the polymer-Cu(II) complexes could bind to CT-DNA principally by electrostatic interactions. Additionally, ionic interactions, van der Waals interactions, hydrogen bonding and other partial intercalation binding modes may have also been present.<sup>91</sup>

In 2014, Abu-Dief and co-workers developed a range of tridentate Schiff base-amino acid ligands that formed octahedral geometries with Fe(II) ions and had the general formula  $[Fe(HL)_2] \cdot nH_2O$  (**76a-e**, **Fig. 23**). The ligands were prepared by condensation of 5-bromosalicylaldehyde with the  $\alpha$ -amino acids (L-alanine, L-phenylalanine, L-aspartic acid, L-histidine and L-arginine). Interaction of the Fe(II) complexes with CT-DNA were investigated by UV-Vis absorption, viscosity and agarose gel electrophoresis measurements. The metal complexes were found to bind to DNA via an intercalative mode, exhibiting binding strengths that followed the order **76e** > **76d** > **76a** > **76c** > **76b**. Antifungal activity assays of the metal complexes on three fungal

strains (*P. purpurogenium*, *A. flavus* and *T. rosium*) showed that the metal complexes were more active than the parent ligands.<sup>92</sup> For comparison, nickelocene-amino acid conjugates (**77a-c**, **Fig. 23**) were also obtained by reaction of amino acid azides with ethynyl nickelocene using a 1,3-dipolar cycloaddition. These organometallic complexes exhibited moderate antifungal activities against *A. niger*, *A. flavus* and *A. alternata*, but were less active than FCZ.<sup>93</sup>

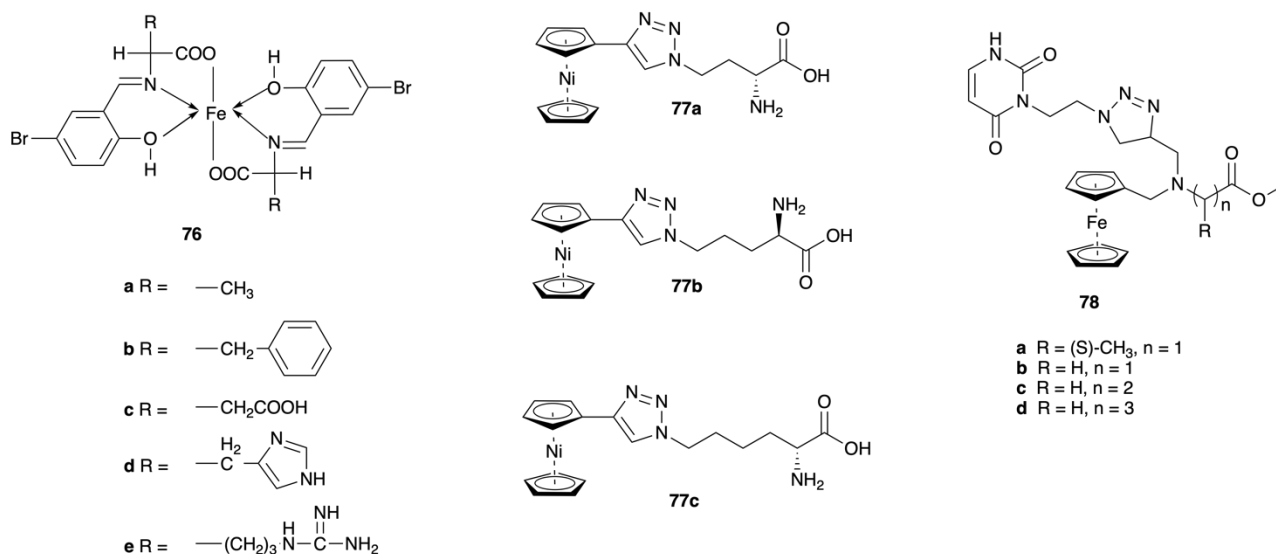


**Fig. 23:** Amino acid-based metal complexes assessed for antifungal activity.

In 2019, Daniluk *et al.* successfully synthesised ferrocenyl amino acid ester-uracil conjugates derived from alanine, glycine,  $\beta$ -alanine and  $\gamma$ -aminobutyric acid via click reactions (**78a-d**, **Fig. 23**). The redox potential of the ferrocene/ferrocenium (Fc/Fc<sup>+</sup>) couple in complexes **78a-d** were also very similar to ferrocene alone, indicating redox activity was not lost or reduced through synthetic modification. Unfortunately, the antifungal activity of these ferrocenyl derivatives against six yeast strains showed that only compound **78a** had significant inhibitory activity against *C. guilliermondii* (IBA 155) with an inhibition zone of 15 mm at a concentration of 0.4 mg per disk. For comparison, the negative control and FCZ (conc. = 0.025 mg per disk) resulted in inhibitory zones of 9 mm and 40 mm, respectively.<sup>94</sup>

## 5. Chalcone-based metal complexes

Recently, Muthukumar *et al.* reported a range of Ru(II) chalconato complexes with the general formula  $[\text{Ru}(\text{CO})(\text{B})(\text{L})_2]$  (**79**) and  $[\text{RuCl}(\text{CO})(\text{EPh}_3)(\text{B})(\text{L})]$  (**80**) (Fig. 24) (E = P or As; B = PPh<sub>3</sub>, AsPh<sub>3</sub> or Py). Octahedral geometries were tentatively proposed for all complexes.<sup>95,96</sup> The antifungal activities of the Ru(II) chalconato complexes against *A. niger* and *Mucor Sp.* strains were greater than the parent ligands alone, but still did not reach the efficacy of the standard drug, Bavistin®. The increase in activity of the metal complexes was explained on the basis of increased lipophilicity of the complexes through metal ion coordination. In 2016, a set of ferrocenyl chalcones were prepared from *O*-alkylated vanillins and acetylferrocene by Muškinja *et al.* (**81a-f**, Fig. 24). The antifungal activities of these complexes were determined against five fungal strains (*M. mucedo*, *T. viride*, *A. niger*, *C. albicans* and *P. italicum*). The ferrocenyl chalcones were found to have moderate antifungal activities with the MIC values ranging from 0.312 to 10 mg·mL<sup>-1</sup>. The *C. albicans* strain was the most sensitive to these compounds, while *A. niger* was the most resistant.<sup>97</sup>

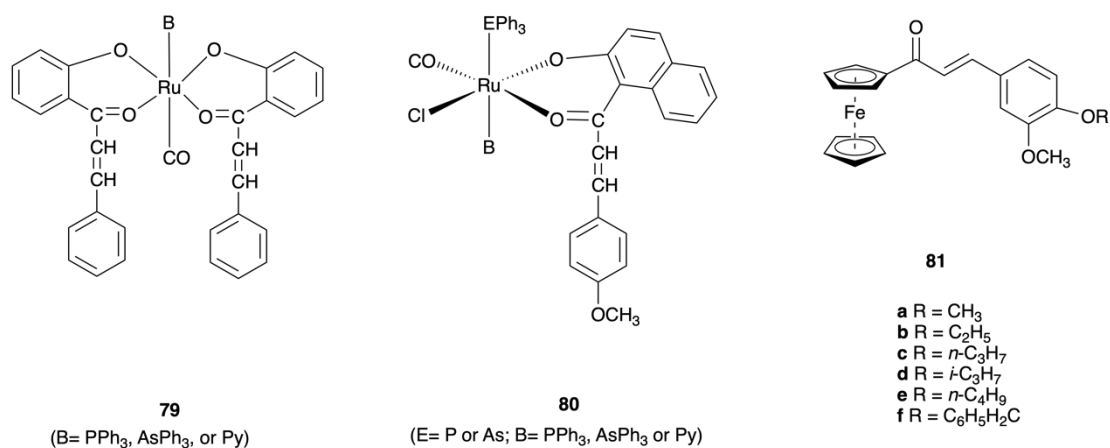


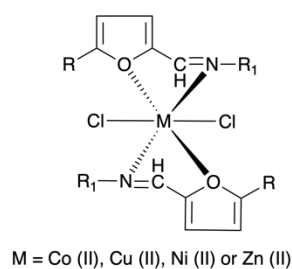
Fig. 24: Chalcone-based metal complexes assessed for antifungal activity.

## 6. Sulfonamide-based metal complexes

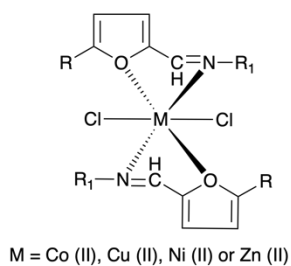
The development of metal complexes based on sulfonamide was stimulated by the discovery of silver sulfadiazine, which is a topical antibiotic used to prevent infections in burn victims.<sup>98</sup> Chohan *et al.* prepared a range of bidentate furanyl-derived sulfonamide ligands which were subsequently coordinated with metal ions (Co(II), Cu(II), Ni(II) and Zn(II)) (**82a-x**, **83a-p**, Fig. 25).<sup>99,100</sup> All resultant metal-based compounds adopted



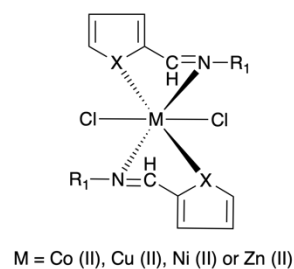
octahedral geometries. The non-electrolytic nature of these metal complexes was determined by molar conductance, confirming that the chloride ions were coordinated to the metal ions. IR spectra indicated that the ligands were coordinated to the metal ion through the furanyl oxygen and the azomethine nitrogen. The antifungal activities of these metal complexes were screened against *M. longifusus*, *C. albicans*, *A. flavus*, *M. canis*, *F. solani* and *C. glabrata* strains and compared with the reference drugs, MCZ and AmB, all complexes had comparable or higher activity than the parent ligands. Complexes **82a-x** only showed ~30% inhibition at 200  $\mu\text{g}\cdot\text{mL}^{-1}$  against the tested fungi, however, most of the complexes **83a-p** exhibited significant inhibition (~80%) at the same concentration. The cytotoxicities of these complexes were tested using a brine shrimp bioassay and, except for some copper complexes, the complexes were found to be non-cytotoxic. Furthermore, pyrrolyl and thienyl-derived sulfonamide ligands and their metal complexes with Co(II), Cu(II), Ni(II) and Zn(II) ions (**84a-t**, **Fig. 25**) were also synthesised by the same authors in a separate article.<sup>101</sup> Shifting of the vibrational modes of the C=N, C-N/S functionalities to lower frequencies, as recorded by IR spectroscopy, suggested that metal coordination occurred through the azomethine nitrogen and pyrrolyl nitrogen/thienyl sulfur. The antifungal activities against the aforementioned six strains showed that most of the complexes possessed significant activity across all tested organisms with inhibition zones greater than 16 mm at 200  $\mu\text{g}\cdot\text{mL}^{-1}$  recorded, however, all metal complex activities were still less than the standard drugs MCZ and AmB (~30 mm).



82



83



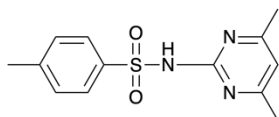
84

**a** = Co(L<sub>1</sub>)<sub>2</sub>Cl<sub>2</sub>    **i** = Co(L<sub>3</sub>)<sub>2</sub>Cl<sub>2</sub>    **q** = Co(L<sub>5</sub>)<sub>2</sub>Cl<sub>2</sub>  
**b** = Cu(L<sub>1</sub>)<sub>2</sub>Cl<sub>2</sub>    **j** = Cu(L<sub>3</sub>)<sub>2</sub>Cl<sub>2</sub>    **r** = Cu(L<sub>5</sub>)<sub>2</sub>Cl<sub>2</sub>  
**c** = Ni(L<sub>1</sub>)<sub>2</sub>Cl<sub>2</sub>    **k** = Ni(L<sub>3</sub>)<sub>2</sub>Cl<sub>2</sub>    **s** = Ni(L<sub>5</sub>)<sub>2</sub>Cl<sub>2</sub>  
**d** = Zn(L<sub>1</sub>)<sub>2</sub>Cl<sub>2</sub>    **l** = Zn(L<sub>3</sub>)<sub>2</sub>Cl<sub>2</sub>    **t** = Zn(L<sub>5</sub>)<sub>2</sub>Cl<sub>2</sub>  
**e** = Co(L<sub>2</sub>)<sub>2</sub>Cl<sub>2</sub>    **m** = Co(L<sub>4</sub>)<sub>2</sub>Cl<sub>2</sub>    **u** = Co(L<sub>6</sub>)<sub>2</sub>Cl<sub>2</sub>  
**f** = Cu(L<sub>2</sub>)<sub>2</sub>Cl<sub>2</sub>    **n** = Cu(L<sub>4</sub>)<sub>2</sub>Cl<sub>2</sub>    **v** = Cu(L<sub>6</sub>)<sub>2</sub>Cl<sub>2</sub>  
**g** = Ni(L<sub>2</sub>)<sub>2</sub>Cl<sub>2</sub>    **o** = Ni(L<sub>4</sub>)<sub>2</sub>Cl<sub>2</sub>    **w** = Ni(L<sub>6</sub>)<sub>2</sub>Cl<sub>2</sub>  
**h** = Zn(L<sub>2</sub>)<sub>2</sub>Cl<sub>2</sub>    **p** = Zn(L<sub>4</sub>)<sub>2</sub>Cl<sub>2</sub>    **x** = Zn(L<sub>6</sub>)<sub>2</sub>Cl<sub>2</sub>

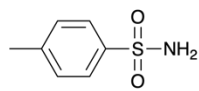
**a** = Co(L<sub>1</sub>)<sub>2</sub>Cl<sub>2</sub>    **i** = Co(L<sub>3</sub>)<sub>2</sub>Cl<sub>2</sub>  
**b** = Cu(L<sub>1</sub>)<sub>2</sub>Cl<sub>2</sub>    **j** = Cu(L<sub>3</sub>)<sub>2</sub>Cl<sub>2</sub>  
**c** = Ni(L<sub>1</sub>)<sub>2</sub>Cl<sub>2</sub>    **k** = Ni(L<sub>3</sub>)<sub>2</sub>Cl<sub>2</sub>  
**d** = Zn(L<sub>1</sub>)<sub>2</sub>Cl<sub>2</sub>    **l** = Zn(L<sub>3</sub>)<sub>2</sub>Cl<sub>2</sub>  
**e** = Co(L<sub>2</sub>)<sub>2</sub>Cl<sub>2</sub>    **m** = Co(L<sub>4</sub>)<sub>2</sub>Cl<sub>2</sub>  
**f** = Cu(L<sub>2</sub>)<sub>2</sub>Cl<sub>2</sub>    **n** = Cu(L<sub>4</sub>)<sub>2</sub>Cl<sub>2</sub>  
**g** = Ni(L<sub>2</sub>)<sub>2</sub>Cl<sub>2</sub>    **o** = Ni(L<sub>4</sub>)<sub>2</sub>Cl<sub>2</sub>  
**h** = Zn(L<sub>2</sub>)<sub>2</sub>Cl<sub>2</sub>    **p** = Zn(L<sub>4</sub>)<sub>2</sub>Cl<sub>2</sub>

**a** = Co(L<sub>1</sub>)<sub>2</sub>Cl<sub>2</sub>    **k** = Ni(L<sub>3</sub>)<sub>2</sub>Cl<sub>2</sub>  
**b** = Cu(L<sub>1</sub>)<sub>2</sub>Cl<sub>2</sub>    **l** = Zn(L<sub>3</sub>)<sub>2</sub>Cl<sub>2</sub>  
**c** = Ni(L<sub>1</sub>)<sub>2</sub>Cl<sub>2</sub>    **m** = Co(L<sub>4</sub>)<sub>2</sub>Cl<sub>2</sub>  
**d** = Zn(L<sub>1</sub>)<sub>2</sub>Cl<sub>2</sub>    **n** = Cu(L<sub>4</sub>)<sub>2</sub>Cl<sub>2</sub>  
**e** = Co(L<sub>2</sub>)<sub>2</sub>Cl<sub>2</sub>    **o** = Ni(L<sub>4</sub>)<sub>2</sub>Cl<sub>2</sub>  
**f** = Cu(L<sub>2</sub>)<sub>2</sub>Cl<sub>2</sub>    **p** = Zn(L<sub>4</sub>)<sub>2</sub>Cl<sub>2</sub>  
**g** = Ni(L<sub>2</sub>)<sub>2</sub>Cl<sub>2</sub>    **q** = Co(L<sub>5</sub>)<sub>2</sub>Cl<sub>2</sub>  
**h** = Zn(L<sub>2</sub>)<sub>2</sub>Cl<sub>2</sub>    **r** = Cu(L<sub>5</sub>)<sub>2</sub>Cl<sub>2</sub>  
**i** = Co(L<sub>3</sub>)<sub>2</sub>Cl<sub>2</sub>    **s** = Ni(L<sub>5</sub>)<sub>2</sub>Cl<sub>2</sub>  
**j** = Cu(L<sub>3</sub>)<sub>2</sub>Cl<sub>2</sub>    **t** = Zn(L<sub>5</sub>)<sub>2</sub>Cl<sub>2</sub>

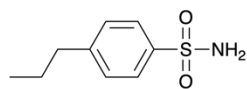
L<sub>1</sub>: R = H, R<sub>1</sub> =



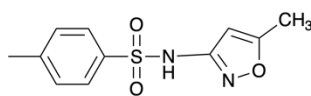
L<sub>2</sub>: R = H, R<sub>1</sub> =



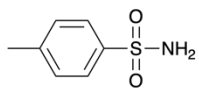
L<sub>3</sub>: R = H, R<sub>1</sub> =



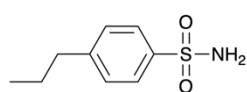
L<sub>4</sub>: R = H, R<sub>1</sub> =



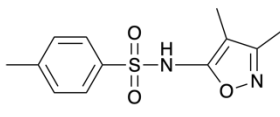
L<sub>5</sub>: R = CH<sub>3</sub>, R<sub>1</sub> =



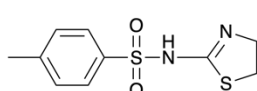
L<sub>6</sub>: R = CH<sub>3</sub>, R<sub>1</sub> =



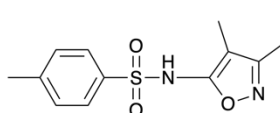
L<sub>1</sub>: R = H, R<sub>1</sub> =



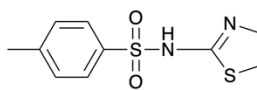
L<sub>2</sub>: R = H, R<sub>1</sub> =



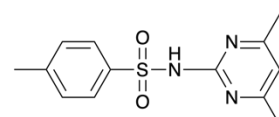
L<sub>3</sub>: R = CH<sub>3</sub>, R<sub>1</sub> =



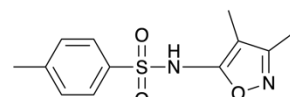
L<sub>4</sub>: R = CH<sub>3</sub>, R<sub>1</sub> =



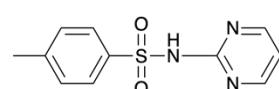
L<sub>1</sub>: X = NH, R =



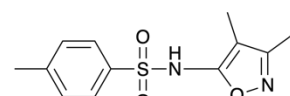
L<sub>2</sub>: X = NH, R =



L<sub>3</sub>: X = S, R =



L<sub>4</sub>: X = S, R =



L<sub>5</sub>: X = S, R =

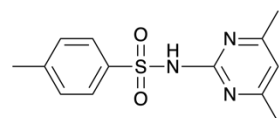


Fig. 25: Sulfonamide-based metal complexes assessed for antifungal activity.

Chohan and co-workers reported a series of sulfonamide derived from salicylaldehyde. The sulfonamide-derived Schiff bases coordinated to Co(II), Cu(II), Ni(II) and Zn(II) with octahedral geometries (**85a-l**, **86a-h** and **87a-l**, Fig. 26) and were tested for their antifungal activity.<sup>102,103,104</sup> Complexes **86a-h** and **87a-l**, substituted with bromo-/chloro- groups in the para-position relative to the phenyl hydroxyl group, had significant inhibitory effects on the growth of the six fungi tested (*M. longifusus*, *C. albicans*, *A. flavus*, *M. canis*, *F. solani* and *C. glabrata*) compared to their respective free ligands. The best inhibition results were achieved by complexes **86a-c** against *F. solani* (73-91%), **86f-h** and **87f/g** against *M. canis* (71-87%), **87c** against *C. glabrata* (85%) and **87l** against *T. longifucus* (76%).

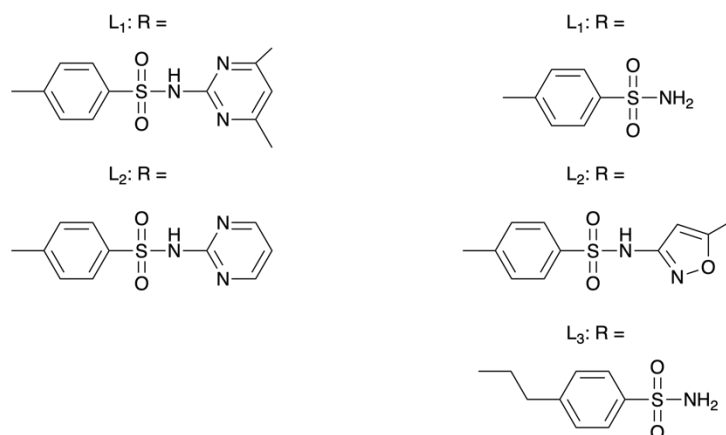
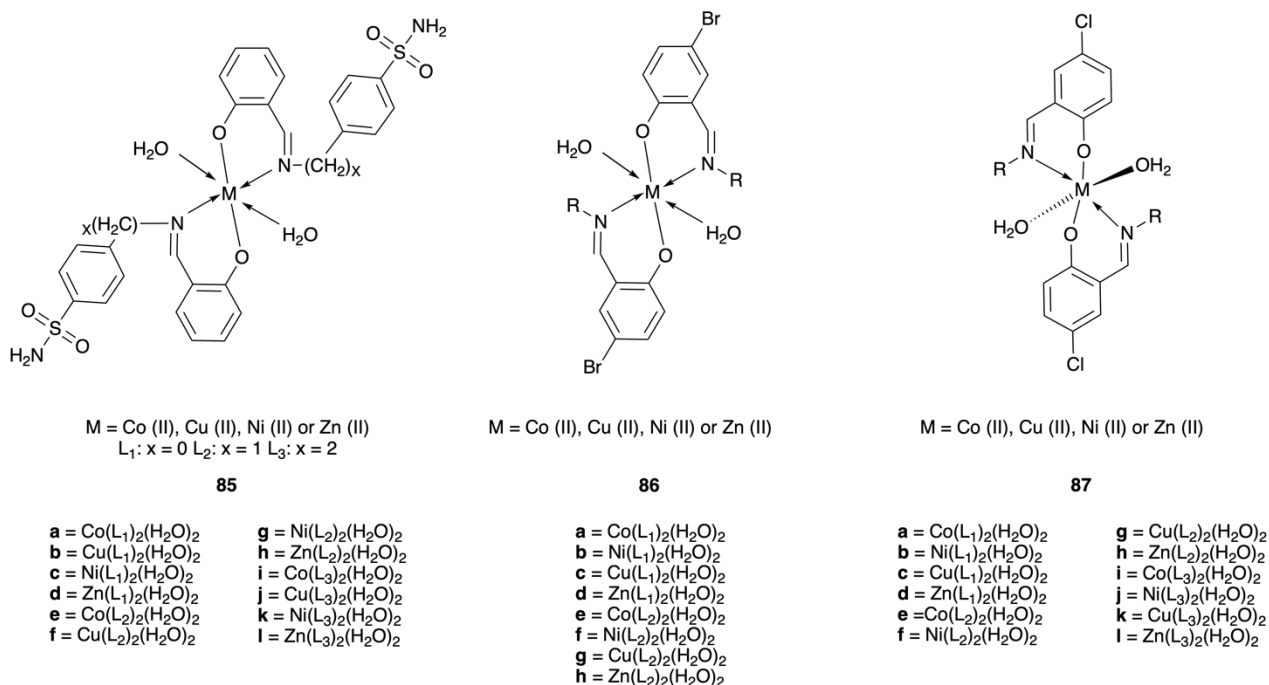


Fig. 26: Sulfonamide-based metal complexes assessed for antifungal activity.

Considering the biological and pharmacological activity of isatin-derived compounds, some isatin bearing sulfonamides and their metal complexes (Co(II), Cu(II), Ni(II) and Zn(II)) were also developed by Chohan and co-workers (**88a-x**, **89a-p**, Fig. 27 and **90a-l**, Fig. 28).<sup>105,106,107</sup> Their antifungal activities were assessed against six fungus strains (*M. longifusus*, *C. albicans*, *A. flavus*, *M. canis*, *F. solani* and *C. glabrata*) at 200  $\mu\text{g}\cdot\text{mL}^{-1}$ . Most complexes (**89a-p** and **90i-l**) significantly inhibited the growth of the various fungal strains by ~65 to 70%. Among those tested, the Zn(II) complexes were found to be the most active, while complexes **88a-x** only showed moderate activity (approximately 30% inhibition). The furanyl-/thienyl-analogues, **90a-h**, exhibited reduced fungicidal activities than the isatin-derivatives **90i-l**. Growth inhibition of uncoordinated ligands was enhanced upon metal complexation and was rationalized on the basis of the Overtone's concept and increased liposolubility due to electron delocalization resulting from metal ion coordination. According to the Overtone's concept of cell permeability, the lipid membrane that surrounds the cell favours the passage of lipid-soluble materials, making liposolubility an important factor that influences drug uptake and activity.<sup>108</sup> Chelation considerably reduces the polarity of the metal ion due to partial sharing of its positive charge with the donor groups and possible  $\pi$ -electron delocalization over the whole chelate ring. This process of chelation could enhance the lipophilic nature of central metal atom, subsequently favouring its permeation through the lipid layers of the cell membrane. It has also been observed that the introduction of azomethine linkages can be helpful in increasing biological activity by similar rationale.<sup>109</sup>

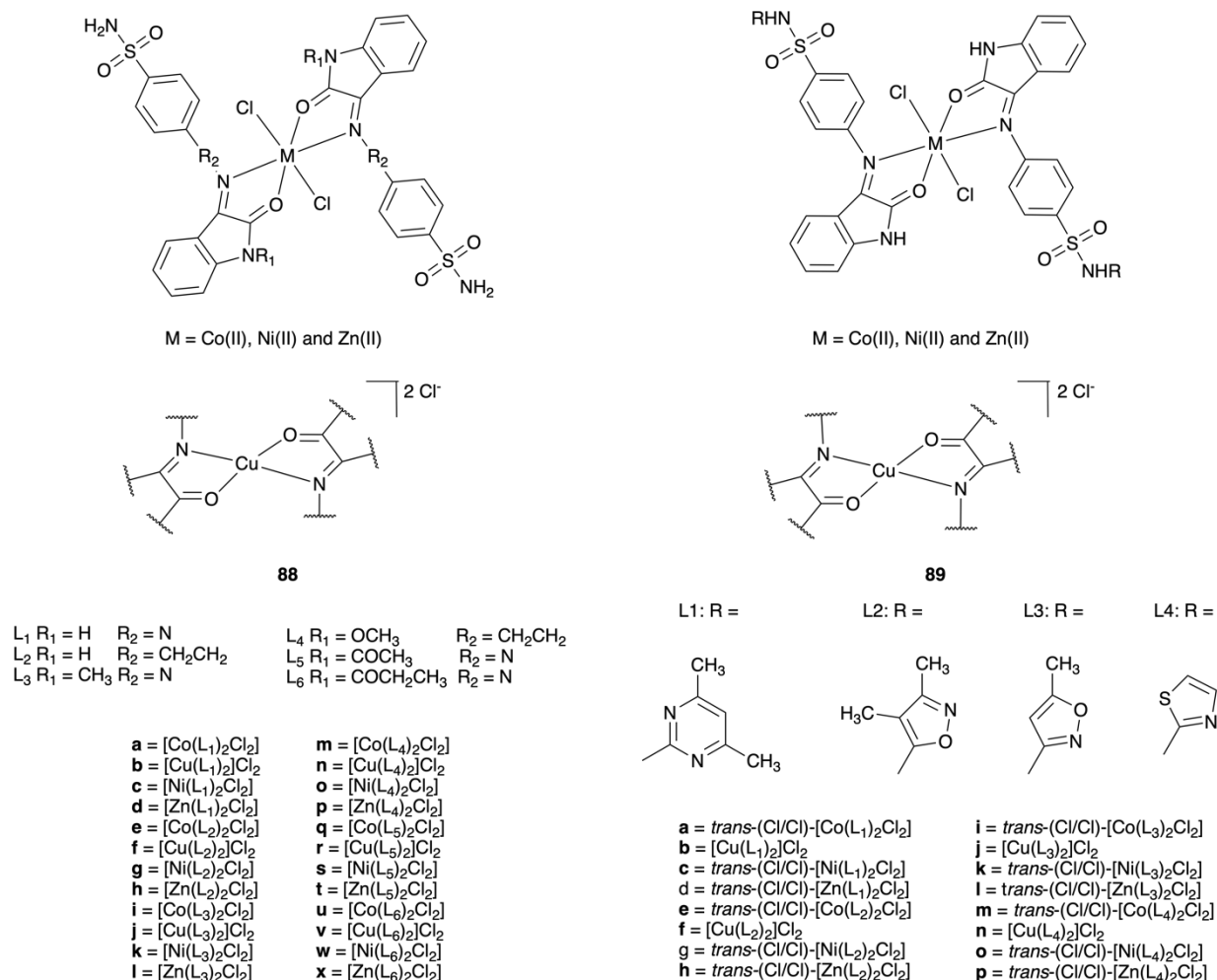
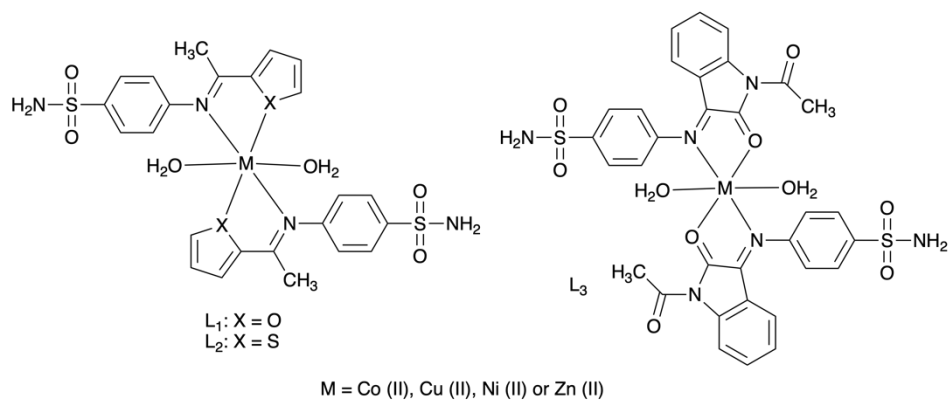
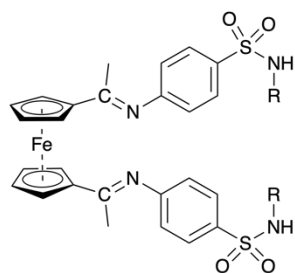
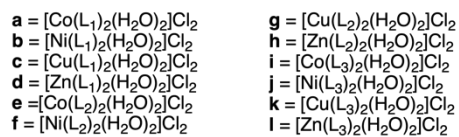


Fig. 27: Sulfonamide-based metal complexes assessed for antifungal activity.

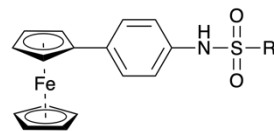
In 2009, Chohan investigated the antifungal activities of ferrocenyl sulfonamide derivatives against the same six fungal strains at 200  $\mu\text{g}\cdot\text{mL}^{-1}$  by disk diffusion (**91a-d**, Fig. 28). All tested complexes displayed significant inhibition of the growth of the tested fungi (22-27 mm), except *C. albicans* (~17 mm), when compared to MCZ and AmB (~30 mm). However, the organometallic complexes also exhibited potent cytotoxicities, as shown by brine shrimp bioassays.<sup>110</sup> In 2013, Yavuz *et al.* evaluated the antifungal activities of ferrocene derivatives containing sulfonamide groups (**92a-d**, Fig. 28) against *S. cerevisiae* and *C. albicans* strains.<sup>111</sup> Complexes **92c-d** with more alkyl chains exhibited a greater inhibitory effect (MICs ranging from 8.25 to 16.5  $\mu\text{g}\cdot\text{mL}^{-1}$ ) than **92a-b** (8.25-66  $\mu\text{g}\cdot\text{mL}^{-1}$ ) on the tested fungal strains, of particular note was compound **92d** which was as active as the positive control, KTZ.



90

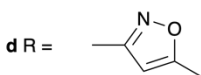
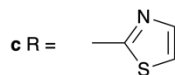
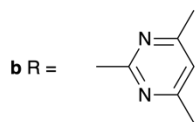


91

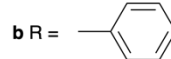


92

**a** R = H



**a** R = -CH<sub>3</sub>



**c** R = -C<sub>2</sub>H<sub>5</sub>

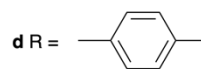
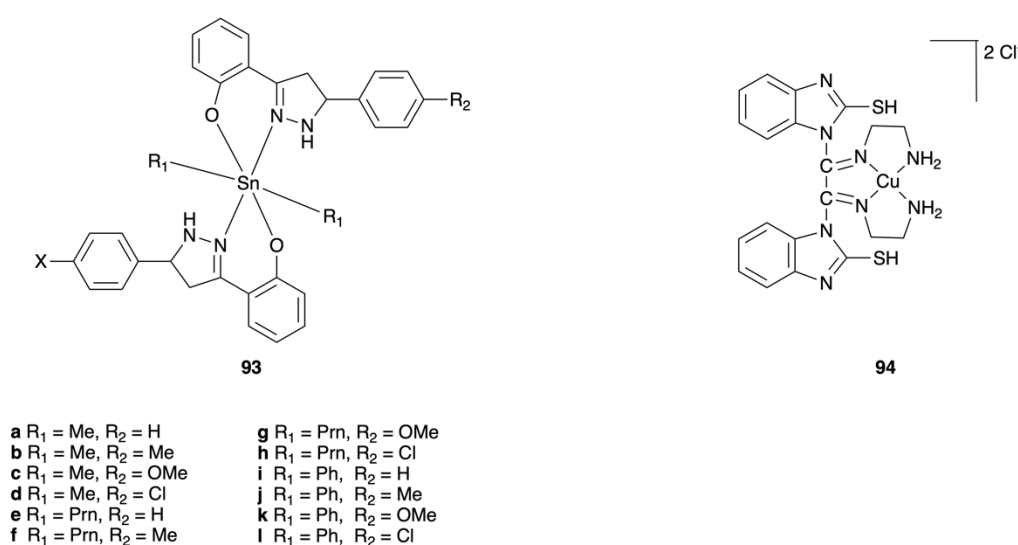


Fig. 28: Sulfonamide-based metal complexes assessed for antifungal activity.

## 6. Heterocycles-based Metal Complexes

Heterocyclic compounds contain at least one non-carbon atom in a ring and there has been considerable interest in the pharmacological applications of heterocycle-based metal complexes. In 2006, Tripathi *et al.* reported a set of diorganotin(IV) dipyrazolates (**93a-l**, Fig. 29) by reaction of diorganotin(IV) dichloride with sodium salts of pyrazolines. The bidentate pyrazoline ligands coordinated to Sn(IV) in distorted *trans*-octahedral geometries. Among the tested complexes, complex **93i** displayed greater inhibitory effect against *A. niger* compared to the free pyrazoline ligand and positive control, TRB.<sup>112</sup>



**Fig. 29:** Metal complexes based on heterocycles assessed for antifungal activity.

A square planar Cu(II) complex with a benzimidazole derivative (**94**, Fig. 29) was synthesised by Arjmand and co-workers in 2005. Hyperchromicity and decreased viscosity in the presence of DNA suggested that the complex interacted with the biomolecule through only partial intercalation. A cyclic voltammogram of the same complex in the absence of CT-DNA showed a quasi-reversible redox wave for a one-electron transfer process, corresponding to the Cu(I/II) couple. The ratio of the anodic and cathodic peak currents  $I_{pa}/I_{pc}$  was 1.33, confirming the quasi-reversible redox process. After addition of DNA to the metal complex solution, the  $I_{pa}/I_{pc}$  ratio for the bound complex decreased to 0.67. The decrease in the current was attributed to the diffusion of an equilibrium mixture of free and DNA-bound metal complex to the electrode surface. The ratio of equilibrium constants could be predicted by the shift in the  $E_{1/2}$  of Cu(I/II) couple following the equation:

$E_b - E_f = 0.0591 \log (K_{1+}/K_{2+})$  (**Fig. 30**), where  $E_b$  and  $E_f$  are the formal potentials of bound and free forms, respectively. The possible mechanism is:<sup>113</sup>

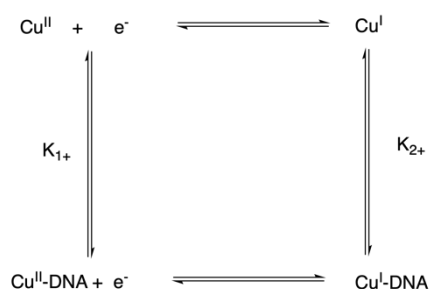


**Fig. 30:** Binding equilibrium of the Cu(I/II) couple with CT-DNA.

The ratio of binding constants ( $K_{1+}/K_{2+}$ ) for DNA binding of the Cu(I/II) couple was close to 1 (0.9), indicating that both Cu(II) and Cu(I) forms interacted with CT-DNA to a similar extent. The Cu(II) complex (**94**) was more active than its precursor ligand and the bis(ethylenediamine) Cu(II) complex against *A. niger*.<sup>114</sup>

In 2018, Mansour synthesised three photo-induced CO-releasing pyridylbenzimidazole-based Ru(II) carbonyl complexes, which were functionalized with alkylated sulfonate, phthalimide or morpholine moieties (**95a-c**, **Fig. 31**). The protein affinities of these compounds with hen egg-white lysozyme (HEWL) were evaluated using electrospray ionization mass spectrometry (ESI-MS). While the protein adducts were stable in the dark, CO release was detected upon illumination at 365 nm. Compound **95b** showed significant antifungal activity against the fungi *C. albicans* and *C. neoformans* with similar MIC values of  $16 \mu\text{g}\cdot\text{mL}^{-1}$  (24 nM). Using the standard octanol-water partition coefficient method, the lipophilicity of compound **95b** ( $\log P_{7.4} = 0.8 \pm 0.06$ ) was found to be higher than **95a** ( $\log D_{7.4} = -0.4 \pm 0.06$ ) and **95c** ( $\log P_{7.4} = 0.3 \pm 0.03$ ). The hydrophobic nature of **95b** enhanced its cellular uptake, therefore increasing its antifungal activity. The cytotoxicity of compound **95b** was assessed on noncancerous human embryonic kidney cells (HEK293) and recorded moderate cell viability of 62% at  $32 \mu\text{g}\cdot\text{mL}^{-1}$ . Additionally, compound **95b** showed good blood compatibility with 10 and 50% haemolysis concentration ( $\text{HC}_{10}$  or  $\text{HC}_{50}$ ) values greater than  $32 \mu\text{g}\cdot\text{mL}^{-1}$ , making compound **95b** the most promising fungicide of this series for further investigations.<sup>115</sup>



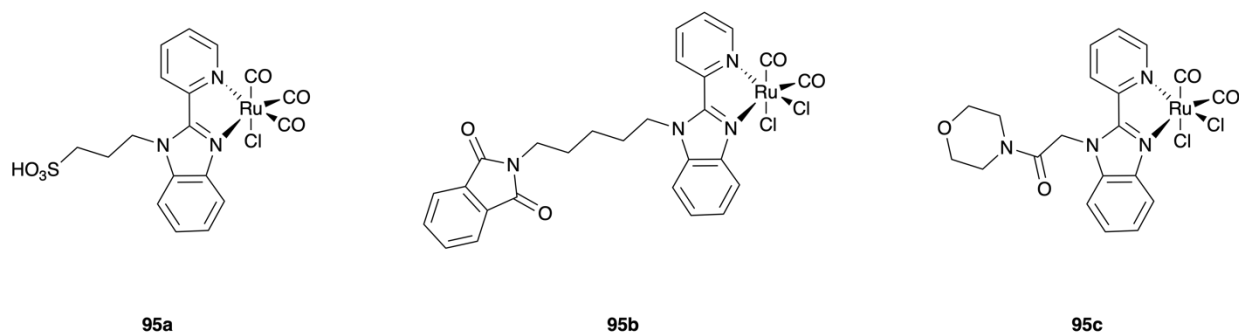


**Fig. 31:** Heterocyclic metal complexes assessed for antifungal activity.

In 2019, Cu(II), Ni(II) and Co(III) complexes with isatin-based ligand and dibenzoylmethane were prepared by Ahmad and co-workers (**96a-c**, **Fig. 32**). The antifungal activities of these complexes were evaluated alone or in combination with FCZ against seven different FCZ-susceptible and FCZ-resistant *C. albicans* strains. The Ni(II) complex exhibited the highest activity when employed alone against FCZ-resistant strains (MIC values ranged from 4 to 8  $\mu\text{g}\cdot\text{mL}^{-1}$ ) and at least two-fold more potent than FCZ against the same organism (8-16  $\mu\text{g}\cdot\text{mL}^{-1}$ ). Moreover, the Ni(II) complex significant antifungal activity against the seven fungal pathogens with MFC values ranging from 8 to 16  $\mu\text{g}\cdot\text{mL}^{-1}$ . Although the Cu(II) complex showed the lowest activity alone, it exhibited impressive synergistic inhibitory effects together with FCZ against 5 out of 7 strains. The mechanism of these complexes was investigated by terminal deoxynucleotidyl transferase dUTP nick end labelling (TUNEL) assay and it was shown that the Ni(II) complex induced apoptosis in *C. albicans*.<sup>116</sup>

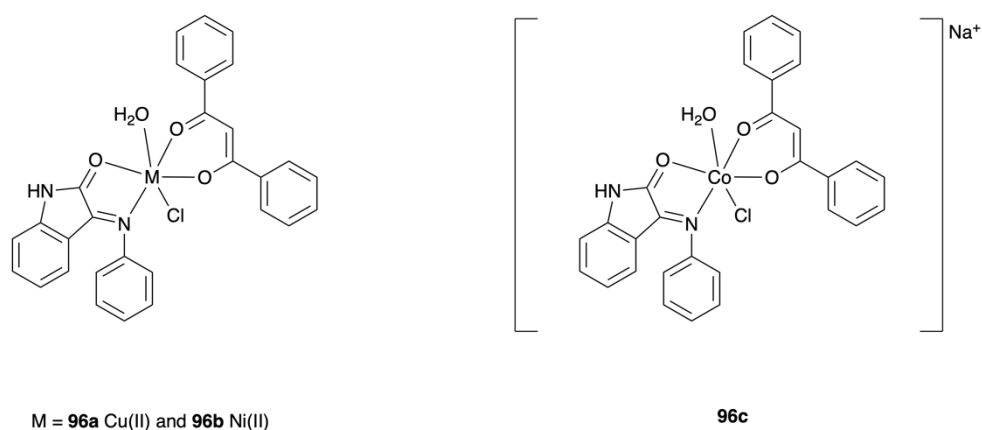


**Fig. 32:** Heterocyclic metal complexes assessed for antifungal activity.

*N,N'*-bis(ferrocenylmethyl)imidazolium salts (**97a-c**, **Fig. 33**) with Cl<sup>-</sup>, Br<sup>-</sup> and BF<sub>4</sub><sup>-</sup> anions were prepared by Demirhan and co-workers. Due to the presence of the ferrocenyl core, the electrochemical properties of these complexes could be studied by cyclic voltammetry. The half wave potentials (E<sub>1/2</sub>) of imidazolium salts **97a-c** were shifted to more positive potentials compared to unsubstituted ferrocene and were influenced by the presence of different counter-ions. The fungal growth inhibition of complexes **97a-c** were screened against *C. albicans* and recorded MIC values ranged from 312 to 416 μg·mL<sup>-1</sup>; significantly less active than nystatin (MIC = 0.68 μg·mL<sup>-1</sup>).<sup>117</sup> Burmudžija *et al.* synthesised two similar series of ferrocenyl pyrazoline derivatives (**98a-l**, **99a-l**, **Fig. 33**) to evaluate the effects of stereochemistry and electronic environment on bioactivity. Complexes **98g**, **i**, **j** and **l** were found to be more efficient at inhibiting the growth of *C. albicans* (MIC = 0.625 mg·mL<sup>-1</sup>) than other tested complexes. Moreover, the interactions between compounds **98g/l** and **99a/e** and DNA or bovine serum albumin (BSA) were determined due to these complexes possessing significant antimicrobial activities. With increasing concentration of the complexes, displacement of ethidium bromide (EB) from EB-DNA (which shows intense fluorescence light due to its strong intercalation between DNA base pairs) was observed through fluorescence quenching. It was therefore assumed that intercalation was the binding mode of these complexes with DNA. The affinities of the complexes with BSA were also investigated by fluorescence spectroscopic methods.<sup>118</sup>

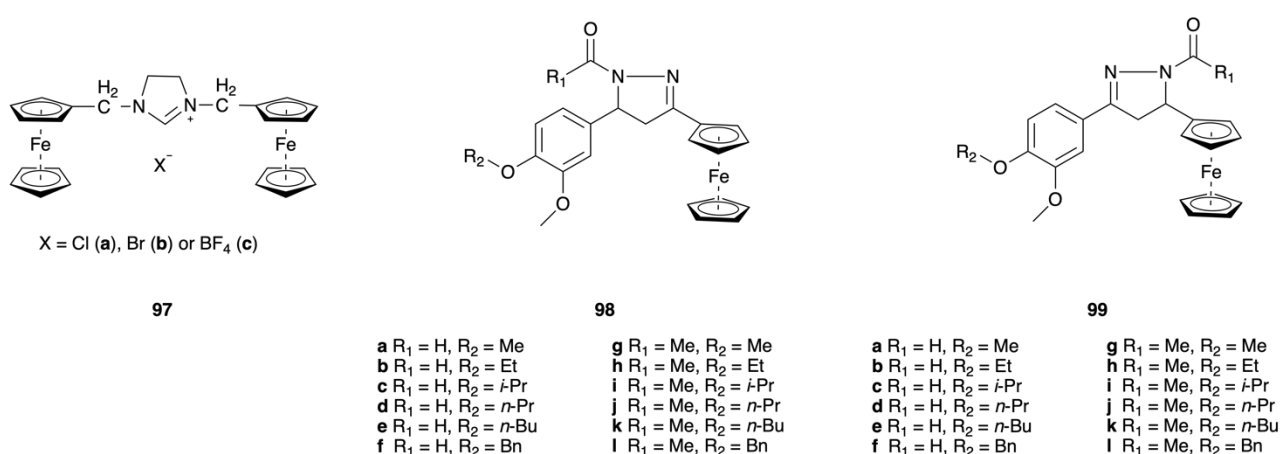


**Fig. 33:** Heterocyclic metal complexes assessed for antifungal activity.

In 2017, ferrocene-containing pyrazoline analogues, 5-ferrocenyl-3-substituted aryl-4,5-dihydro-1H-pyrazol-carbothioamides (**100a-f**, **Fig. 34**) and their cyclized products 2-(5-ferrocenyl-3-aryl-4,5-dihydro-1H-pyrazol-1-yl)-4-(4-substituted-aryl) (**101a-f**, **Fig. 34**) were prepared by Parveen *et al.* All complexes were screened *in vitro* against seven strains of fungi (*C. albicans*, *C. dubliniensis*, *C. glabrata*, *C. parapsilosis*, *C. tropicalis*, *C. kefyr* and *C. krusei*). FCZ was used as a reference drug and had a MIC values of 64  $\mu\text{g}\cdot\text{mL}^{-1}$  against all tested strains. Among all the metal-based compounds, complex **101f**, which contained a para-nitro group on the phenyl ring, showed comparable or higher antifungal activity than FCZ against *C. glabrata* (32  $\mu\text{g}\cdot\text{mL}^{-1}$ ), *C. parapsilosis* (32  $\mu\text{g}\cdot\text{mL}^{-1}$ ) and *C. tropicalis* (16  $\mu\text{g}\cdot\text{mL}^{-1}$ ).<sup>119</sup> In continuation of this study, a series of ferrocenyl pyrazoline complexes containing quinolone units (**102a-f**, **Fig. 34**) were synthesised by the same authors. The antifungal activities of these compounds were screened against the seven strains of fungi mentioned above. Interestingly, all compounds exhibited equivalent or higher antifungal activities than FCZ against the fungal organisms, with MIC values ranging from 8 to 64  $\mu\text{g}\cdot\text{mL}^{-1}$ . Compound **102d**, which contained a para-chloro group on the phenyl ring, showed the highest antifungal activity with MIC values of 8  $\mu\text{g}\cdot\text{mL}^{-1}$  against *C. dubliniensis* and *C. tropicalis*.<sup>120</sup>

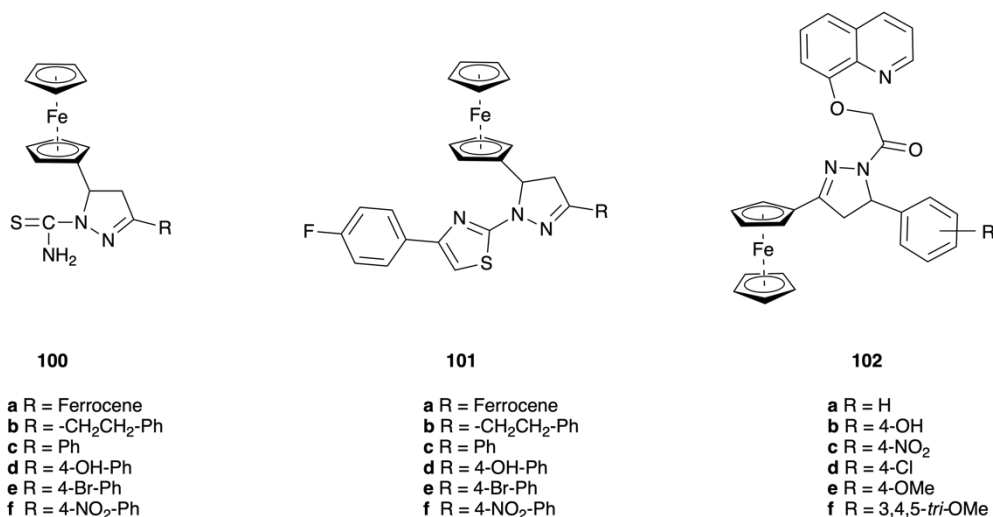


**Fig. 34:** Heterocyclic metal complexes assessed for antifungal activity.

In 2018, Damljanović and co-workers synthesised a class of ferrocenyl pyrazolidinone derivatives derived from acryloylferrocene and *N,N'*-cyclic azomethine imines. The mixture of two diastereoisomers (*trans* and

*cis*-5-arylethrahydropyrazolo [1,2- $\alpha$ ]pyrazol-1(5*H*)-ones were separated and isolated as pure substances (**103a-n** and **104a-n**, **Fig. 35**). All complexes were screened *in vitro* against bacteria or fungi. Contrary to many antimicrobial agents, which are often more sensitive to bacteria than fungi, the inverse was found to be true of the complexes reported in this article when tested against *C. albicans*, *A. brasiliensis*, *P. canescens*, and *F. oxysporum*. Compound **103c** was the most effective complex of this series (MIC <0.02 mM), compared to the reference drug KTZ (MIC = 0.0753 mM) against *C. albicans*. The antifungal activities of the ferrocenyl pyrazolidinone derivatives were found to be more significant than the *N,N'*-cyclic azomethine imine derivatives, but lower than those of acryloylferrocene. Overall, most of the ferrocenyl pyrazolidinone derivatives showed inhibitory effects at low concentrations.<sup>121</sup>

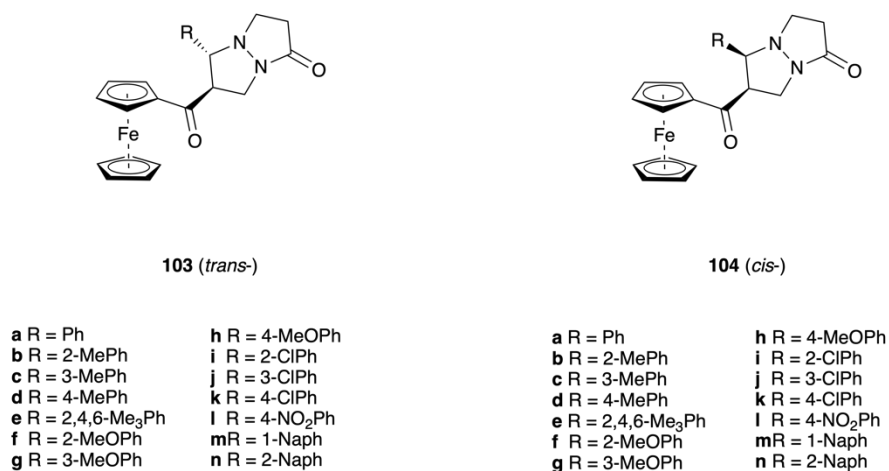


**Fig. 35:** Heterocyclic metal complexes assessed for antifungal activity.

The antifungal activities of a series of 5-arylidene-2-ferrocenyl-1,3-thiazolidin-4-ones (**105a-t**, **Fig. 36**) against *F. oxysporum*, *D. stemonitis*, *P. canescens* and *A. brasiliensis* were investigated by Pejović *et al.* These complexes had lower activities (MIC = 0.5 to 2 mg·mL<sup>-1</sup>) than the standard drug, KTZ (1.25-40 µg·mL<sup>-1</sup>).<sup>122</sup> Based on earlier observations that the ferrocene-substituted porphyrin RL-91 (**106a**, **Fig. 36**) had a considerable impact on *C. albicans* biofilm formation without photoactivation,<sup>123</sup> Lippert *et al.* further developed *trans*-ferrocenyl porphyrin (**106b**, **Fig. 36**) by replacing two ferrocenylphenyl moieties with methoxy methylene substituted *tert*-butylphenyl entities. The modified compound, **106b**, possessed higher lipophilicity and lower toxicity against human lung fibroblast cells (MRC5) than **106a**. In addition,

electrochemical studies showed that the ferrocenyl moieties of porphyrins **106a** and **106b** were more easily oxidized to ferricenium ions, compared to ferrocene alone. Compound **106b** also showed higher inhibition of *C. albicans* (ATCC10231) than **106a** by disk diffusion assay. The interaction of **106b** with DNA was investigated using *in silico* modelling which determined binding to the major DNA groove to be dominant.<sup>124</sup>

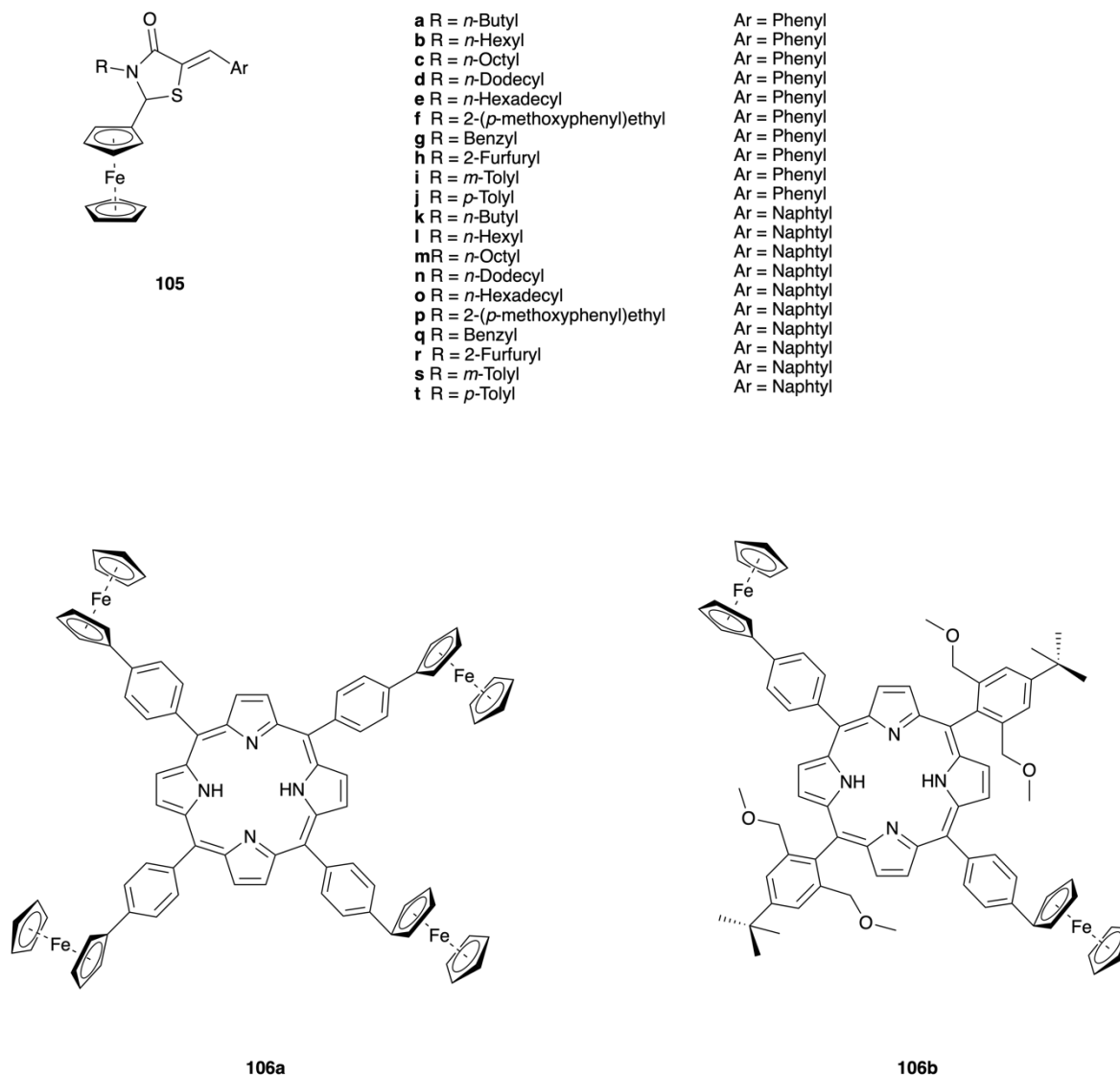


**Fig. 36:** Heterocyclic metal complexes assessed for antifungal activity.

## 7. $\beta$ -diketone/dithione-based metal complexes

In 2002, hexacoordinated binuclear Ru(III) complexes with the general formula  $\{[\text{RuX}_2(\text{EPh}_3)_2]_2(\text{bis-}\beta\text{-dk})\}$  (X = Cl or Br; *bis- $\beta$ -dk* = thiobis( $\beta$ -diketone)) (**107**, **Fig. 37**) were prepared by Natarajan and co-workers. The antifungal activities of these complexes were screened *in vitro* against *A. flavus*, *F. oxysporium* and

*Rhizoctonia solani*. Under identical experimental conditions, the ruthenium complexes displayed two-fold greater activities than the parent ligands, but were still less effective than the standard drug, Bavistin.<sup>125</sup> In 2009, Jayabalakrishnan and co-workers prepared a series of binuclear Ru(II) complexes containing *bis*- $\beta$ -diketones (**108**, Fig. 37). The binuclear Ru(II) complexes showed two to three-fold higher activities against *C. albicans* and *A. niger* than the free ligands or metal salts alone. The improved antifungal activities on the metal complexes were attributed to increased lipophilicity and improved penetration of the cellular membrane by the compounds.<sup>126</sup> In 2006, Chohan and co-workers investigated the antifungal activities of ferrocene derivatives incorporating dithiothione or dithioketone moieties (**109**, Fig. 37) against *M. longifusus*, *C. albicans*, *A. flavus*, *M. canis*, *F. solani* and *C. glabrata*. The ferrocene derivatives exhibited excellent inhibitory effects with inhibition zone ranging from 24 mm to 32 mm against all tested fungal species. The values were similar or greater than standard drugs, MCZ and AmB, which had inhibition zones of 20-30 mm.<sup>127</sup>

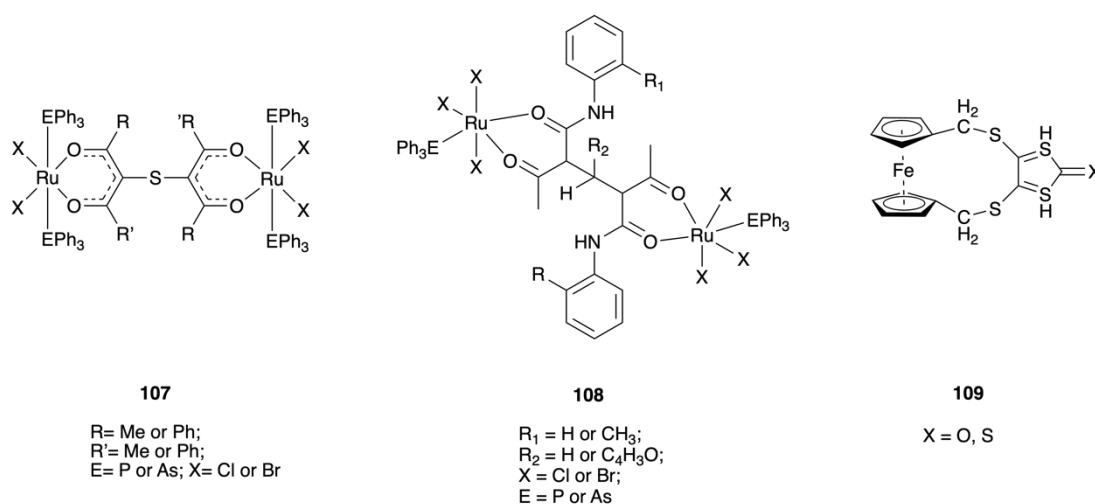


**Fig. 37:** Metal complexes based on  $\beta$ -diketone/dithione were assessed for antifungal activity.

In 2020, Dkhar *et al.* evaluated the antifungal activities of six cationic [Ru(II)(Cp/Ind)( $\kappa^2$ (SS)L)(PPh<sub>3</sub>)]PF<sub>6</sub> complexes (**110a-f**, Fig. 38) against *C. albicans*.<sup>128</sup> The results showed that all the tested complexes (except **110a**) displayed significant inhibition against fungal cells, while the ligand and metal precursors did not. Among all compounds, the morpholine-substituted complexes, **110b** and **110e**, showed greater inhibitory zones than FCZ ( $\geq 20$  mm vs. 18mm for FCZ). In 2021, McGowan and co-workers screened a set of Ru(II) bis(bipy) ferrocenyl  $\beta$ -diketone complexes (**111a-o**, Fig. 38) against *C. albicans* and *C. neoformans*.<sup>129</sup> The

results showed that all the tested complexes (except **111a**) had >100% inhibition against *C. neoformans* at a concentration of 32  $\mu\text{g}\cdot\text{mL}^{-1}$ . However, compounds **111b-c**, **111f-h** and **111k-o** displayed reduced efficacies against *C. albicans* with inhibitory zones ranging from 89.90% (**111h**) to 100.44% (**111n**). A lack of aromatic substituents on the ferrocenyl  $\beta$ -diketone ligands for complexes **111a**, **111d**, and **111e** were thought to be responsible for their inactivity against *C. albicans*. Compound **111e** was found to be 2-fold more selective towards *C. neoformans* over human blood cells making it one of the most promising complexes studies. No positive controls were reported.

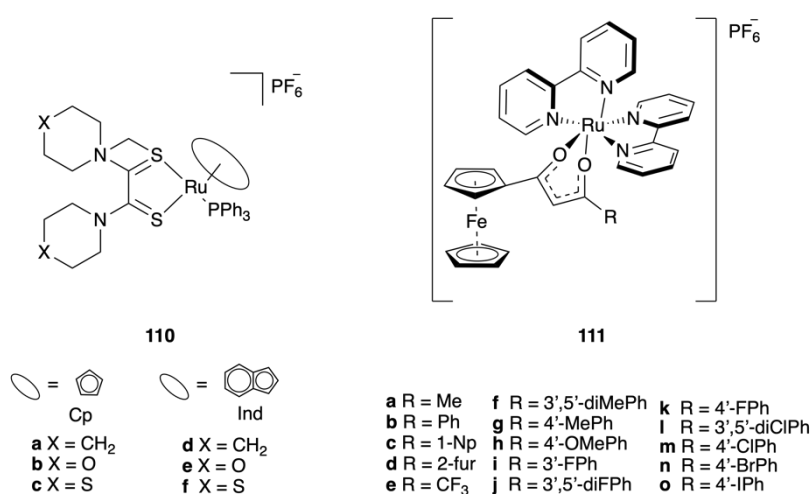


**Fig. 38:** Metal complexes based on  $\beta$ -diketone/dithione were assessed for antifungal activity.

## 8. Guanidine-based metal complexes

Gul *et al.* investigated the antifungal activity of ferrocenyl guanidines (**112a-h**, **Fig. 39**) against three fungal strains, namely *F. moniliforme*, *A. fumigatus* and *A. flavus*. The interactions of these ferrocenyl guanidine compounds with DNA were determined to be predominantly electrostatic modes by cyclic voltammetry and UV-visible studies. Among the tested compounds, complexes **112a-c**, which contained electron-withdrawing substituents, possessed inhibitory properties comparable to or greater than the reference drug, TRB (65-96% vs. 92%). However, complexes **112d-h** – containing electron-donating substituents – displayed less activity with only 13 to 47% inhibition of fungal growth. Of note, the tested compounds displayed significant stability as they did not decompose for up to seven day in ethanol or DMSO.<sup>130</sup> In 2018, Sadler and co-workers synthesised a series of 16- and 18-electron organo Ir(III) complexes containing derivatives of widely used

biguanides as chelating ligands. The resulting complexes had general formulae  $[(\eta^5\text{-Cp}^x)\text{Ir}(\text{Big})\text{X}]\text{Y}$ , where  $\text{Cp}^x = \text{Cp}^*$ ,  $\text{Cp}^{\text{XPh}}$  or  $\text{Cp}^{\text{Xbiph}}$ , Big = biguanide or sulfonyl-substituted biguanide ligands, X and Y = Cl, Br, or I (**113a-n**, **Fig. 39**). Evaluation of the antifungal activities of the series of complexes against *C. albicans* and *C. neoformans* showed that complexes **113d-i** possessed excellent efficacies with MICs ranging from 0.25 to 1  $\mu\text{g}\cdot\text{mL}^{-1}$  (0.34-1.45  $\mu\text{M}$ ), approximately 76-fold more effective against *C. neoformans* than the standard drug, FCZ (26.1  $\mu\text{M}$ ). Conversely, the biguanide ligands alone showed no activity against the fungi tested. Complexes **113d-i** exhibited good selectivity towards microorganisms over mammalian cells with low cytotoxicities towards human embryonic kidney cells with half maximal cytotoxic concentrations ( $\text{CC}_{50} = 17$  to  $>32 \mu\text{g}\cdot\text{mL}^{-1}$  (19 to 47  $\mu\text{M}$ )) and low haemolytic activities ( $\text{HC}_{50}$ , 6-21  $\mu\text{g}\cdot\text{mL}^{-1}$  (8-28  $\mu\text{M}$ )) against human red blood cells. The hydrophobicities of these compounds were investigated via reverse phase-HPLC and comparison of retention times. The fact that the least hydrophobic complexes **113a** and **113b** were inactive with MICs greater than 32  $\mu\text{g}\cdot\text{mL}^{-1}$  indicated that the activities were related to the hydrophobicity-dependent uptake of the complexes into the cell membranes. To investigate the potential target sites of these active compounds, their interactions with nucleobases and amino acids were also studied. No indication of binding to DNA nucleobase models (9-ethylguanine and guanosine 5'-monophosphate disodium hydrate) or the amino acids tryptophan, leucine, *N*-acetyl-L-methionine, L-histidine and L-cysteine (L-Cys) were found. However, using NMR spectroscopic methods and liquid chromatography-mass spectrometry (LC-MS), the authors discovered that displacement of the biguanide ligand rapidly led to the formation of the dinuclear dimer,  $[(\text{Cp}^{\text{Xbiph}})\text{Ir}(\text{L-Cys})]_2^{2+}$ . The mechanism of action was postulated to be due to the intracellular release of active biguanides from the organometallic complexes. These biguanides then bound to endogenous metal ions, thus inhibiting the biosynthesis of proteins and important cofactors. Conversely, the biguanide ligands themselves were inactive when screened to the microorganisms.<sup>131</sup>



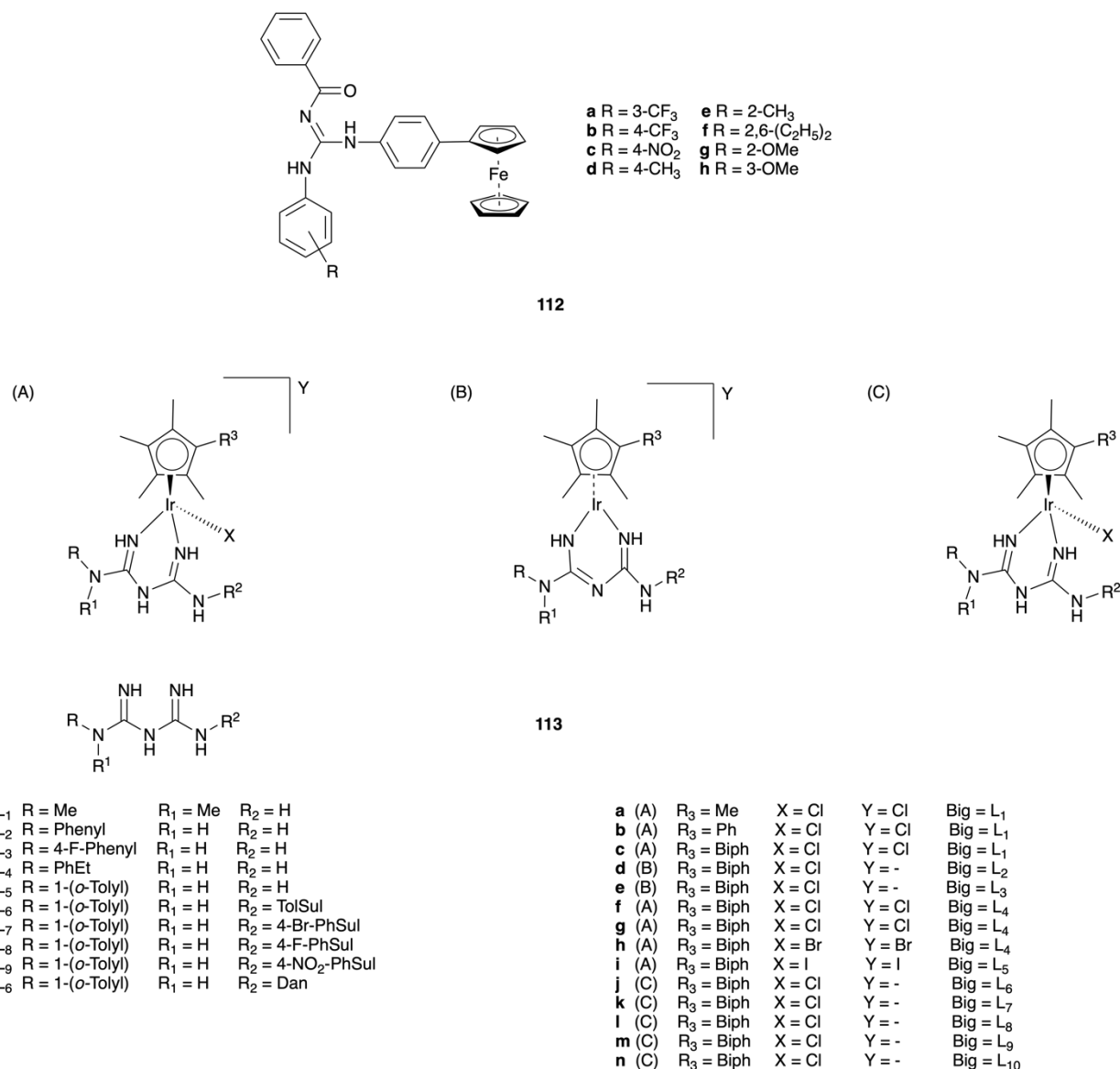
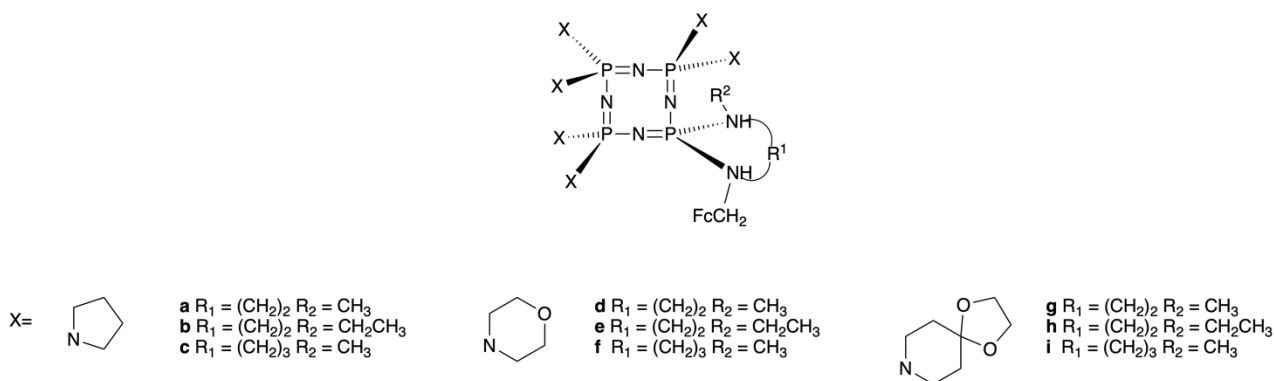


Fig. 39: Metal complexes based on guanidine assessed for antifungal activity.

## 9. Cyclotetraphosphazene-based metal complexes

Kilic and co-workers evaluated the antifungal activities of fully substituted monoferrocenyl-spirocyclotetraphosphazenes with pyrrolidine, morpholine and 1,4-dioxo-8-azaspiro[4,5]decane (DASD) (**114a-i**, Fig. 40) against three yeast strains (*C. albicans*, *C. krusei* and *C. tropicalis*). Six out of nine compounds were found to be more active against *C. albicans* than the standard drug, KTZ. In addition, compounds **114c** and **114f** (MFC  $\leq 19.5 \mu\text{M}$ ) were 7-fold more active than KTZ against *C. krusei* and *C. tropicalis* (MFC  $\geq 153 \mu\text{M}$ ).<sup>132</sup> Based on these promising results, bis-ferrocenyl pendant-armed dispirocyclotetraphosphazenes (**115a-l**, Fig. 40) were also synthesised by the same group. Among all tested compounds, **115l** was found to

be the most active agent MFC of 15.63  $\mu\text{M}$  against *C. albicans*, much higher than KTZ (MFC = 312.5  $\mu\text{M}$ ).<sup>133</sup> However, when compared to the antifungal activities of bis-ferrocenyl- and mono-ferrocenyl-cyclotetraphosphazenes with the same substituents, bis-ferrocenyl-cyclotetraphosphazenes were less effective than the mono-substituted compounds. The DNA interactions of these compounds were studied using agarose gel electrophoresis. It was observed that bis-ferrocenyl phosphazene derivatives **115a**, **115c** and **115d** decreased DNA mobility, while the corresponding mono compounds, cleaved DNA to linear form III through different interaction with DNA. The cytotoxicities of these complexes were studied against L929 fibroblast and DLD-1 colon cancer cell lines. Most of the compounds were found to be less toxic than cisplatin and doxorubicin.



114

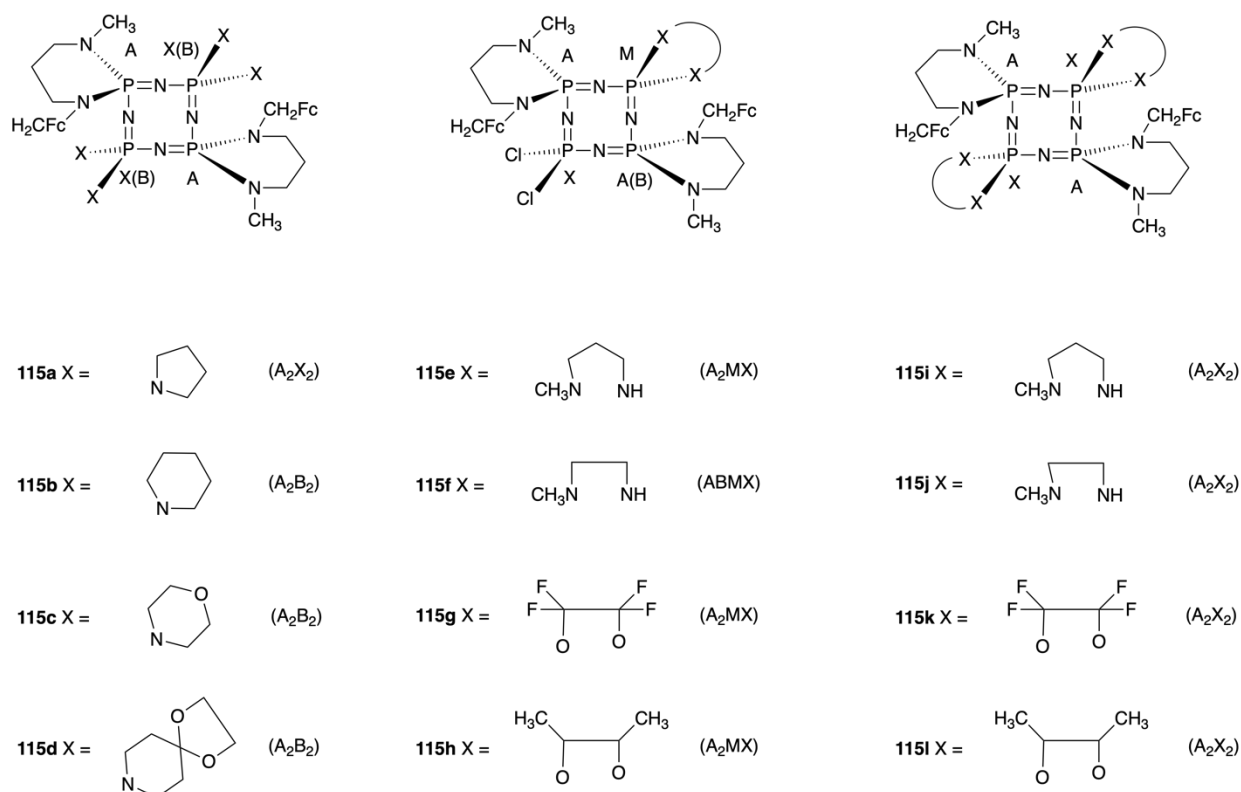
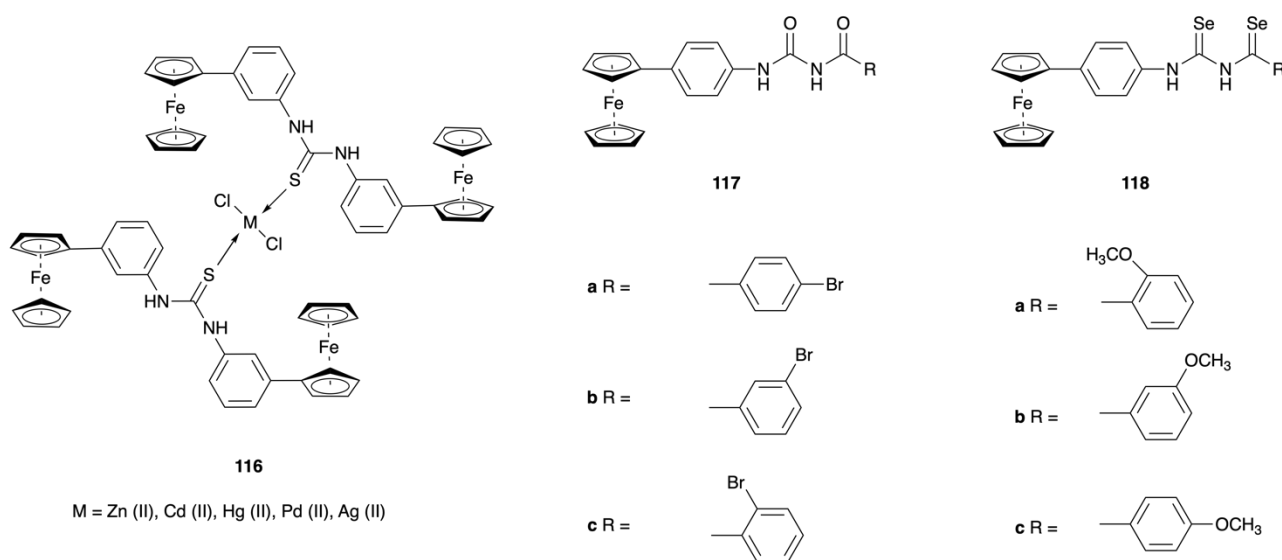


Fig. 40: Metal complexes based on cyclotetraphosphazene assessed for antifungal activity.

## 10. Urea-based Metal Complexes

In 2015, 1,1'-(4,4'-di-ferrocenyl)di-phenyl thiourea and their metal complexes (Zn(II), Cd(II), Hg(II), Pd(II) and Ag(I)) (116, Fig. 41) were prepared by Ali *et al.* These complexes showed moderate antifungal activities against *A. niger*. Possible DNA intercalation of the complexes was supported by cyclic voltammetry and viscosity measurements. In addition, the dose-dependent inhibition of these metal complexes on the activity of the enzyme, alkaline phosphatase, was also observed.<sup>134</sup> Asghar *et al.* synthesised three ferrocene-

containing urea ligands by the deprotection of ferrocene-based thioureas, using alkaline Hg(II) as a sulfur capturing agent (**117a-c**, **Fig. 41**). The DNA binding modes of these compounds were studied by UV-vis spectroscopy and cyclic voltammetry which indicated that an electrostatic mode of interaction between the positively charged **117** and the negatively charged DNA phosphate backbone was likely. The antifungal activities of these complexes were determined and compound **117c** was found to be the most active compared to the other analogues, with >70% inhibition against all the tested fungal strains (*F. moniliforme*, *A. fumigatus* and *A. flavus*). The enhanced activity might be due to a more pronounced inductive effect of the bromo group at the ortho position than at the meta and para positions.<sup>135</sup> Three ferrocene-containing selenourea ligands (**118a-c**, **Fig. 41**) displayed moderate activity (~50% inhibition) on *F. solani* and *Helmentosporium sativum* strains.<sup>136</sup>



**Fig. 41:** Metal complexes based on urea assessed for antifungal activity.

## 11. Miscellaneous

In 2004, Chohan and co-workers used bis-(1,1'-disubstituted ferrocenyl)thiocarbohydrazone and bis-(1,1'-disubstituted ferrocenyl)carbohydrazone as ligands to chelate Co(II), Ni(II), Zn(II), and Cu(II). The Co(II), Ni(II), and Zn(II) complexes had the general formula  $[M(L)Cl_2]$  and adopted distorted octahedral geometries, while the Cu(II) which formed a  $[Cu(L)]Cl_2$  complex with square-planar geometry (**119a-h**, **Fig. 42**). All compounds were tested against six fungal strains (*M. longifusus*, *C. albicans*, *A. flavus*, *M. canis*, *F. solani* and *C. glaberata*).

The metal complexes showed moderate antibacterial activities and significant antifungal activities compared to the ligands alone, but did not perform as well as the positive controls, imipenem, MCZ and Amb.<sup>137</sup> In 2006, Ramesh and co-workers reported a series of orthometallated Ru(II) complexes (**120a-e**, **Fig. 42**) derived from reaction of 2-(aryloxy)phenol ligands with the Ru(II) precursor, [RuH(Cl)(CO)(PPh<sub>3</sub>)<sub>3</sub>]. The crystal structures of **120a** and **120b** revealed a distorted octahedral environment around the ruthenium centre. *In vitro* studies against *C. albicans* and *A. niger* demonstrated that the metal complexes had higher activities than the respective free ligands, while RuCl<sub>3</sub>·3H<sub>2</sub>O and the Ru(II) carbonyl precursor complex displayed no antifungal effects under identical experimental conditions. *A. niger* displayed higher sensitivity to these metal complexes than *C. albicans*.<sup>138</sup> In 2014, Al-Noaimi *et al.* synthesised two heterotrimetallic Ru(II)-Pd(II)-Ru(II) complexes, with the general formula [Ru<sup>II</sup>Cl<sub>2</sub>(PPh<sub>3</sub>)<sub>2</sub>(triamine)]<sub>2</sub>[Pd<sup>II</sup>X<sub>2</sub>] (X = Cl, OAc) (**121a-b**, **Fig. 42**). Complexes **121a-b** showed significant antifungal activities against *A. niger*, *C. albicans* and *P. digitatum* with inhibition zones greater than 19 mm, and moderate activities against *F. oxysporum* (<16.2 mm). As positive control, nystatin displayed inhibition zones in the range of 20.8 to 33.7 mm against the tested fungi.<sup>139</sup> Yuan *et al.* evaluated the antifungal activities of Cu(II), Ru(II) and Pt(II) complexes with a tridentate *N,N,N*-coordinating anthracene-based tripodal ligand, 9-[(2,2'-dipicolylamino)methyl]anthracene (ADPA) (**122**, **Fig. 42**). This resulted in complexes with the formulae [Cu(ADPA)Cl<sub>2</sub>]·H<sub>2</sub>O, [Ru(ADPA)Cl<sub>2</sub>DMSO]·4CH<sub>3</sub>OH·H<sub>2</sub>O and [Pt(ADPA)Cl]PF<sub>6</sub>·DMSO·2CH<sub>3</sub>OH·H<sub>2</sub>O. The Pt(II) and Ru(II) complexes were two-fold more active than the free ligand against *C. albicans*.<sup>140</sup>

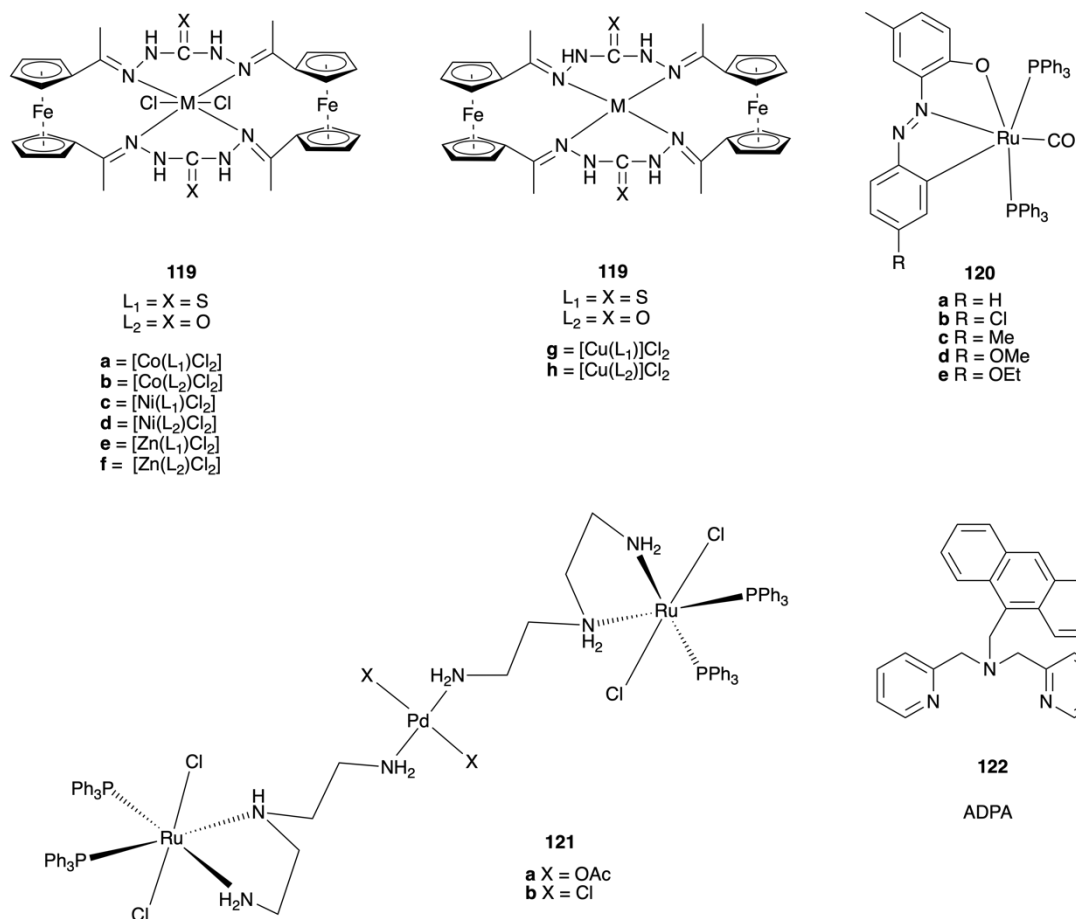


**Fig. 42:** Various metal complexes assessed for antifungal activity.

Recently, the antifungal activities of a series of transition metal complexes (Mn(II), Ni(II), Cu(II), Zn(II), Rh(III) and Cd(II)) with the tridentate ligand, N-(2-aminoethyl)-1,3-propanediamine (AEPD), (**123a-f**, **Fig. 43**) were evaluated against *C. albicans* by Khalaf-Alla. Among all tested compounds, the Cd(II) and Rh(III) complexes had excellent activities with inhibition zones of  $32.0 \pm 0.5$  mm and  $21.5 \pm 0.5$  mm, respectively, which were comparable or higher than the standard drug, nystatin ( $21 \pm 0.5$ mm).<sup>141</sup>

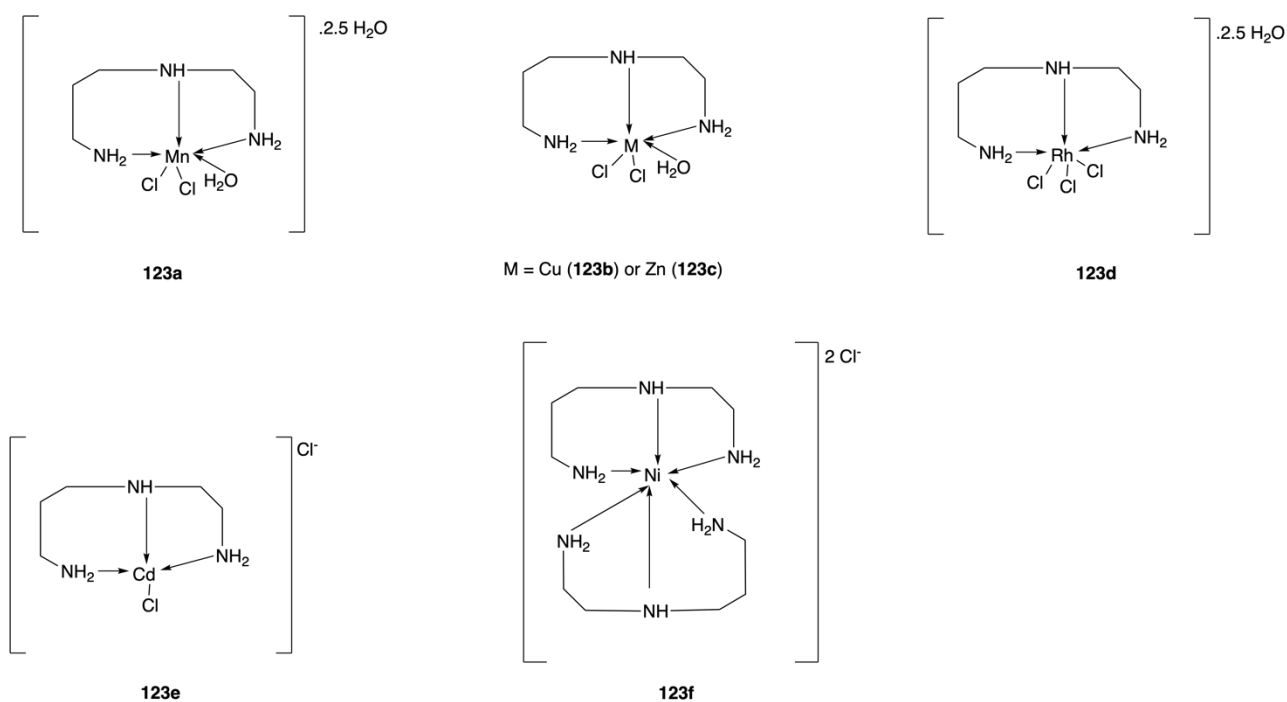


**Fig. 43:** Transition metal complexes derived from AEPD assessed for antifungal activity.

## 12. Schiff bases

Imines and azomethines, commonly known as Schiff bases after German-Italian chemist Hugo Schiff, are the product of aldehyde or ketone condensation with an amine. These species are naturally occurring, for example, in corrin which forms the core of vitamin B<sub>12</sub> and binds Co(II) as a cofactor. Schiff bases have been identified as versatile pharmacophores that possess antifungal, antibacterial, antiviral, anti-inflammatory, antiproliferative, and antiparasitic properties. The electrophilic carbon and nucleophilic nitrogen that form the backbone of Schiff bases facilitate reactions with many nucleophiles and electrophiles. Such reactivity allows interactions with important biological target sites, such as enzymes, proteins, and DNA. Schiff bases have been shown to be excellent ligands for a multitude of metal ions – from main groups to transition metals to the *f*-block, covering a wide range of complex geometries and oxidation states.

The antifungal properties of some Schiff bases and related compounds are well known, however, many compounds and their metal complexes lacking significant antifungal (or antibacterial, anticancer, etc.) activities have also been published. Several reports are devoted to the characterisation of complexes, and application seen as an afterthought. Often the discussion of any antifungal activity is justified by the idea that

the metal complex of a ligand would increase lipophilicity by delocalisation of the metal ion charge, thereby improving cellular uptake and fungicidal activity. While this may be true in some cases, it does not necessarily indicate a successful or effective antifungal agent has been developed. For example, a series of amino acids (glycine, alanine, phenylalanine, methionine, cysteine) were condensed with salicylaldehyde to form Schiff bases (**Fig. 44**), and complexed with Co(II), Cu(II), Ni(II), Zn(II) to form 25 compounds (including the free ligands).<sup>142</sup> The compounds were tested against six fungal strains (150 experiments) and ~77% displayed no antifungal activity while the remaining 23% achieved a maximum inhibitory effect of 35%, relative to positive controls, MCZ and AmB. Similar studies with lacklustre antifungal results are common in the literature, however, there are also positive examples of metal complexes resulting in significant fungicidal activities.

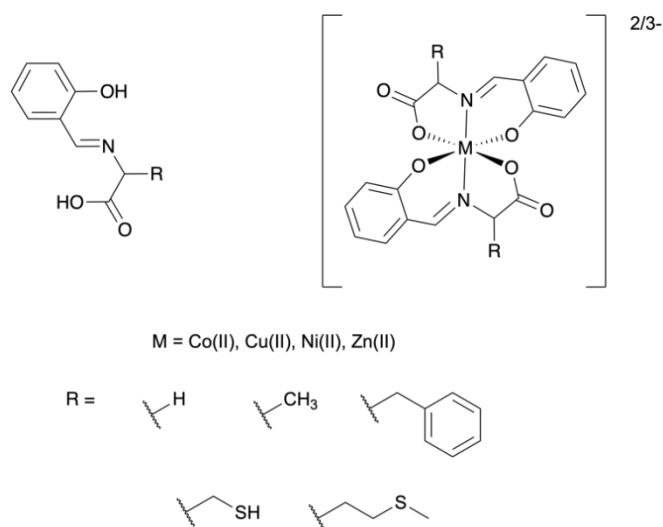


**Fig. 44:** Salicylaldehyde amino acid Schiff base ligands and coordination complexes formed by various first-row transition metals.

### 12.1. Triazole-based ligands

Over the course of nearly a decade, a range of triazole-based Schiff base ligands have been synthesised, characterised and complexed with metal ions, in-effect constituting an extensive Structure Activity Relationship (SAR) study. The triazole core has been appended with Schiff base groups such as salicylaldehyde (and substituted species thereof), heterocycles and various other motifs (**Fig. 45**). Metal complexes were formed with first row transition metal ions (including Fe(II), Co(II), Ni(II), Cu(II), Zn(II), V(IV)) and antifungal testing was carried out against a common range of fungal strains (*T. longifucus*, *C. albicans*, *A. flavus*, *M.*



*canis*, *F. Solani*, *C. glaberata*, *A. niger*, and *A. flavus*). In general, complexation of the triazole ligands with metal ions increased the bioactivities, however, in some instances complexation either abolished activity of active ligands or provided minimal improvement.<sup>143,144</sup>

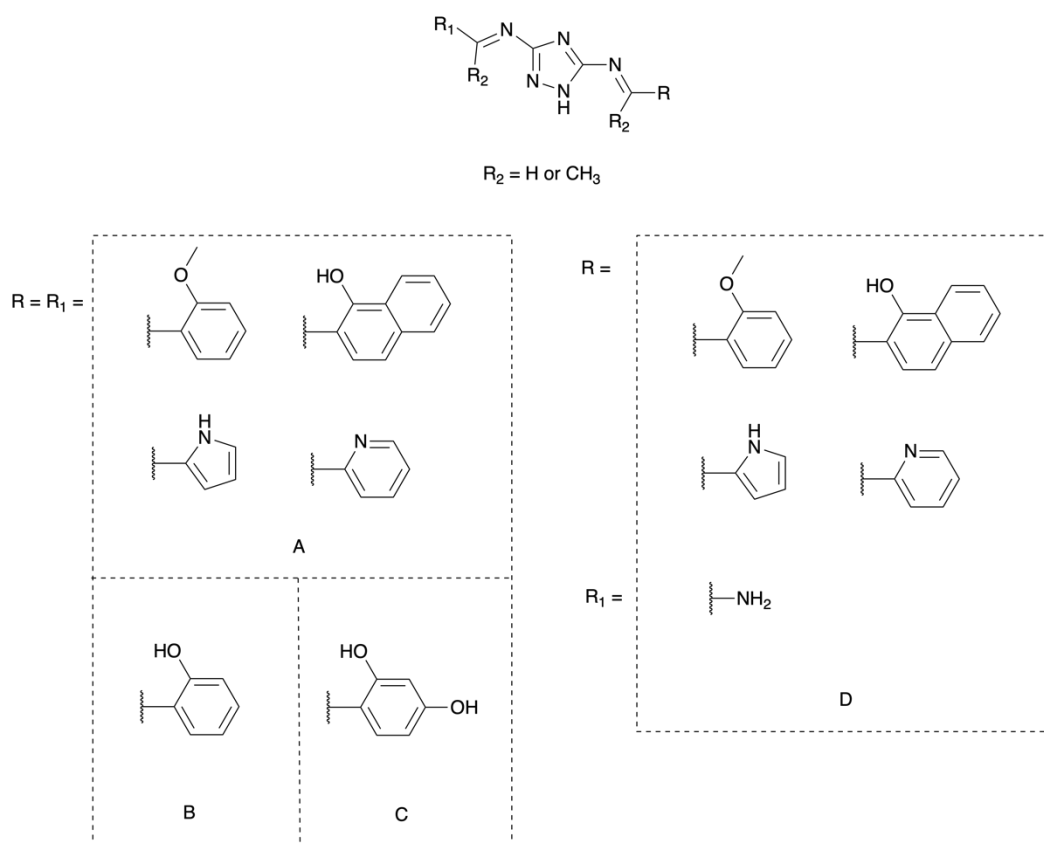


**Fig. 45:** Triazole-containing Schiff based ligands complexed with a range of first-row transition metals (not shown) and assessed for antifungal properties.

Of these investigations, a vast number of tested compounds yielded poor antifungal activities relative to positive controls but some promising insights can be gleaned from the studies as a whole. Comparison of antifungal experiments revealed that nitrogen-containing heterocycles (pyrrole or pyridine) and their derivatives had the most prominent activities. For example, Chohan *et al.* found that treatment with 200  $\mu\text{g}\cdot\text{mL}^{-1}$  solutions of triazole-pyrrole/pyridine oxovanadium complexes (**Fig. 46**) achieved up to 80% fungal growth inhibition against all tested organisms. Similarly, 75-80% inhibition was achieved against *M. canis*, *F. solani*, and *C. glabrata* for a methyl-pyridinyl compound.<sup>145,146</sup>

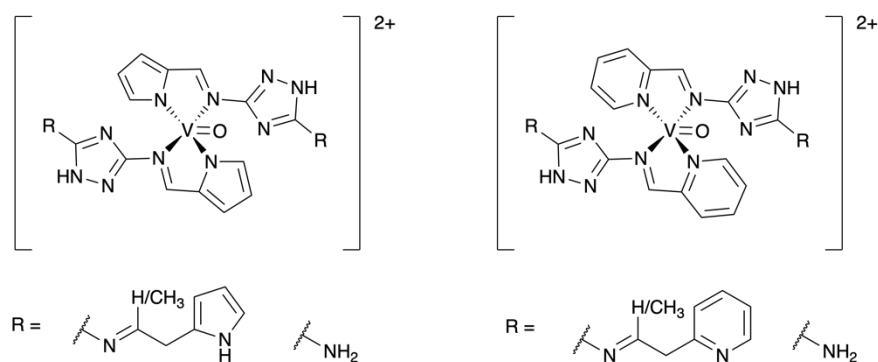


**Fig. 46:** Oxovanadyl complexes with triazole-pyridinyl and -pyrrole derivatised Schiff base ligands.

Conversely, Co(II), Ni(II), Cu(II) and Zn(II) complexes of triazole-furanyl ligands (**Fig. 47A**) barely reached 60% inhibition and had average inhibitory values of 44-49% across six fungal strains.<sup>147</sup> Chlorobenzyl derivatives (**Fig. 47B**) in complex with metal ions displayed poor activities against *A. niger* and *A. flavus*, achieving only 40-50% inhibition of both organisms relative to FCZ.<sup>144</sup>

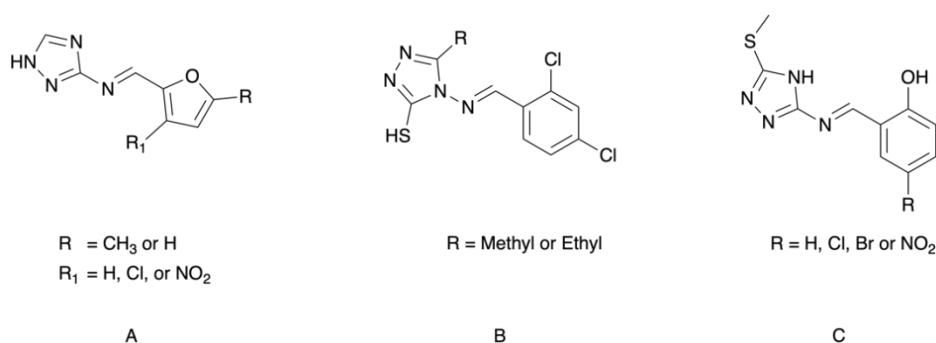


**Fig. 47:** Triazole-containing Schiff based ligands complexed with a range of metals (not shown) and assessed for antifungal activity.

Salicylaldehyde-triazole derivatives including *p*-bromo/chloro/nitro functionalities (**Fig. 47C**) were found to be effective against selected fungi (*C. glabrata*, *F. solani*, *A. niger*, *A. flavus*) and achieved ~70% inhibition.<sup>143,148,149</sup> However, in this instance, the free ligand displayed significant antifungal activity and complexation with the metal ions only increased the activity by 5 to 10%.

## 12.2 Pyrazoloyl-based

Pyrazolyl-Schiff bases formed between 3-methyl-1-phenyl-4-acetylpyrazolin-5-ol and 1,2-diaminobenzene or 2-aminophenol were reported in 2010.<sup>150</sup> Complexation with V(IV), Fe(III), Cu(II), and Co(II) ions yielded eight different complexes. The tridentate ligands coordinated as ONN or ONO donors via the pyrazolyl oxygen, azomethine nitrogen and phenol or amino O/N (**Fig. 48**). The compounds and free ligands were tested for antifungal efficacy against three species (*C. albicans*, *Rhizopus sp.*, and *A. niger*) through disk diffusion experiments at  $200 \mu\text{g}\cdot\text{mL}^{-1}$  with AmB as positive control. Interestingly, the free 2-aminophenol Schiff base displayed significant activity against *A. niger*, resulting in similar inhibition diameters to the positive control. Complexation of the ligand with Co(II) increased the antifungal properties against *Rhizopus* spp. where the complex approached the efficacy of AmB, and against both *A. niger* and *C. albicans* where inhibitory zone surpassed the positive control. Similarly, the Co(II) complexes with the diaminobenzene derived ligand displayed equivalent inhibitory effects against *A. niger*, and greater than 80% inhibition against *C. albicans*.

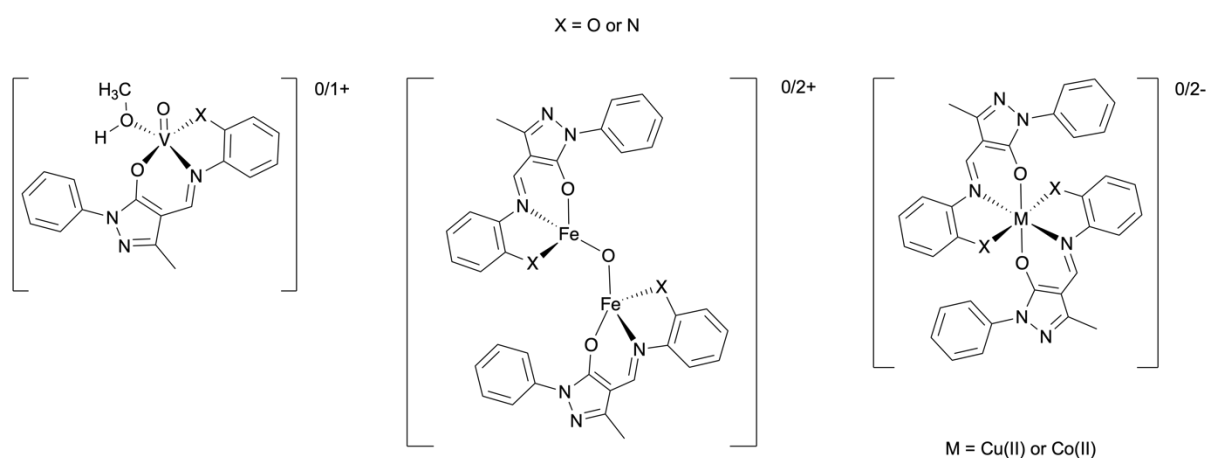


**Fig. 48:** Pyrazoloyl-diamino/aminophenol ligands complexed with V(IV), Fe(III), Co(II), and Cu(II).

Two Schiff based ligands – phenazone-furfural and aminophenol-nitrobenzaldehyde – were synthesised and used to form mixed ligand complexes with Fe(III) and other divalent first row transition metal ions (**Fig. 49**).<sup>151</sup> Against the chosen fungal strains, all complexes were found to have lower MIC values than either the free ligands or metal salt sources. The lowest MIC reported was for the Co(II) complex against *A. niger* ( $15 \mu\text{g}\cdot\text{mL}^{-1}$ )

and *C. albicans* ( $16 \mu\text{g}\cdot\text{mL}^{-1}$ ) which approached the MIC values of the three positive controls (nystatin: 12 and  $16 \mu\text{g}\cdot\text{mL}^{-1}$ ; KTZ: 14 and  $15 \mu\text{g}\cdot\text{mL}^{-1}$ ; CTZ: 10 and  $8 \mu\text{g}\cdot\text{mL}^{-1}$  against *A. niger* and *C. albicans*, respectively).

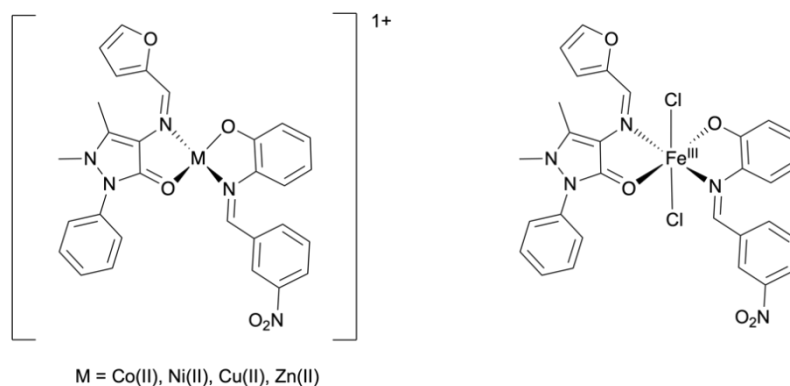


**Fig. 49:** Mixed ligand complexes formed between a range of transition metal ions and Schiff base-type ligands.

Mixed ligand Mn(IV) complexes of 2,2'-bipy and a pyrazolinone ethylenediamine, ethanolamine or glycine Schiff base (**Fig. 50**) were tested against *C. albicans* by determination of MIC values to assess antifungal properties.<sup>152</sup> All complexes were reported to have lower MICs than the parent pyrazolinone Schiff base ligands. Both the ethanolamine and glycine derivatives were found to be two-fold more effective than the positive control. However, the positive control used for all antimicrobial experiments (bacterial and fungal) was streptomycin, not a drug commonly used as an antifungal agent. Despite this, experimental MIC values of  $5 \mu\text{g}\cdot\text{mL}^{-1}$  for the tested complexes were significant.

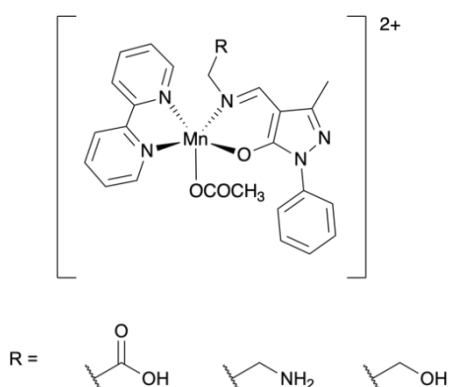


**Fig. 50:** Mixed 2,2'-bipy/pyrazoyl Mn(IV) complexes, derivatised with glycine, ethylenediamine and ethanolamine.

### 12.3 Salicylaldehyde-based ligands

Salicylaldehydes are a commonly used carbonyl in the synthesis of Schiff bases, likely due to their own bioactivity and the stabilising effect that conjugation between the azomethine nitrogen and the aromatic core provides. A study of binuclear Ru(III) complexes coordinated by bis(salicylaldehyde) ligands bridged by a range of flexible and rigid spacers was reported but the greatest inhibitory effects against *A. flavus*, *F. oxysporum*, and *R. solani* were 19% (**Fig. 51**).<sup>153</sup>

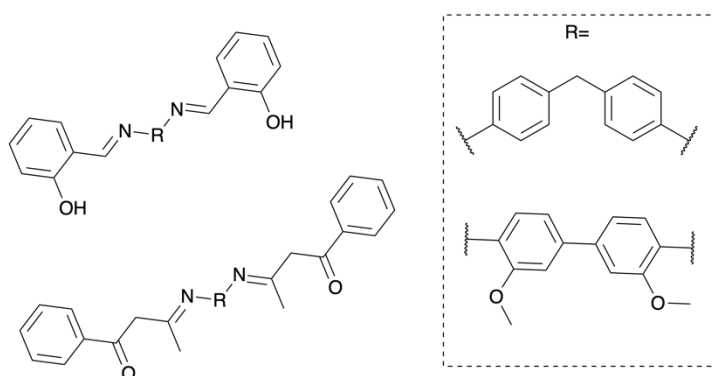


**Fig. 51:** Schiff bases, based on salicylaldehyde, which were coordinated to a range of metals (not shown) and assessed for antifungal activity.

Schiff bases formed between salicylaldehyde, aniline and *o*-/*m*-/*p*-toluidine were complexed with Ru(II) in mixed ligand systems (**Fig. 52A**). The resultant compounds were tested against *A. flavus* at concentrations of 100 and 200 ppm with Bavistin as a positive control. The antifungal results of only four complexes and the free ligands were reported, with the highest achieved inhibition was only 65%.<sup>154</sup>

Similar salicylaldehyde-based compounds that differed by the inclusion of methylamine, cycloamine or 2-aminopyridine were complexed with Ru(III) ions to form mixed ligand systems with triphenyl arsane/phosphane and halogen ions (**Fig. 52B**). The compounds were tested against *A. flavus* and *Flusarium* spp. at concentrations of 100 and 200 ppm. Similarly, only a subset of the antifungal measurements were reported, but the compounds achieved up to 76% inhibition of *F. spp.* and 68% of *A. flavus*.<sup>155</sup>

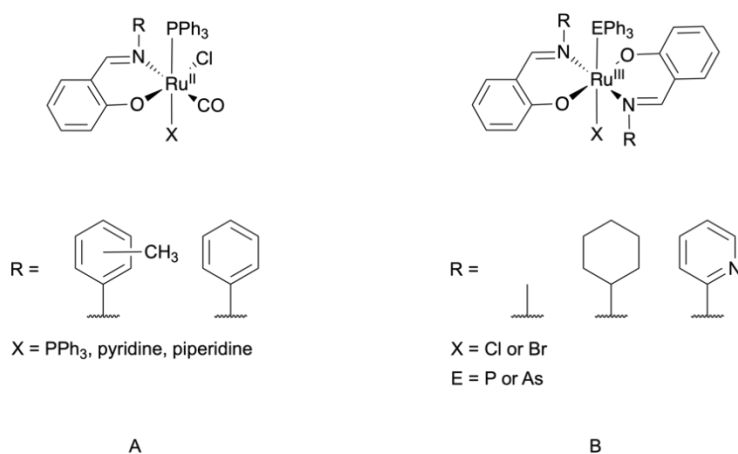


**Fig. 52:** Ru(II/III) complexes formed between salicylaldehyde-Schiff base derivatives.

A mixed-ligand Cu(II) complex was synthesised with Schiff base salicylalanine derivatives, phen, and dodecylamine (**Fig. 53A**). Characterisation of the complex included determination of its micelle forming properties, interactions with DNA, and antimicrobial activity.<sup>156</sup> The two fungal strains used in the agar well diffusion studies were *A. albicans* and *C. albicans*. Interestingly, after incubation of *C. albicans* with 3 mg·mL<sup>-1</sup> solutions of the complex for 24 and 48 h, the inhibitory diameter exceeded that of the positive control (KTZ). For the treatment of *A. albicans* the inhibition zone diameter approached the positive control (25 ± 0.54 and 29 ± 0.58 mm for 24 and 48 h, respectively, compared to 30 ± 0.58 mm for KTZ after 24 h – 48 h measurement not reported). Potentially, the results could be due to the combined effect of the different complex components used, which were explained to have been chosen for the bioactivity of Schiff bases, copper ions and phen as well as the surfactant properties of dodecylamine.

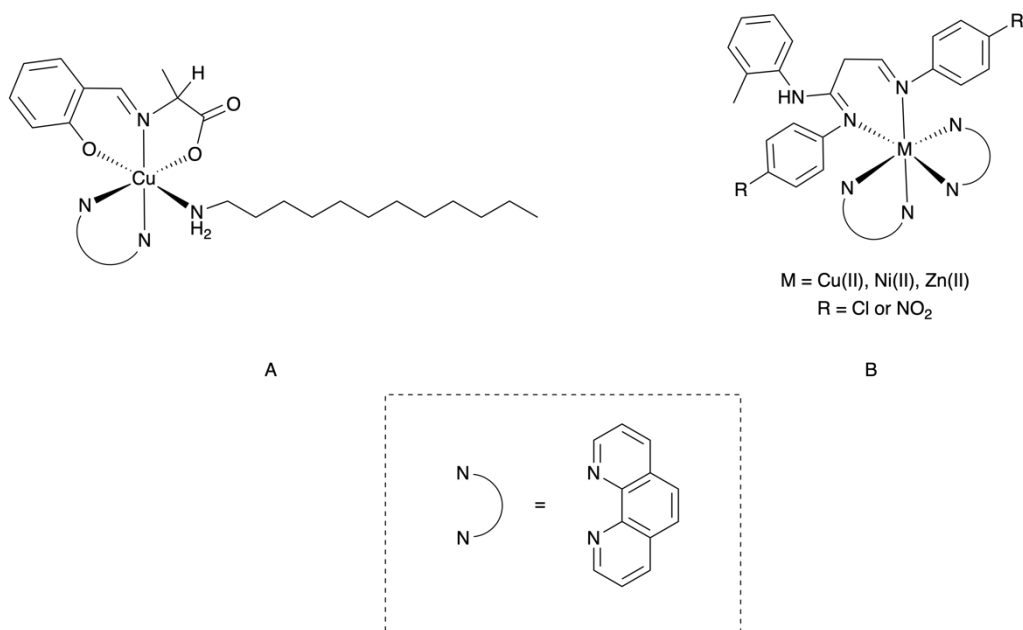


**Fig. 53:** Mixed ligand complexes formed between synthesised Schiff base ligands and 1,10-phen.

In 2014, Raman *et al.* aimed to develop mixed ligand, DNA intercalating M(II) complexes with two structurally similar Schiff bases and phen (**Fig. 53B**).<sup>157</sup> The two synthesised Schiff bases differed by the para-aminobenzene species used (either chloro or nitro) that were condensed with N-acetylaceto-*o*-toluidine. The free ligand and metal complexes (Cu(II), Ni(II) and Zn(II)) were characterised by a range of spectroscopic and spectrometric techniques and the ligand was determined to have NNNN coordination via two azomethine nitrogen atoms and two phen ligands. The chloro and nitro Cu(II) complexes were the most potent against all organisms against five strains of fungi. The MIC values of these complexes approached or reached the MICs of FCZ. Such results showed promise for the use of the metal complexes to treat fungal infections, while at the same time raising questions about their modes of action. The authors did not address the biochemical possibilities behind the observed differences between the metal ions used, however, the redox properties of the Cu(I/II) couple could provide additional fungicidal effects through the generation of ROS.

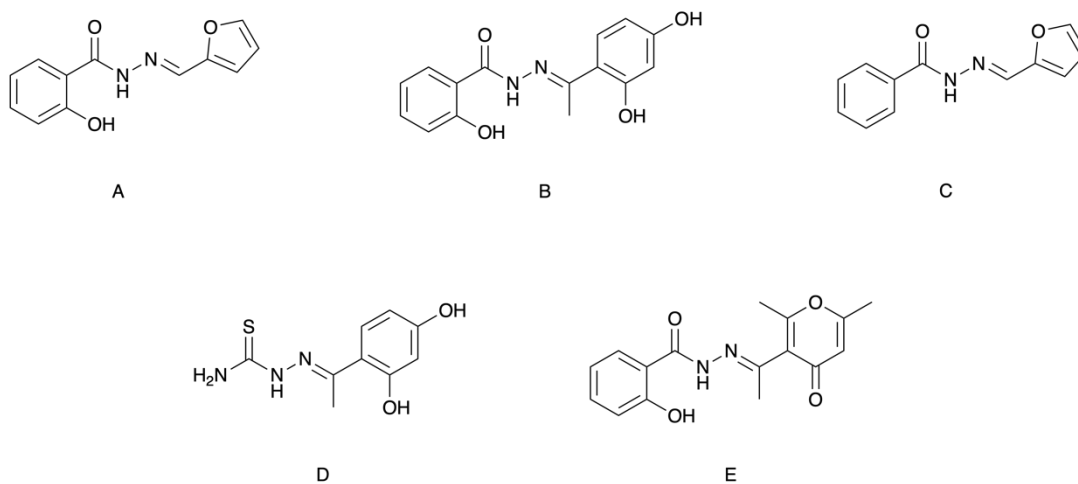


**Fig. 54:** Schiff bases complexed with a range of metals (not shown) and assessed for antifungal activity.

One study investigated the efficacies of Schiff base metal complexes against pathogenic fungal strains that cause sheath blight/rot and other diseases in rice crops (*R. solani* and *A. oryzae*).<sup>158</sup> Five Schiff derivatives (**Fig. 54A-E**) were synthesised and complexed with a range of divalent first row transition metals. While many of the characterised complexes were highly insoluble and therefore too inconvenient to test, a few standout results were reported. Complexation of the salicylaldehyde hydrazone-furfuryl ligand (**Fig. 54A**) with VO(IV) or Mn(IV) ions achieved 100% and 95% inhibition, respectively, against *R. solani* at a concentration of 1000 ppm by poison agar experiments (relative to Dithane M-45). Similarly, the VO(IV) complexes of **54B** and **54C** resulted in 100% and 98% inhibition, respectively, of the aforementioned fungus under the same experimental conditions. Both manganese and vanadium have been identified as important micronutrients for the growth and function of microorganisms. While the potential biochemical reliance of fungi on these metals might only partially explain the efficacies of the complexes, it could highlight another avenue of attack for antifungal agent development. Mammals are not known to have biochemical reliance on vanadium or manganese, nor are these metals highly toxic to humans.

Despite controversy around the incorporation of heavy metals in drug design, tin-based antifungal agents are common. In 2011, Shujah *et al.* synthesised and characterised a range of organotin(IV) complexes with the Schiff base N'-(5-bromo-2-oxidobenzylidene)-N-(oxidomethylene)hydrazine (**Fig. 55A**).<sup>159</sup> The complexes differed by their ancillary ligands, which depended on the organotin precursor used, e.g., dimethyl, dibutyl,



diphenyl, dioctyl Sn(IV) halides and oxides. The compounds were characterised by standard analytical methods: IR spectroscopy, mass spectrometry,  $^1\text{H}$  and  $^{13}\text{C}$ , as well as  $^{119}\text{Sn}$  NMR spectroscopic measurements. Single crystal structures of the free ligand, dimethyl, and diphenyltin(IV) complexes were also reported. The structures confirmed that the Schiff base acted as a tridentate ONO ligand, coordinating via the phenol oxygen, azomethine nitrogen and enolized aldehyde. The metal complexes and the parent ligand were tested against six fungal strains via agar tube dilution. The Schiff base ligand alone showed significant levels of activity against *F. solani* and *M. canis* with approximately 65 and 90% inhibition, respectively (relative to the positive control). Against the same strains of fungi, complexation with the organotin species decreased activities significantly. For most other tin complexes studied, however, complexation of the Schiff base with the metal resulted in an observable increase of the fungal inhibition. The most significant activity enhancement, relative to the free ligand, was observed for the dibutyl, diphenyl, and dioctyltin(IV)-Schiff base complexes against *A. flavis*, which resulted in approximately 90, 80 and 85% increases in efficacy, respectively.

While organotin complexes have shown promising antifungal activity, the inclusion of a heavy metal in the drugs raises concerns regarding mammalian toxicity of the compounds as well as tin-based metabolites leaching into the environment, particularly in agricultural or veterinary fungal treatments.

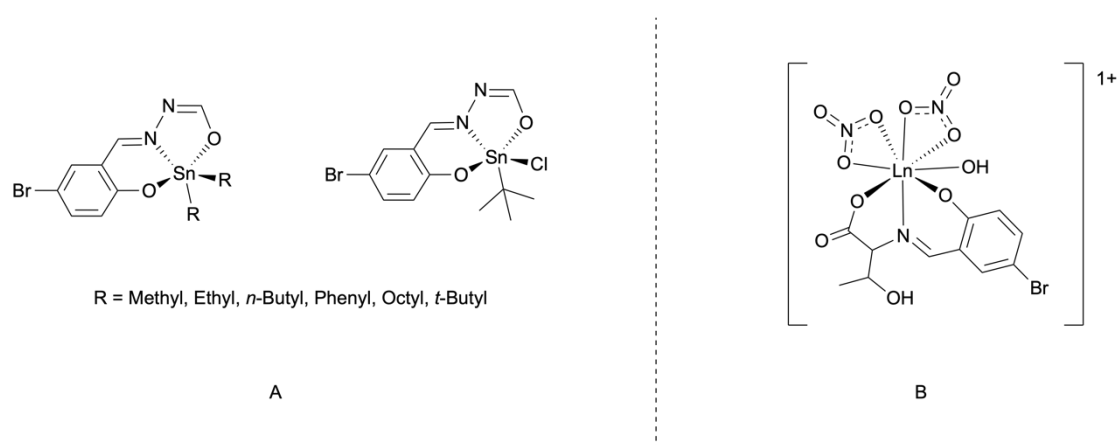


**Fig. 55:** **A** Complexes formed between a bromosalicylic hydrazine Schiff base ligand and various organo Sn(IV) sources. **B** Complex formed between Ln(III) ions and a threonine-bromosalicylic Schiff base ligand; structure not displayed in original article by Logu *et al.*, but was drawn by the authors of this review from the originally reported spectroscopic data.

A range of rare earth element complexes (Pr(III), Sm(III), Gd(III), Tb(III), Er(III), Yb(III)) with threonine-bromosalicylaldehyde Schiff base ligands (**Fig. 55B**) were tested for their efficacies against *Candida* and *Aspergillus* spp.<sup>160</sup> Interestingly, at 60  $\mu\text{g}\cdot\text{mL}^{-1}$  treatments, all compounds except for Pr(III) complex and the free ligand recorded >90% inhibition against *Candida* relative to KTZ. Similarly, >80% inhibition of *Aspergillus* was achieved for all complexes except the Pr(III) and Gd(III) compounds. While the sustainability of including rare earth elements in fungal treatments is questionable, the luminescence properties of such complexes could open doors to a greater understanding of metal complex uptake and distribution in *in vitro* fungal cultures by means of confocal microscopy and X-ray fluorescence spectroscopy.

#### 12.4 Indole-based ligands

Several indole-containing Schiff base ligands have been synthesised to incorporate the bioactivities of the indole moiety, imine species and metal ions into one drug. A series of mixed ligand Ru(III) indole-inspired Schiff base complexes with phosphane/arsane, and bromide/chloride ligands (**Fig. 56A**) were synthesised, characterised and tested for bioactivity against *B. cineria* and *A. niger* by disk diffusion at concentrations of 0.25, 0.5 and 1.0% w/v.<sup>161</sup> While the antifungal results initially appeared promising against both organisms tested – almost all diameters of inhibition exceeded that of the positive control – examination of the positive control drug raised questions regarding experimental design. The synergistic antibiotic ‘co-trimoxazole’ is used to treat severe bacterial infections (being sulfonamide-based) but does not appear to be commonly used against fungal infections. In the cases where it is prescribed for antifungal treatment, the drug acts as a facilitator for entry of the active antifungal drug into the cell by increasing cell permeability.<sup>162</sup> It is unclear whether the authors of the paper assumed co-trimoxazole was synonymous with CTZ (an azole based antifungal commonly used to treat yeast infections) or if this was perhaps a misspelling (despite the same name appearing twice in the paper), but without a suitable positive control for comparison, the fungal inhibition studies do not provide much insight into the antifungal activities of this series of complexes.

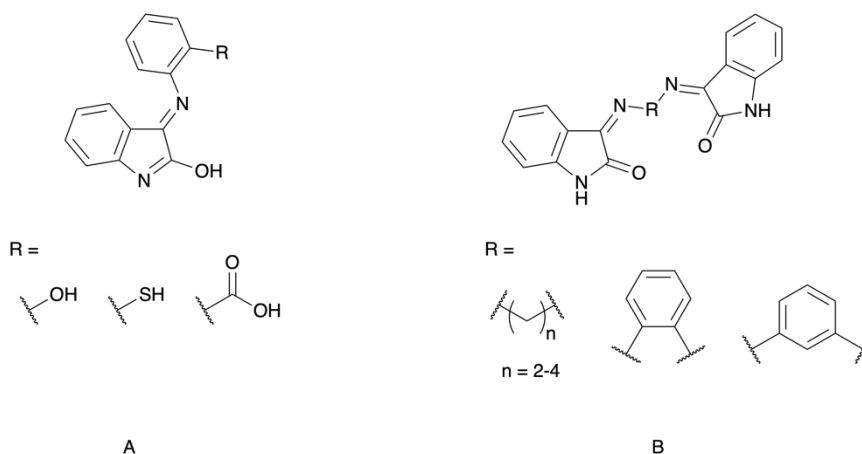


**Fig. 56:** Indole-containing Schiff base ligands which were coordinated to a range of metals (not shown) and assessed for antifungal properties.

Sharma *et al.* developed a series of linked di-indole ligands that differed by the bridging moiety (**Fig. 56B**).<sup>163</sup> The ligands chelated M(III) ions (M = Ru, Rh, Ir) through the carbonyl oxygen and azomethine groups. At a concentration of 1000 ppm, all metal complexes achieved at least 60% inhibition of *A. niger* and *F. oxysporium* after 96 h incubation, as determined by poison agar experiments. *F. oxysporium* exhibited a higher susceptibility to the tested complexes. All compounds displayed a dose-dependent response as the concentration was increased from 100 to 1000 ppm.

Indole/quinoline-based Schiff base Cu(II) complexes were reported by Karekal *et al.* (**Fig. 57**) and found to have MIC values similar to FCZ against *C. oxysporum* and *A. niger* ( $12.5 \mu\text{g}\cdot\text{mL}^{-1}$ ), but not *C. albicans* ( $25 \mu\text{g}\cdot\text{mL}^{-1}$ ). Other compounds (including Co(II), Cd(II), Ni(II), and Hg(II) complexes) had similar MIC values against the three tested fungal strains.<sup>164</sup> Additionally, the Cu(II) complex was also found to have superior antioxidant activity compared to the other five complexes and more than double that of the free ligand.

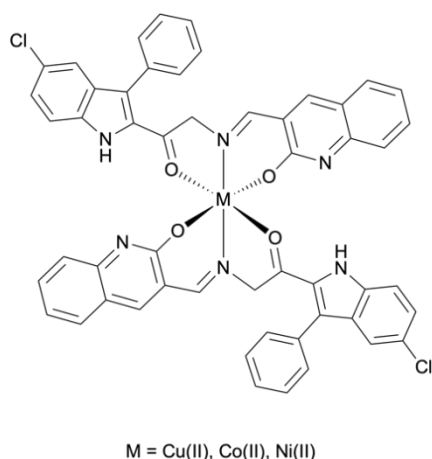


**Fig. 57:** Postulated complex geometry formed between the indole-quinoline derived Schiff base ligand and various divalent first-row transition metal ions.

## 12.5 Ferrocenyl-containing ligands

As has been mentioned above, improved drug bioactivity can sometimes be achieved by the inclusion of ferrocene moieties into drug molecules<sup>165</sup> as the ferrocene motif possesses its own fungicidal activity. In this vein, many groups have sought to complex Schiff-functionalised ferrocenyl moieties with metal ions.

Mahmoud *et al.* condensed L-alanine with 2-acetyl ferrocene and complexed a range of first row transition metal ions (**Fig. 58A**). It was found that more than 70% of the compounds had no antifungal activity when tested against *A. fumigatus* and *C. albicans* by zone of inhibition experiments.<sup>166</sup> However, of the 30% of compounds that elicited a fungicidal response, the Co(II) complex exceeded the positive control (KTZ) – 20 mm·mg<sup>-1</sup> vs. 17 mm·mg<sup>-1</sup>, respectively – while the Cd(II) complex achieved an inhibitory zone equal to that of KTZ. In another report, the same group synthesised, characterised and tested mixed ligand ferrocenyl-salicylaldehyde (L, **Fig. 58B**), phen first row transition metals complexes.<sup>167</sup> Four fungal strains (*A. fumigatus*, *S. racemosum*, *G. candidum* and *C. albicans*) were treated with solutions of the metal complexes in zone of inhibition experiments. It was shown that all metal complexes were more potent antifungal agents than the free ligand. One standout result was that of the [Fe(III)(L)(phen)(H<sub>2</sub>O)<sub>2</sub>]Cl complex which, across all four fungal strains, achieved the same inhibition diameter as AmB. Several of the other complexes approached the positive control, but none to the same extent.

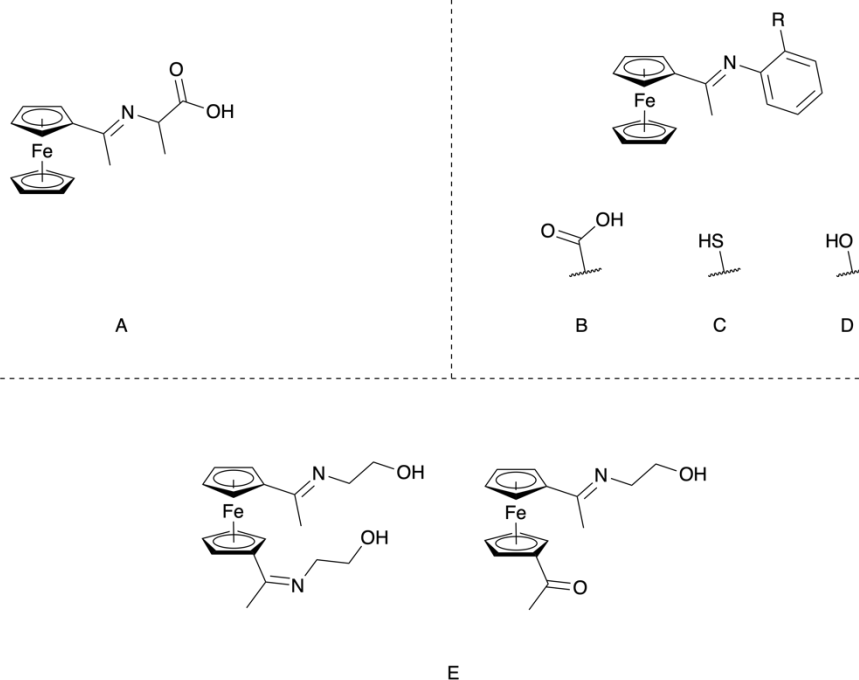


**Fig. 58:** Ferrocene-containing Schiff base ligands complexed with a range of metals (not shown) and assessed for antifungal properties.

One example refuting the theory that metal chelation of an organic species improves bioactivity was found in the work of Abou-Hussein *et al.*<sup>168</sup> Mono and diacetyl ferrocene species were condensed with *o*-aminothiobenzene (**Fig. 58C**) in either 1:1 or 1:2 molar ratios, depending on the ferrocenyl species used. When tested against *F. oxysporium*, both free ligands possessed appreciable antifungal activities, however, all ligand-metal complexes with Ru(III), V(IV) or U(VI) showed no improvement in fungicidal response or a decrease in activity.

A very similar *o*-aminophenol-monoacetyl ferrocene Schiff base ligand (**Fig. 58D**) complexed with first row transition metal ions and Cd(II) elicited more significant fungicidal responses.<sup>169</sup> The compounds were tested against four fungal and four bacterial strains in disk diffusion experiments, with AmB as positive control against the fungi. The Cu(II) complex displayed significant antifungal activities against *A. fumigatus*, *S. racemosum* and *G. candidum* by reaching or exceeding the inhibition zones of AmB. Other promising results were recorded for the Fe(III), Co(II) and Zn(II) complexes which all approached the positive control result

against the tested fungi. None of the tested complexes had considerable effect against *C. albicans*, relative to AmB.

A diacetyl-ferrocene-ethanolamine ligand (**Fig. 58E**) was coordinated to Co(II), Cu(II), Ni(II) and Zn(II) and tested against the six strains of fungi.<sup>101</sup> The Zn(II) metal complex performed best with zone of inhibition areas approaching those of both MCZ and AmB (except against *C. albicans*). Against *C. albicans* none of the compounds displayed significant inhibitory effects, relative to the positive controls.

Condensation of diacetylferrocene with 2-furoic/thiophene/salicylic hydrazide (**Fig. 59**) yielded a family of Schiff base ligands which were used to form metal complexes with Co(II), Ni(II), Cu(II) and Zn(II).<sup>170</sup> A total of 15 compounds (including the free ferrocene-containing ligands) were tested against *T. longifusus*, *C. albicans*, *A. flavus*, *M. canis*, *F. solani*, *C. glabrata* for antifungal activities. Most metal complexes performed slightly better than their parent ligands with some displaying inhibition values greater than 70%. However, the Co(II)-salicylaldehyde complex achieved 96% inhibition of *C. albicans* relative to AmB.

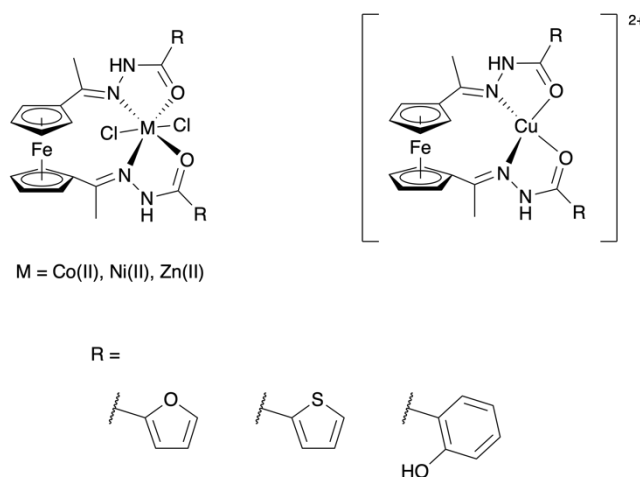


**Fig. 59:** Dicarbohydrazone ferrocene Schiff bases derivatised with various aromatic groups and complexed with first row transition metal ions.

## 12.6 Miscellaneous Schiff bases

Coumarin-based ligands appended with heterocycles (pyrimidine, triazine, thiazole, thiadiazole) and hydrazine(thio)carbamides (**Fig. 60**) via Schiff base condensation were complexed with first row transition

metals and tested against six pathogenic fungi.<sup>171</sup> When tested against *C. albicans*, the thiazole-Co(II) complex had an inhibition zone greater than MCZ and 96% inhibition relative to AmB. Against *A. flavus*, the Zn(II) complexes of the hydrazinecarboxamide-coumarin and thiazole-coumarin derivatives had the greatest inhibitory effects. Against *M. canis*, all complexes with the hydrazidethiocarboxamide derivative as a ligand had >80% inhibition and a similar result was observed for the pyrimidine-Zn(II), Ni(II) and Cu(II) complexes.

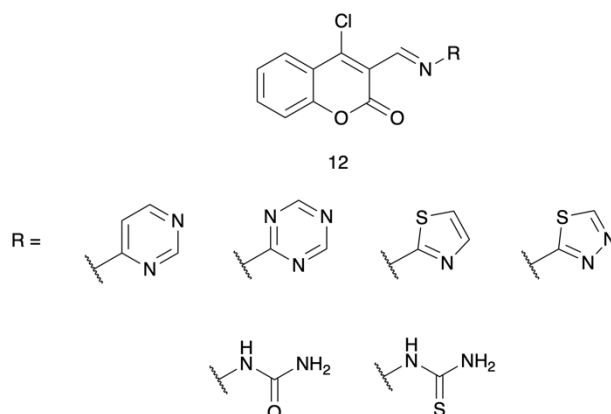


**Fig. 60:** Coumarin-based Schiff base ligands which were coordinated to a range of metal ions – Ni(II), Zn(II), Cu(II) – and assessed for antifungal activity.

Coordination of Ru(III) with bis(aminophenol), bis(aminothiophenol)glyoxal or bis(aminophenol)benzyl (**Fig. 61A**) was investigated and the antifungal efficacies of the resultant complexes tested against *Fusarium* spp. at 200 and 150  $\mu\text{g}\cdot\text{mL}^{-1}$ .<sup>172</sup> Unfortunately, no complex/ligand tested recorded greater than 22% inhibition of the organism. No positive control drug was stated in the article and percent inhibition was only determined relative to a 'control plate'.

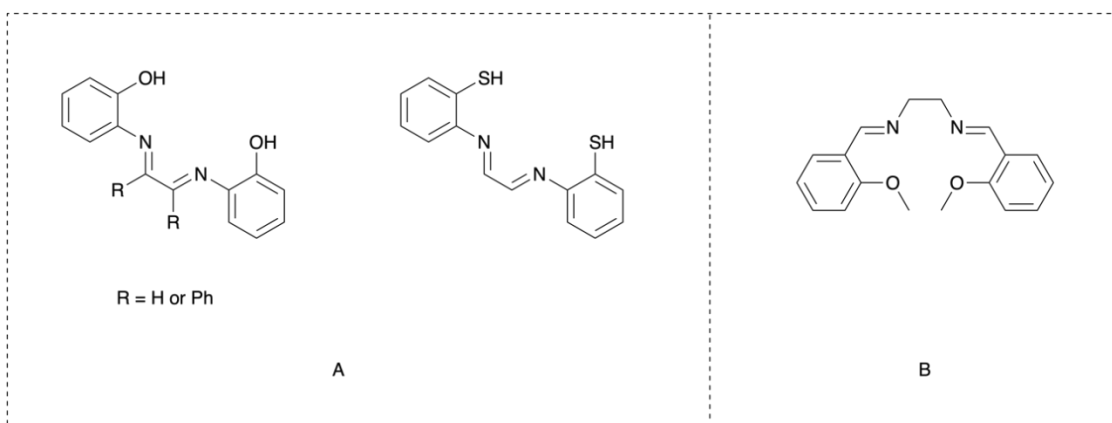


**Fig. 61:** Tetradentate acyclic Schiff base ligands complexed with metal ions (not shown) and assessed for antifungal activity.

A salen-based ligand (**Fig. 61B**) coordinated with Cu(II), Cr(III) or La(III) was found to have zero inhibitory effect against *A. flavus*, however, the free ligand had moderate antifungal activity.<sup>173</sup> Conversely, against *C. albicans*, both the free ligand and the La(III) complex had zero inhibitory effect, but the Cu(II) and Cr(III) complexes reached inhibition of approximately 10 and 15 mm per mg of complex, respectively. No compound tested approached AmB.

Various length diamines (ethyl, propyl or butyl) were condensed with 2-acetylthiophene to form a series of ligands (**Fig. 62A**) and complexes with first row transition metals were formed.<sup>174</sup> By disk diffusion it was determined that >70% inhibition was reached by the Co(II)-butyldiamine complex (against *F. solani*), Cu(II)-propyldiamine complex (against *C. albicans*), Co(II)-ethyldiamine complex (against *T. longifusus*), Zn(II)-ethyldiamine complex (against *A. flavus*), and the Ni(II)-butyldiamine complex (against *M. canis*). Against *C. glabrata*, the highest inhibition measured was 62% for the Zn(II)-propyldiamine complex. All inhibitions were reported as percentages relative to MCZ and AmB.



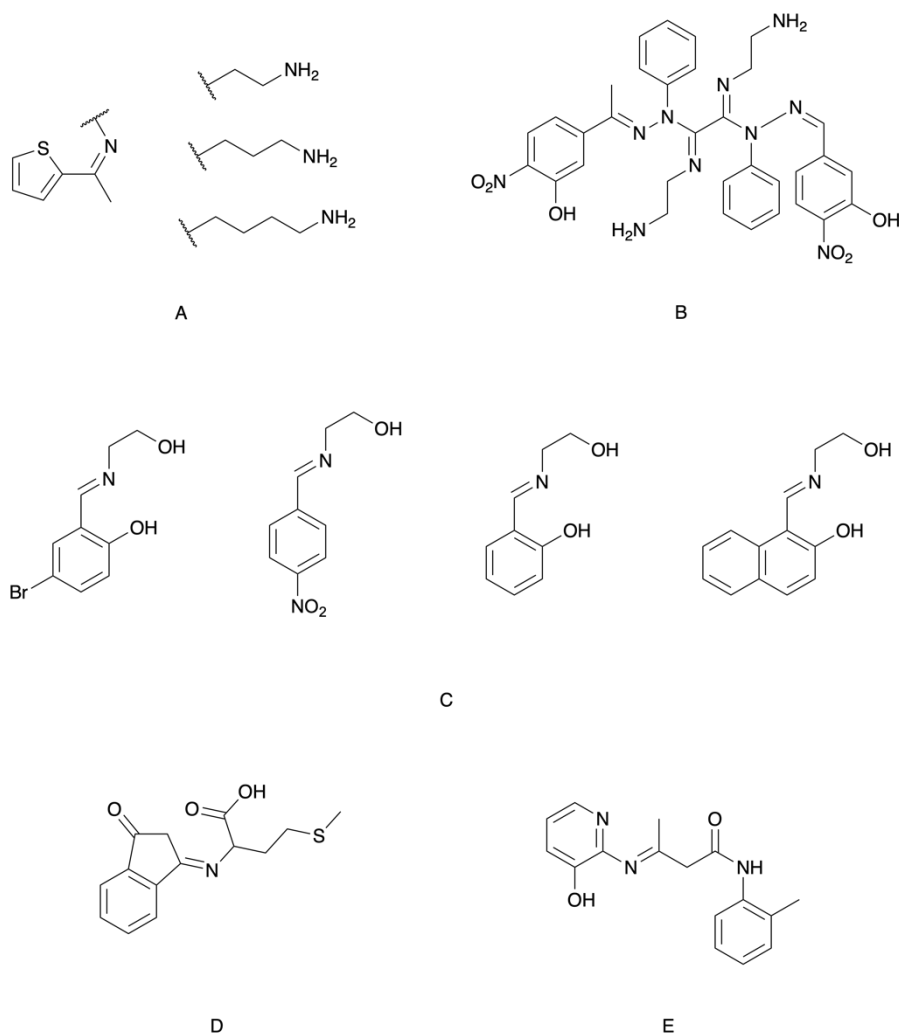


**Fig. 62:** Schiff base ligands complexed with metal ions (not shown) and assessed for antifungal activity.

A hydrazine Schiff base developed by Raman *et al.* (**Fig. 62B**) and complexed to Cu(II), Ni(II) or Zn(II) ions was tested against *A. niger*, *R. stolonifera*, *C. albicans* and *R. bataicola* by determination of MIC values.<sup>175</sup> Relative to the parent ligands, the metal complexes had three-fold lower MIC values against all fungi (15-20  $\mu\text{g}\cdot\text{mL}^{-1}$  to 4-7  $\mu\text{g}\cdot\text{mL}^{-1}$ ). However, the metal complex MIC values were still four to five times higher than the positive control (nystatin).

Schiff bases formed between substituted aromatic aldehydes and ethanolamine (**Fig. 62C**) and subsequently complexed with Co(II), Cu(II), Ni(II) and Zn(II) were tested for antifungal properties against *T. longifusus*, *C. albicans*, *A. flavus*, *M. canis*, *F. solani*, and *C. glabrata*.<sup>176</sup> In general, all metal complexes with the bromo- and nitro-derivatised ligands had greater antifungal responses than the naphthyl and salicylaldehyde compounds.

This was reflected in the average zone of inhibition distances (averaged over all experiments with a particular compound), which were ~19-22 mm for the bromo/nitro complexes and 15-17 mm for the naphthyl/salicylaldehyde complexes. The standard drugs had inhibitory zones greater than 25 mm.

Indandione condensed with methionine (**Fig. 62D**) was reported to have MIC values ranging from 9.6  $\mu\text{g}\cdot\text{mL}^{-1}$  against *C. albicans* to 12.5  $\mu\text{g}\cdot\text{mL}^{-1}$  against *A. flavus*.<sup>177</sup> However, when complexes were formed with Co(II), Cu(II), Ni(II) or Zn(II) the MIC values against the four tested fungal strains increased, indicating they were less toxic against the organisms. FCZ was measured to have inhibitory concentrations between 6.1 and 9.4  $\mu\text{g}\cdot\text{mL}^{-1}$ .

Condensation of 2'-methylacetoacetoanilide with 2-amino-3-hydroxypyridine yielded an ONO chelating ligand (**Fig. 62E**).<sup>178</sup> Subsequent complexation with Co(II), Ni(II), Cu(II) or Zn(II) and determination of MIC values against *A. niger*, *R. bataicola*, *R. stolonifer*, and *C. albicans* showed that, while the metal coordination improved the antifungal effect, the resulting MIC values were at least 10-40 times higher than nystatin.

A macrocyclic compound formed through Schiff condensation of 2,4-diaminotoluene and benzil (**Fig. 63A**) was coordinated with Mn(II), Fe(II), Co(II) or Ni(II).<sup>179</sup> Testing against *C. albicans* by zone of inhibition experiments found that the Mn(II) and Fe(II) complexes approached the positive control, gentamycin, achieving ~80% inhibition of organism growth. The Co(II) and Ni(II) compounds reached between 60 and 70% inhibition.

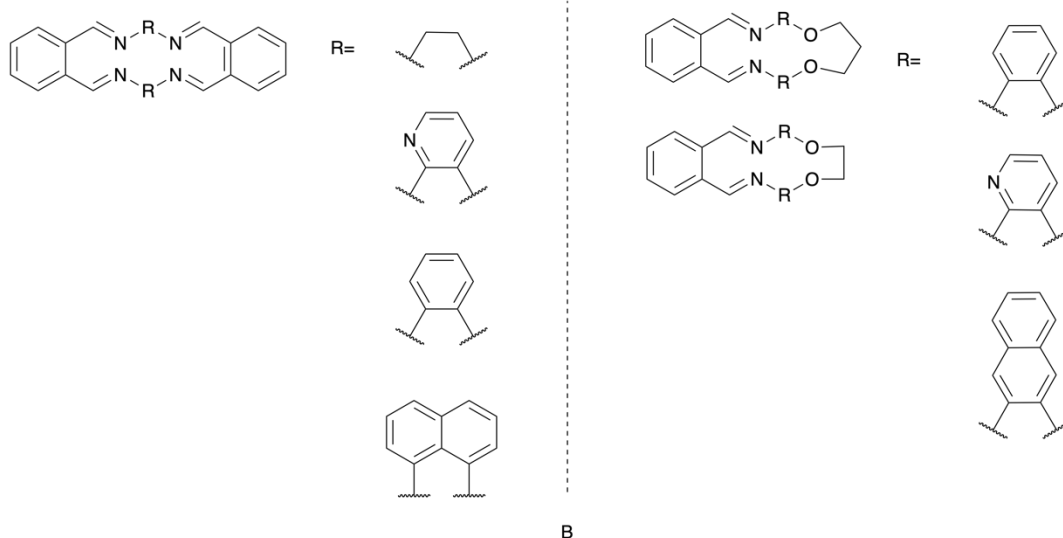
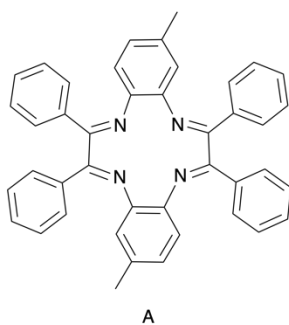


**Fig. 63:** Macrocyclic tetradentate  $N_4$  and  $N_2O_2$  Schiff base ligands complexed with metal ions (not shown) and assessed for antifungal activity.

A series of macrocyclic NNNN and NNOO donor ligands with different bridging spacers (**Fig. 63B**) were coordinated to Ru(II) ions and tested against *A. flavus* and *Fusarium* spp. at 0.5 and 1.0 mg·mL<sup>-1</sup> by zone of inhibition experiments.<sup>180</sup> The free ligands all had moderate inhibitory effects and increased as a result of Ru(II) complexation. Despite this, no compound achieved significant inhibition relative to the positive controls, AmB or Bavistin.

### 13. Thiosemicarbazone complexes

#### 13.1 Aliphatic thiosemicarbazone ligands

Condensation of 1-hydroxyacetone with a thiosemicarbazide yielded (E)-1-(1-hydroxypropan-2-ylidene)thiosemicarbazide which was subsequently complexed with Co(II), Ni(II), Cu(II) and Zn(II) ions, as reported by Netalkar *et al.* (**Fig. 64A**).<sup>181</sup> The biocidal activities of these complexes were determined based on their MIC values against various bacteria, *C. albicans* and *A. niger*. Promisingly, most of the metal-thiosemicarbazide complexes reported MIC values lower than the positive control (FCZ, MIC = 8  $\mu\text{g}\cdot\text{mL}^{-1}$  *i.e.* 26  $\mu\text{M}$ ), ranging from 1.6 to 12.5  $\mu\text{g}\cdot\text{mL}^{-1}$ , *i.e.* 3.17 to 26.9  $\mu\text{M}$  (with the Zn(II) and Co(II) complexes being most effective against *C. albicans* and *A. niger*, respectively). The metal chloride salts from which the complexes were synthesised were also tested. Relative to the metal source testing, coordination of the thiosemicarbazide with Co(II) and Ni(II) ions reduced the measured MIC values by between three and six-fold, coordination with the Cu(II) ion resulted in a seven-fold reduction against *C. albicans* and a greater than double MIC against *A. niger*. For the Zn(II) complex, relative to the metal salt source, the MICs only reduced by between two and three-fold. Against *A. niger* ZnCl<sub>2</sub> was an effective antifungal agent (5.87  $\mu\text{M}$ ) while the Zn(II) thiosemicarbazide complex was only slightly more effective (3.72  $\mu\text{M}$ ), the lowest reduction of any complex tested.

A fused tricyclic thiosemicarbazone (TSC) was functionalised with furanyl or propyl moieties (**Fig. 64B**) and complexed by Cu(II) and Pd(II) ions as reported by Rosu *et al.* in 2010. MIC values for each complex were determined against a range of bacteria, and *C. albicans*.<sup>182</sup> All complex/ligand MIC values were at least two orders of magnitude higher than the antifungal positive control (FCZ) and in a number of experiments, complexation of the ligands with Cu(II) or Pd(II) decreased antifungal activities.

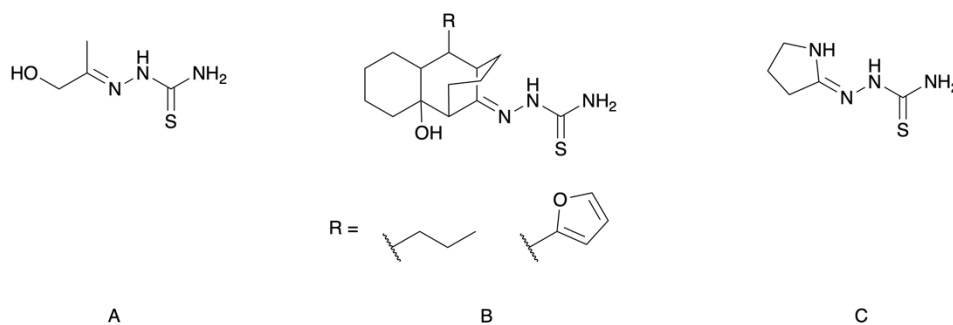


**Fig. 64:** Aliphatic TSCs complexed with a range of metals (not shown) and assessed for antifungal activity.

Al-Amiery *et al.* synthesised and characterised Cu(II), Co(II) and Ni(II) complexes of (Z)-2-(pyrrolidin-2-ylidene)pyrazol-5(1H)-ylidenehydrazinecarbothioamide in 2011 (**Fig. 64C**).<sup>183</sup> The group proposed octahedral binding by two ligands through sulfur, a bridging nitrogen and two axial chlorides. Antifungal activities of these complexes and the free ligand were determined by zone of inhibition experiments against *A. niger* and *C. albicans*. Against both organisms, all complexes exhibited linear dose-dependent responses from 125  $\mu\text{g}\cdot\text{mL}^{-1}$  to 1.0  $\text{mg}\cdot\text{mL}^{-1}$  and were active over all concentrations. Conversely, the free ligand only displayed antifungal activity at the two highest concentrations tested (0.75 and 1.0  $\text{mg}\cdot\text{mL}^{-1}$ ). None of the compounds tested were more effective than the positive control, FCZ. However, the Cu(II) complexes reached 80-96% inhibition, against *C. albicans*, and 60-93% inhibition against *A. niger*. The bioactivities of the tested compounds were ranked as such: FCZ > Cu(II)L<sub>2</sub>Cl<sub>2</sub> > Ni(II)L<sub>2</sub>Cl<sub>2</sub> > Co(II)L<sub>2</sub>Cl<sub>2</sub> > L.

### 13.2 Non-heterocyclic aromatic TSC ligands

A phenyl-pyrazoyl TSC (**Fig. 65A**) Cu(II) complex developed by Pahontu *et al.* was tested against *C. albicans* and recorded MIC values between 1.4 and 4.0  $\mu\text{g}\cdot\text{mL}^{-1}$  (1.78 and 7.26  $\mu\text{M}$ ).<sup>184</sup> These results were improved relative to the parent metal salts and free ligand and also exceeded the positive control, nystatin, by an order of magnitude (80  $\mu\text{g}\cdot\text{mL}^{-1}$ , *i.e.* 86  $\mu\text{M}$ ).

Similarly, a range of phenyl-pyrazoyl TSC derivatives, differing by the TSC-terminal N-substituent (**Fig. 65B**) were complexed with Cu(II) ions to give compounds with general formula of [Cu(L)Br<sub>2</sub>/Cl<sub>2</sub>], depending on the metal salt source used.<sup>185</sup> The antifungal activities of these complexes against *A. niger* and *P. variotii* were



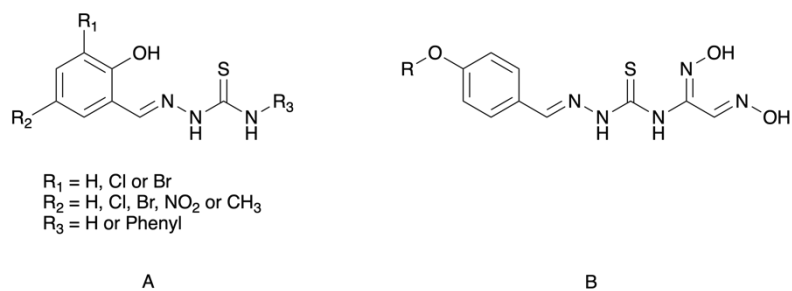


**Fig. 66:** Derivatised aromatic TSC ligands complexed with divalent transition metals and tested for antifungal activities.

Ni(II), Cu(II) and Co(II) complexes with 4-methoxy/ethoxybenzaldehyde TSC glyoxime derivatives (**Fig. 66B**) were tested by disk diffusion against *C. utilis*, *C. albicans*, *C. tropicalis*, and *S. cerevisiae*.<sup>188</sup> Only 25% of attempted antifungal tests yielded results. None of the tested compounds had an inhibitory effect against *C. utilis*, while the highest zone of inhibition against *C. tropicalis* was from that of the free ligands (>80%, relative to nystatin). The Cu(II)-methoxy derivative inhibited growth of *C. tropicalis* by 66%, and the Ni(II)-ethoxy derivative inhibited the growth of *C. albicans*, *C. tropicalis* and *S. cerevisiae* (65-74%).

Mixed ligand Ru(II) complexes ( $[\text{Ru}(\text{phen})_2(\text{L})]\text{Cl}_2$ ) consisting of two phen ligands and a 2-nitro/hydroxy-phenyl TSC were reported by Anchuri *et al.* (**Fig. 67A**)<sup>189</sup> Antifungal activities was determined by agar diffusion experiments against *A. clavatus*, *A. niger*, *Colletotrichum* spp. and *P. notatum*. When treated with a 1 mg·mL<sup>-1</sup> solution of the complex, the zones of inhibition ranged from 6 to 18 mm for three of the organisms; no measurements were reported for *A. niger*. When tested against *P. notatum* the Ru(II)-nitro derivative approached the positive control, griseofulvin, with ~85% inhibition. Additionally, the hydroxyderivative achieved ~75% inhibition against *Colletotrichum* while all other fungal strains were only inhibited by ~60%.

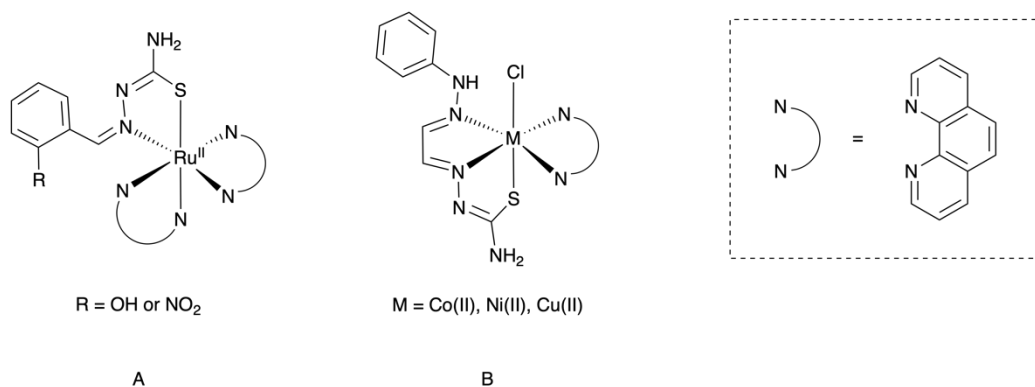


**Fig. 67:** Mixed ligand metal complexes with TSC and phen ligands.

Similarly, mixed ligand complexes [M(phen)(L)Cl] (M = Cu(II), Ni(II), and Co(II), L = 2-(1-(2-phenyl-hydrazono)-propan-2-ylidene)hydrazine-carbothioamide) (**Fig. 67B**) were tested against *A. flavus*, *P. italicum*, *C. albicans*, and *G. candidum* by disk diffusion.<sup>190</sup> At 1 mg·mL<sup>-1</sup>, the free ligand displayed moderate antifungal activity relative to AmB (65-67%), and all metal complexes achieved >70% inhibition against all organisms, except *C. albicans*. The Cu(II) complexes inhibited the growth of *A. flavus*, *P. italicum*, and *G. candidum* by 92, 90 and 86%, respectively and also displayed significant antibacterial properties, inhibiting all bacterial strains by 85-96%.

### 13.3 Heteroaromatic TSC ligands

Mono and di-coordinated titanocene/zirconocene complexes of 2-acetylpyridine TSC (**Fig. 68A**) were tested against *A. niger*, *A. alternata* and *M. phaseolina* for antifungal efficacies over a range of concentrations (20, 40, 60, 80 ppm).<sup>191</sup> All metal complexes achieved 90% inhibition of *A. alternata* growth at 80 ppm and <85% inhibition of *M. phaseolina*, relative to an unspecified control.



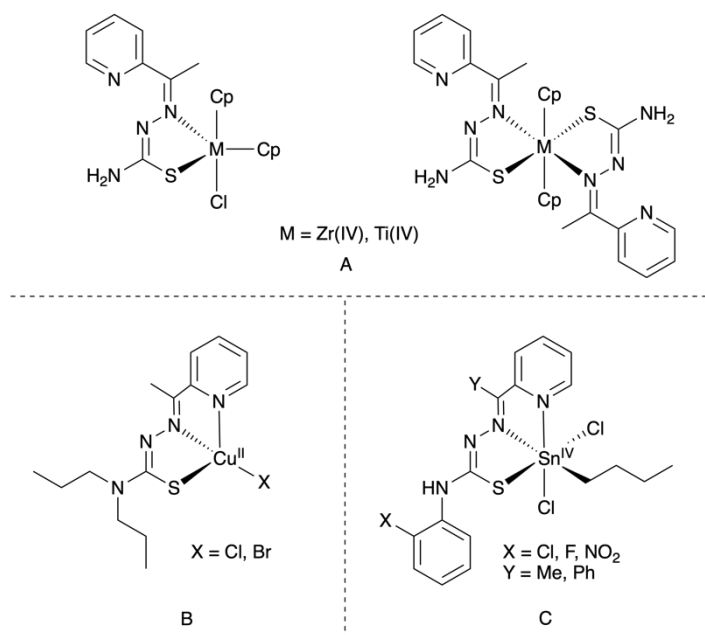


**Fig. 68:** Heterocyclic TSC ligands complexed with a range of metals and assessed for antifungal properties.

2-acetylpyridine N-diethyl TSC (**Fig. 68B**) chloro/bromo Cu(II) complexes tested against seven fungal organisms by disk diffusion yielded inhibition zones ranging from 9 to 17 mm.<sup>192</sup> No inhibition zones for the positive control (nystatin) were reported, however, against various organisms, identical MIC values were recorded for both the bromo complex and nystatin (31.5-62.5  $\mu\text{g}\cdot\text{mL}^{-1}$ ).

2-Acetylpyridine and 2-benzoylpyridinyl TSC (**Fig. 68B**) used as ligands to form organo Sn(IV) complexes from *n*-butylSnCl<sub>3</sub> managed to approach, and exceed, some MIC values of the positive control against *Candida* spp. (*C. albicans*, *krusei*, *glabrata*, and *parapsilosis*).<sup>193</sup> Of note were the pyridinyl-4-orthonitro phenyl complex which had an MIC against *C. glabrata* that was half that of FCZ (5.16  $\mu\text{M}$  vs. 21.32  $\mu\text{M}$ ) and the pyridinyl-4-ortho fluoro phenyl complex which had similar potency (3.74  $\mu\text{g mL}^{-1}$ , *i.e.* 6.28  $\mu\text{M}$ ). Given the relatively high MIC of FCZ against *C. krusei* (104.5  $\mu\text{g mL}^{-1}$ -0.341 mM), all complexes and free ligands tested were found to be more potent against this organism, despite the values ranging from 6.32  $\mu\text{g mL}^{-1}$  to 53.68  $\mu\text{g mL}^{-1}$  (20.64  $\mu\text{M}$  to 175.27  $\mu\text{M}$ ).

A 3-acetylpyridine 4N-(2-pyridyl) TSC ligand (**Fig. 69**) was complexed with Cu(II), Hg(II), Ni(II), UO<sub>2</sub>(IV), VO(IV) and Zn(II) and tested against 'yeast', as reported by the authors.<sup>194</sup> The free ligand, Cu(II), Hg(II), and Ni(II) complexes had zones of inhibition ranging from 18 to 28 mm, with the Hg(II) and Ni(II) being the most potent.

However, ampicillin – not commonly used as an antifungal agent – was used as the positive control for all experiments (bacterial and fungal). As such, compared with the positive control, all complexes had equal or greater fungal zones of inhibition.

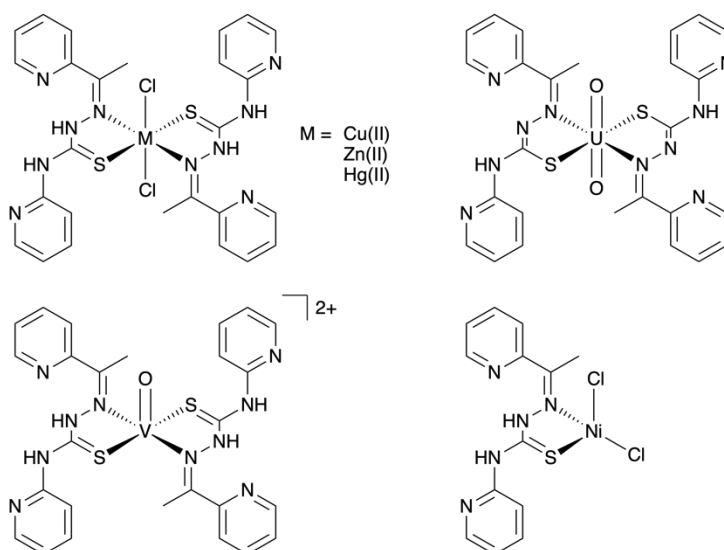


**Fig. 69:** Heterocyclic TSC ligands complexed with a range of metals and assessed for antifungal properties.

Antifungal properties of tridentate (ONS) dehydroacetic acid-TSC Ru(II) mixed ligand complexes (**Fig. 70A**) reported by Kannan *et al.* were assessed by disk diffusion.<sup>195</sup> Against *C. albicans* and *A. niger*, no complex achieved a greater inhibitory effect than 15 mm at 50 and 100 ppm (only reported for the [Ru(TSC)(CO)(pyridine)(PPh<sub>3</sub>)] complex). This was stated by the authors to not approach the positive control, CTZ (data not reported).

Ru(II) thiophene-TSC carbon monoxide complexes (**Fig. 70B**) recorded no antifungal activity in disk diffusion experiments against *C. albicans* at concentration of 50, 75 or 100 µg per disk.<sup>196</sup>

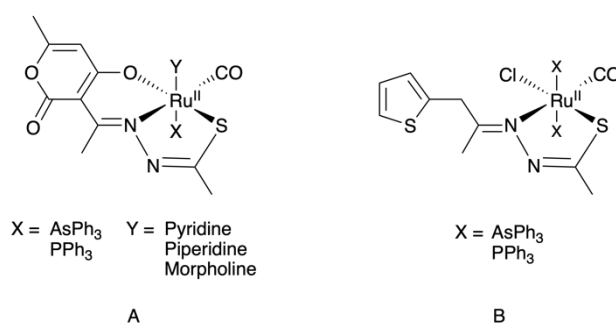


**Fig. 70:** Heterocyclic TSC Ru(II) complexes assessed for antifungal activity.

Quinoline-TSC ligands with a terminal N-methyl or pyridinyl group were complexed with a range of divalent first row transition metal ions (**Fig. 71A**).<sup>197</sup> The ligand coordinated all metal ions as a tridentate ONS ligand, however, the pyridinyl derivatives was identified to form binuclear species where the tautomerized TSC-thiol formed a  $\mu_2$ -bridge between two metal centres. Against both evaluated fungal organisms (*A. niger* and *Cladosporidium* spp.), the Cu(II)-quinoline TSC-methyl derivative outperformed FCZ in disk diffusion experiments. Similarly, the Cu(II)-pyridinyl complex performed best for that class of ligands, although it did not exceed the positive control.

For a thiophene-2,3-bis(TSC) ligand (**Fig. 71B**) in complex with Ni(II), Cu(II) and Cd(II) ions, Alomar *et al.* reported MIC values ranging from 8-62  $\mu\text{g}\cdot\text{mL}^{-1}$  against *C. albicans*, *C. glabrata*, and *A. fumigatus*.<sup>198</sup> While the positive control (AmB) was far more potent against the latter two organisms (0.125 and 0.5  $\mu\text{g}\cdot\text{mL}^{-1}$ , respectively), the Cd(II) complexes (either bromo or chloro, depending on the metal salt source) had the same MIC values as AmB against *A. fumigatus* (8.0  $\mu\text{g}\cdot\text{mL}^{-1}$ ).

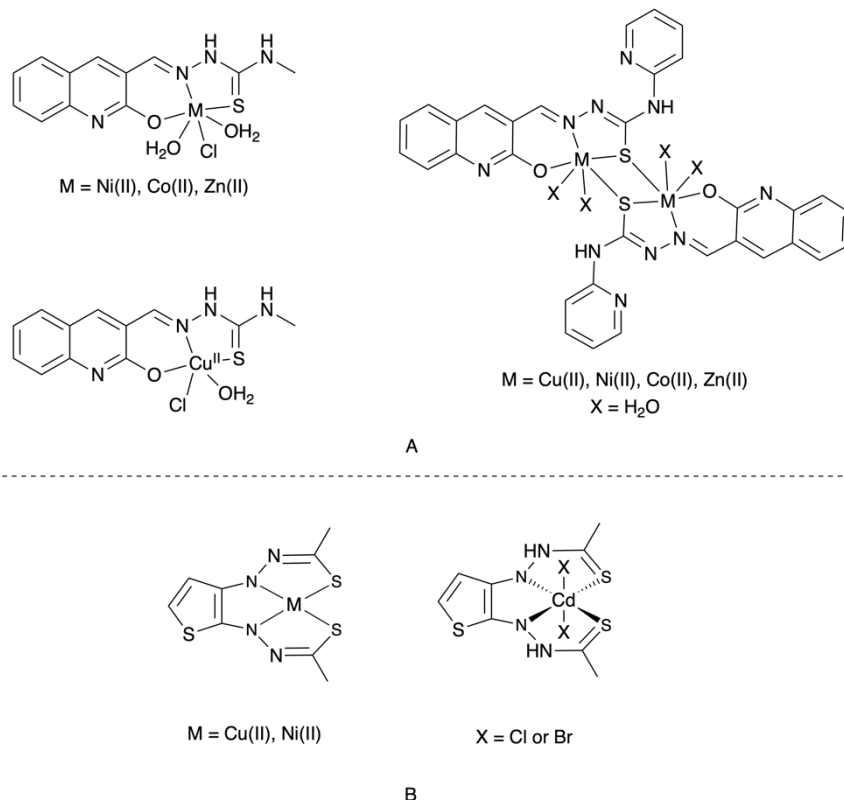


**Fig.71:** Heterocyclic TSC metal complexes assessed for antifungal activity.

## 14. NO donor ligand-based complexes

### 14.1 Diazene/hydrazine-based ligands

Against *C. albicans* and *A. niger*, a Pd(II) complex with (*E*)-4-((2-hydroxyphenyl)diazenyl)-3-phenyl-1H-pyrazol-5(4H)-one (**Fig. 72A**) was found to have moderate activity ( $8.2 \pm 0.2$  and  $10.1 \pm 0.1$  mm, respectively).<sup>199</sup> The free ligand and two other metal complexes (Ni(II) and Pt(II)) were tested, but no results recorded. Additionally, FCZ was listed as a positive control against the fungal organisms, however no measurements were provided in the article.

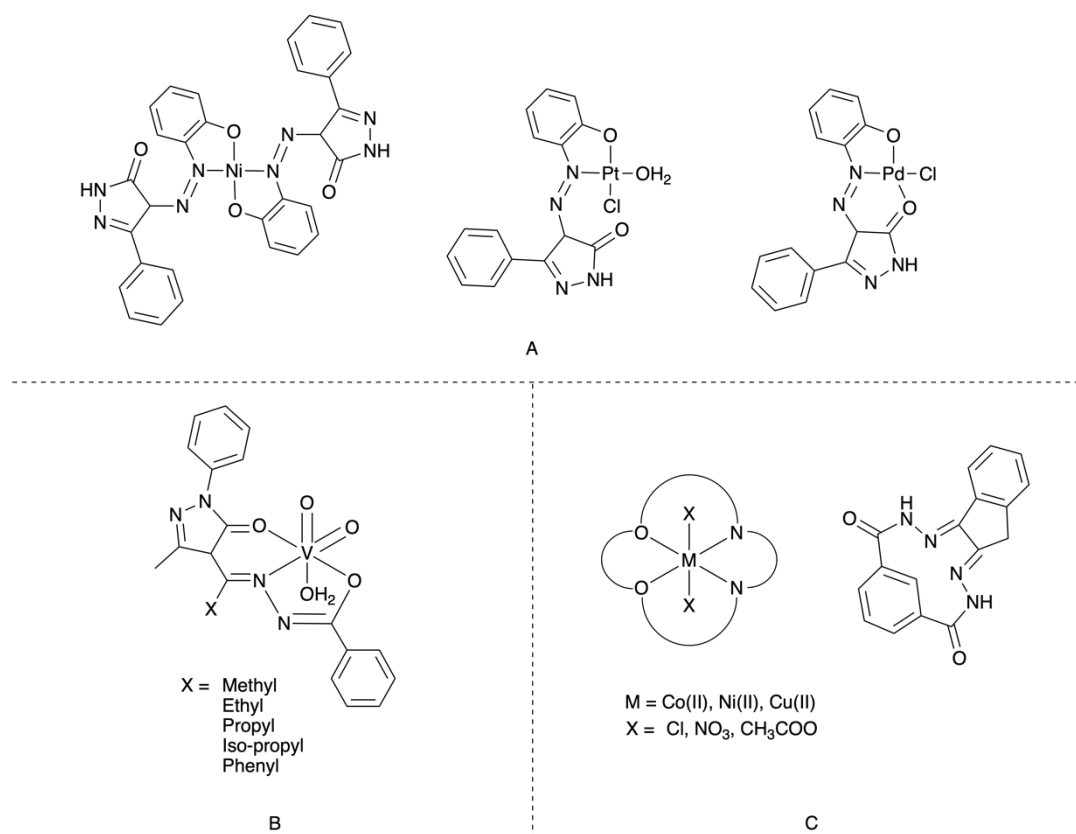


**Fig. 72:** Diazene/hydrazine-containing ligands complexed with a range of metals and assessed for antifungal properties.

A range of isonicotinic acid hydrazide derivatives were synthesised and complexed with VO<sub>2</sub>(V) ions (**Fig. 72B**) by Maurya and Rajput.<sup>200</sup> Of the reported complexes, only one was tested for antifungal activity: N-(4'-butyrylidene-3'-methyl-1'-phenyl-2'-pyrazolin-5'-one)-isonicotinic acid hydrazide. Against *A. niger*, the compound inhibited ~19% of fungal growth after 7 days, which was a decrease of ~40% when compared to

the free ligand. Conversely, against *S. cerevisiae*, the same complex achieved ~91% inhibition over the same time period, a 15% increase on the efficacy of the free ligand (76%). All percentages were calculated relative to an unspecified control.

A tetraazamacrocyclic ligand comprising an ortho carbonyl hydrazide and indole-dione was complexed with Co(II), Ni(II) and Cu(II) ions (**Fig. 72C**).<sup>201</sup> When tested against *C. albicans*, the Cu(II) macrocyclic chloro complex exceeded AmB (14.8 vs. 12.5 mm inhibition zone) and the equivalent Ni(II) complex exceeded the positive control against *S. cerevisiae* (14.2 vs. 13.6 mm).

A benzoyl-pyridinyl hydrazide in complex with Ni(II) (**Fig. 73A**) recorded an inhibitory zone of 29 mm after 48 h incubation with *C. albicans*, far in excess of the AmB control (21 mm).<sup>202</sup> The measurement was recorded at a concentration of 50 µg complex per disk, however, doubling of the concentration to 100 µg per disk resulted in an approximate halving of the inhibitory zone; all experiments were conducted over 24 and 48 h. Strangely, for some of the complexes (including Co(II) and Cu(II) complexes) at the given concentrations, the initial 24 h measurement appeared significant, only to decrease at the 48 h time point. Whether this was a result of complex stability or perhaps an initial fungistatic inhibition which the organism could overcome was not addressed.

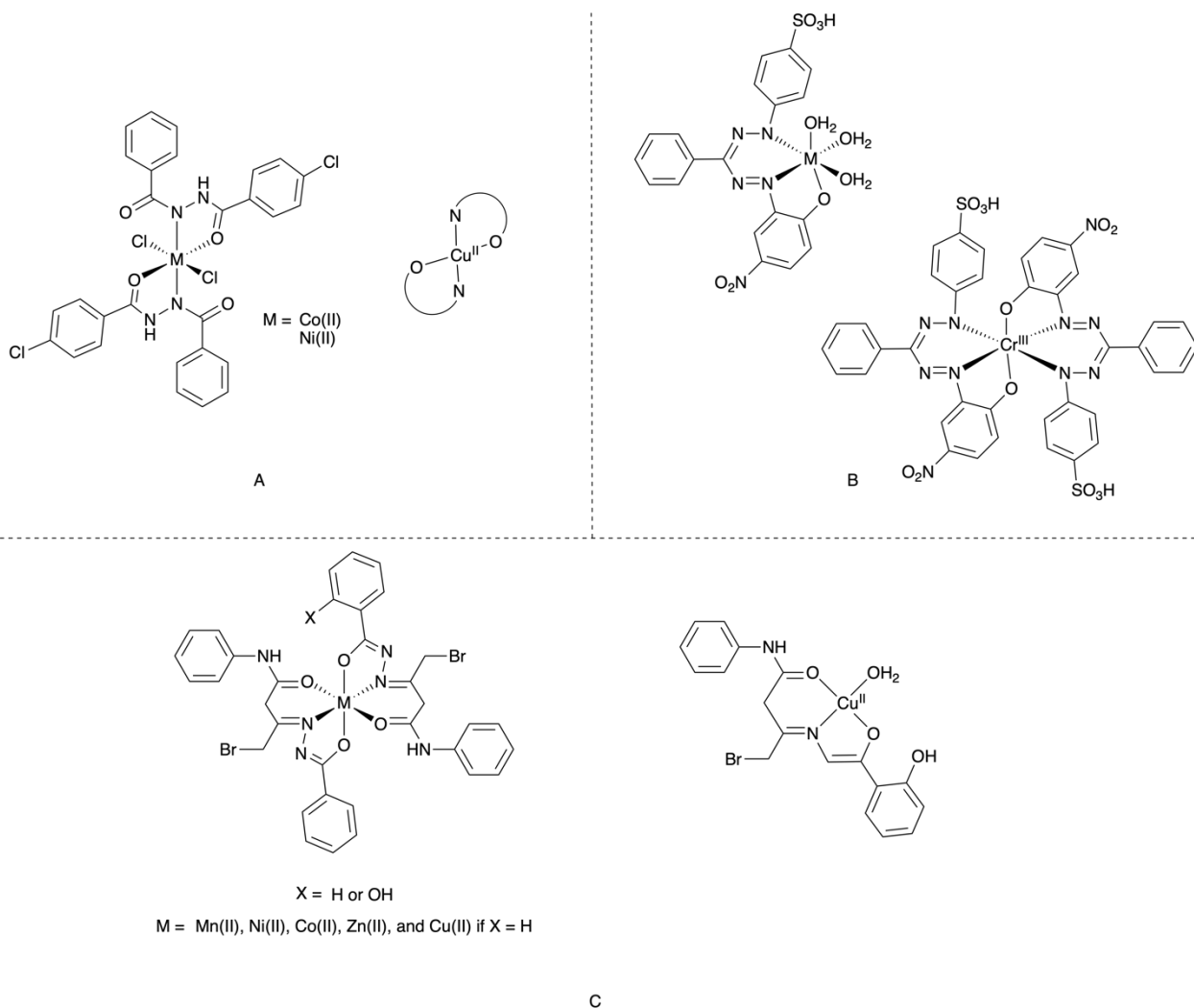


**Fig. 73:** Diazene/hydrazine-containing ligands complexed with a range of metals and assessed for antifungal properties.

A substituted formazan Cr(II) complex reported by Khan *et al.* (**Fig. 73B**) was found to have high activity against five fungal strains.<sup>203</sup> In disk diffusion studies, the complex reached zones of inhibition ranging from  $29 \pm 0.09$  mm against *C. albicans* and up to  $39 \pm 0.01$  mm against *A. niger*.

Benzoyl and salicylylhydrazones (**Fig. 73C**) in complex with Mn(II), Co(II), Ni(II) and Cu(II) were synthesised and characterised by Deepa *et al.*<sup>204</sup> Not only were DMSO solution of the complexes more active fungicidal agents than the parent ligands at 500 ppm, many of the complexes recorded zones of inhibition  $>25$  mm against four strains of pathogenic fungi. Whether the 10 mm diameter of the holes bored into the agar plates was subtracted from the reported values, however, was not specified. Additionally, the DMSO negative control recorded between 10-14 mm inhibition zones for all organisms.

## 14.2 Miscellaneous NO donor ligands

A quinolinol-benzotriazole ligand in complex with Cu(II), Ni(II), Co(II), Mn(II) and Zn(II) (**Fig. 74A**) was found to inhibit the growth of seven fungal strains at 1000 ppm.<sup>205</sup> Most compounds were found to inhibit growth from 63 to 89% relative to an unspecified positive control. The free ligand was also found to have significant antifungal properties with 70% inhibition of *C. glabrata*.

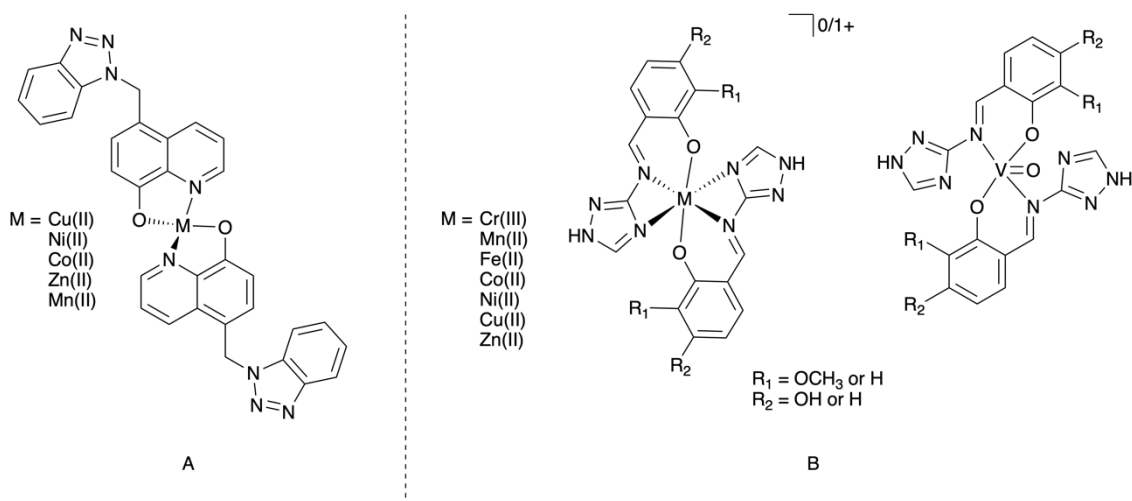


**Fig. 74:** NO coordinating ligands complexed with a range of metals and assessed for antifungal properties.

The Zn(II) complexes of a methoxy and diol phenyl-triazole Schiff base (**Fig. 74B**) were found to be effective against all fungal strains tested with percent inhibitions ranging from 73-82% for the methoxy derivative and 59-76% for the diol derivative.<sup>206</sup> Complexes with other first row transition metals (Cu(II), Ni(II), Co(II), Mn(II), Zn(II)) were also tested and recorded inhibition of fungal growth approaching 70%, relative to MCZ.

A study by Madzivire *et al.* investigated a range of Ru(III) mono-substituted ketoiminates complexes (**Fig. 75A**) and found that, for the 2-ethoxyethanol derivative, the metal centre was reduced to Ru(II). The ketoiminato carbonyl complex that formed was suggested to be the active compound and could possibly act as a carbon monoxide releasing molecule (CORM).<sup>207</sup> While selectivity towards *C. albicans* over other fungal strains was identified, only an inhibitory effect of ~44% was determined.

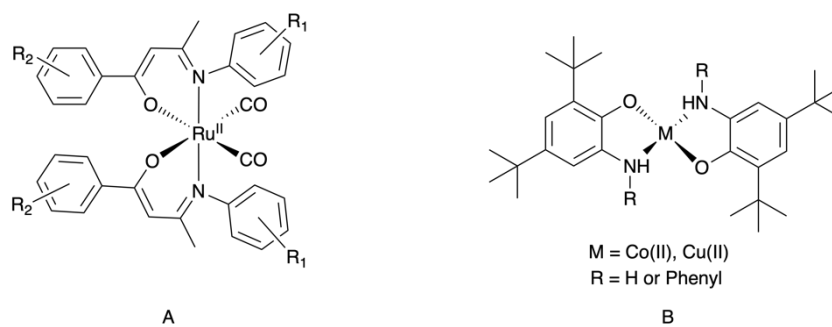


**Fig. 75:** NO coordinating ligands complexed with a range of metals and assessed for antifungal properties.

Sterically hindered *o*-aminophenol derivatives in complex with Co(II) or Cu(II) ions (**Fig. 75B**) – tentatively assigned with square-planar geometries by the authors – were found to have significant fungal inhibitory activities against eight fungi. In some cases the complexes exceeded the positive controls (nystatin, TRB, questiomycin B) by a factor of two.

### 15. Carboximide-based complexes

Relatively few papers concerning the antifungal properties of carboxamide metal complexes (**Fig. 76**) have been reported and, unfortunately, several of the articles reported don't include positive controls for relevant comparison of results.



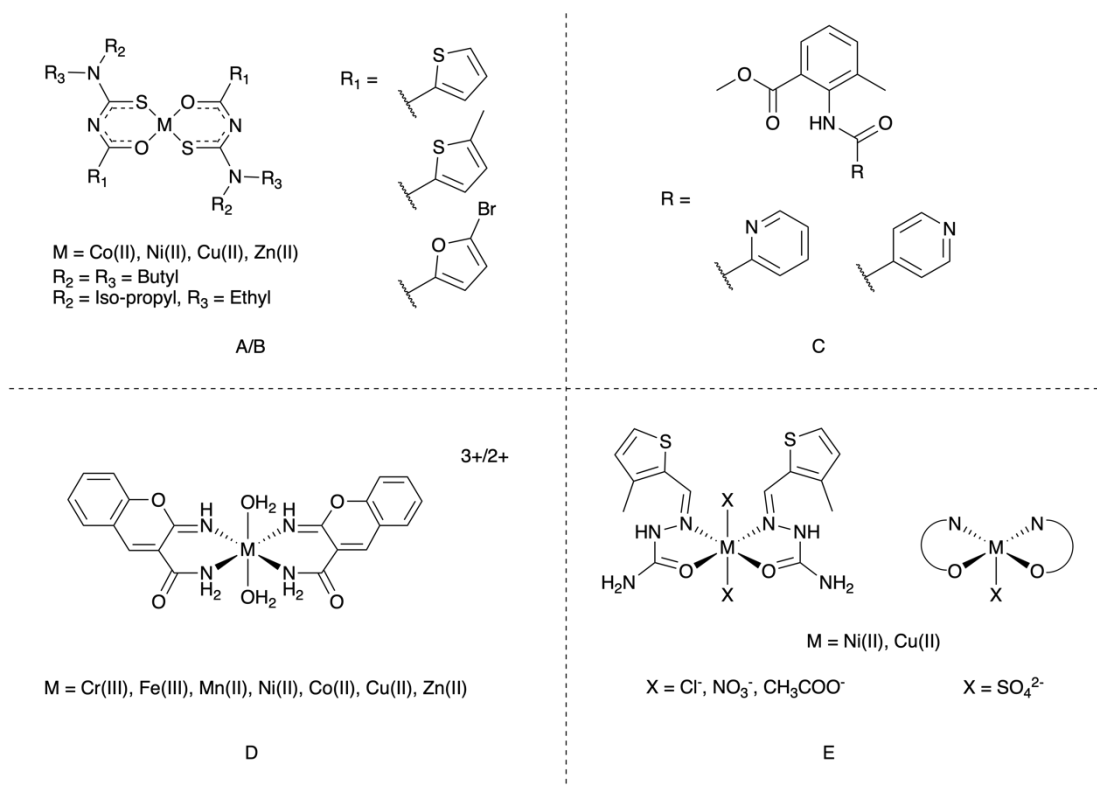


**Fig. 76:** Carboxamide-based ligands complexed with a range of metals and assessed for antifungal properties.

Two articles published by the same group presented asymmetric carboxamide thiourea ligands substituted with thiophene, 4-methylthiophene, and 4-bromofuran. Between the studies, the ligands only differed by the N-alkylation species (dipropyl, and a mix of ethyl/isopropyl, respectively) (**Fig. 76A/B**). Antifungal testing against six organisms provided an average inhibition of <50%. The highest achieved fungicidal activity was for the 4-methylthiophene derivative which approached 70% inhibition of *M. canis* for all metal complexes.<sup>209</sup> Similarly, the 4-bromofuran derivatives approached 70% inhibition against *C. glabrata* for all metal complexes.<sup>210</sup>

Pyridine derivatised carboxamide ligands (**Fig. 76C**) complexed with Cu(II), Co(II) and Zn(II) at a concentration of 10 µg·mL<sup>-1</sup> were found to reduce the growth of *F. californicum* by only 28% relative to the DMSO negative control.<sup>211</sup> No positive control was reported.

A coumarin-based carboxamide (**Fig. 76D**) complexed with a range of M(II) ions showed no activity against *C. albicans* except for the Co(II) and Ni(II) complexes, which approached and exceeded the positive control, KTZ,

respectively.<sup>212</sup> The antibacterial properties of these complexes were far more prominent than the antifungal properties.

Thiophene-containing hydrazine carboxamide Ni(II) and Cu(II) complexes (**Fig. 76E**) were tested for antifungal activities at 250  $\mu\text{g}\cdot\text{mL}^{-1}$  and found to have a maximum inhibitory diameter against *A. flavus* of 16 mm, and 10 mm against *A. niger*.<sup>213</sup> No positive control was reported.

#### 16. Thiocarbamate-based complexes

A range of derivatised dithiocarbamate ligands in complex with dimethyl Sn(IV) (**Fig. 77A**) were found to approach 90% inhibition of *R. solani* at 1.0 mM and close to 100% inhibition of *B. cinerea* at 240  $\mu\text{M}$ .<sup>214</sup> The positive controls used in the studies were mancozeb and ziram which are a mixture of Zn(II)/Mn(II) dithiocarbamate complexes and a Zn(II) dithiocarbamate, respectively. Dimethyl Sn(IV) was found to only inhibit the fungal strains by ~15%. Inhibitory properties of the free ligand were not reported due to poor aqueous stability.

Another study was published reported a similar derivatised dithiocarbamate ligand in complex with di-*n*-butyl Sn(IV) (**Fig. 77B**). Some of the fluorinated complexes approached 75% inhibition of *C. gloeosporioides* at concentrations of 98  $\mu\text{M}$  and had  $\text{IC}_{50}$  of approximately 6  $\mu\text{M}$ .<sup>215</sup>

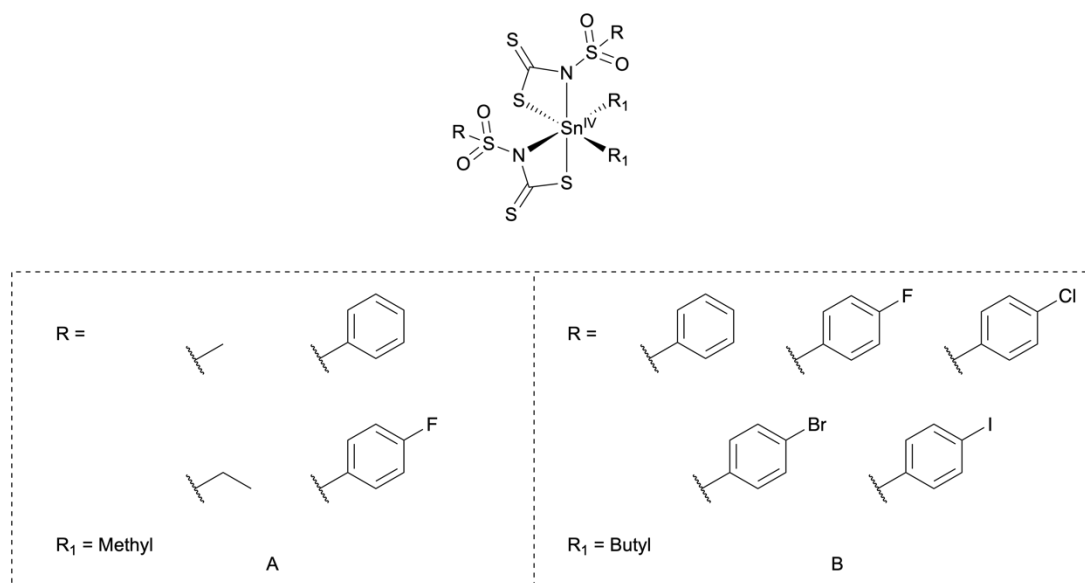


**Fig. 77:** Thiocarbamide-containing ligands complexed with organo Sn(IV) compounds and assessed for antifungal properties.

Another series of organotin(IV) complexes were synthesised and characterised using pyrrolidine dithiocarbamate (**Fig. 78A/B**) and a range of tin precursors:  $\text{SnCl}_2$ ,  $\text{SnPh}_2\text{Cl}_2$ ,  $\text{SnPh}_3\text{Cl}$ ,  $\text{Sn}(n\text{-Bu})_2\text{Cl}_2$  and  $\text{Sn}(\text{cyclohexane})_3\text{Cl}$ .<sup>216,217</sup> The Sn(IV)-derivatives were tested for antifungal activities against *C. albicans* by agar well diffusion with nystatin as positive control (concentration used was ~22 mM). Most complexes were required to be dissolved in a mixed solvent system (dichloromethane/pentane) and were tested at a range of concentrations (0.25 mM to 3.2 mM, with two-fold dilutions). The *n*-butyl Sn(IV) complex exceeded the positive control zone of inhibition at a concentration of 0.4 mM (approximately 50 times more dilute) and the Sn(IV) chloride complex exceeded the positive control by 5.5 mm at a concentration of 1.6 mM. While effective in the inhibition of *C. albicans*, the use of Sn(IV)-derived drugs raises concerns for environmental pollution and mammalian toxicity.

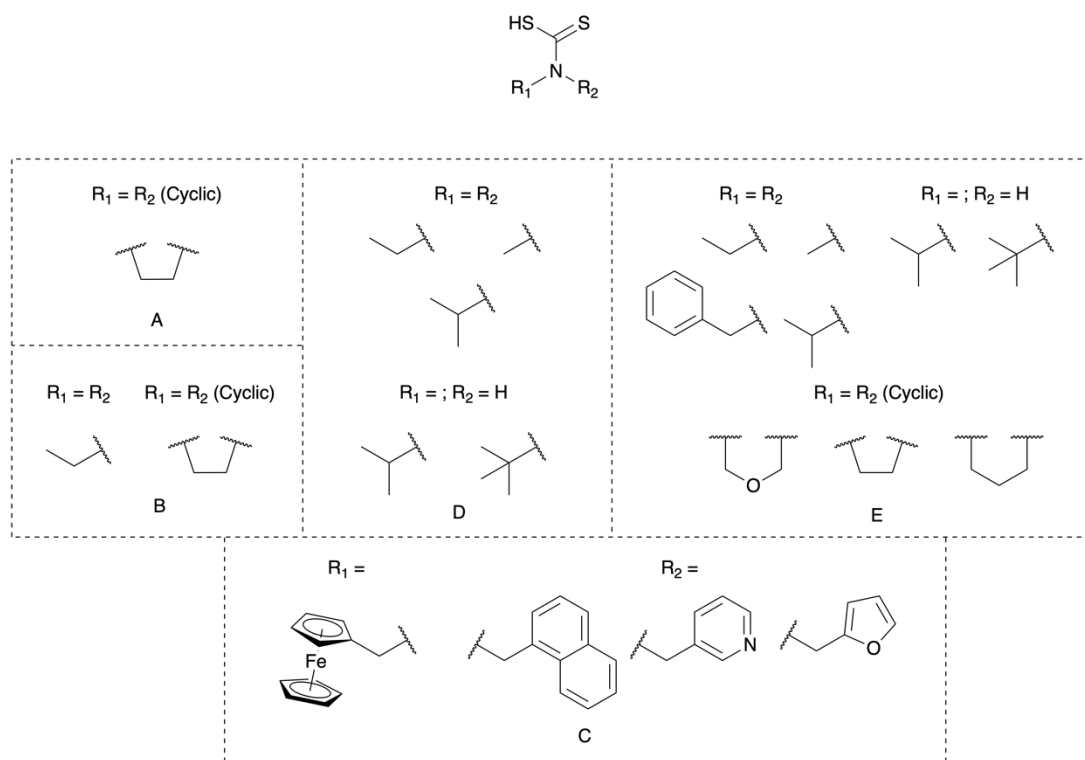


**Fig. 78:** Dithiocarbamate-based ligands complexed with a range of metals (not shown) and assessed for antifungal properties.

A series of ferrocene-derived thiocarbamate species (differing by naphthyl, pyridyl or furanyl pendant groups) were complexed with Co(II), Cu(II), Ni(II) and Zn(II) (**Fig. 78C**) with coordination exclusively occurring through the sulfur donors.<sup>218</sup> Tetrahedral species were reported for the latter three metal ions, and an octahedral complex for the Co(II) ion. Antifungal efficacies were evaluated through determination of the complex and ligand MIC values against *C. albicans* and *A. niger* with FCZ as a positive control. All metal complexes were reported to have MIC values 5-20 times higher than the positive control, however, the Ni(II) 3-pyridyl complex achieved an MIC equal to that of FCZ for *C. albicans* and only  $10 \mu\text{g}\cdot\text{mL}^{-1}$  higher than for *A. niger*.

Another dithiocarbamate appended with aliphatic groups (**Fig. 78D**) was synthesised and used to form tetrakis Ru(III) complexes. MIC values against seven different *A.* species were determined (AmB as positive control).<sup>219</sup> The lowest MIC values were reported for the dimethyl and diethyl Ru(III) complexes ( $4 \mu\text{g}\cdot\text{mL}^{-1}$ , *i.e.*  $4.98 \mu\text{M}$ ) which was  $\sim 15$  times less potent than AmB ( $0.32 \mu\text{M}$ ).

Comparable ruthenium pentakis dithiocarbamate complexes with similar aliphatic decoration (**Fig. 78E**) were tested against six species of *Candida*, *P. bradliensis*, *C. neoformans* and *S. schenkii* by MICs determination.<sup>220</sup> While all Ru(III) complexes were more effective than the free ligand against the organisms, none approached the efficacies of FCZ or AmB.

Liu *et al.* synthesised a range of ferrocenyl-chalcone-dithiocarbamate Schiff bases metal complexes (Cu(II), Hg(II), Zn(II), Fe(II), Cd(II), Ni(II), Pb(II)) (**Fig. 79**).<sup>221–223</sup> All metal complexes (except Hg(II)) were determined to have NNOSS coordination through the two azomethine nitrogen atoms, enolized thiols of the Schiff base ligand and two water molecules; the Hg(II) was found to have NNSS coordination, lacking the axial waters. The antifungal effects of the synthesised complexes were tested against *C. albicans*, *A. fumigatus*, *A. niger*, *A. flavus*, and *S. cerevisiae*. All metal complexes had efficacies against the fungal strains of 50% or greater activity relative to nystatin. While complexation of the metal ions appeared to generally increase the activities of the ferrocenyl Schiff bases, the free ligands also had appreciable fungicidal properties, likely due to the organometallic nature of the ferrocene ligands. Of the myriad complexes tested, the three Zn(II) derivatives containing the phenyl, para-phenyl-dimethylamine, and para-phenyl-bromo groups showed the greatest efficacies against all fungal strains tested (~80% relative to positive control).

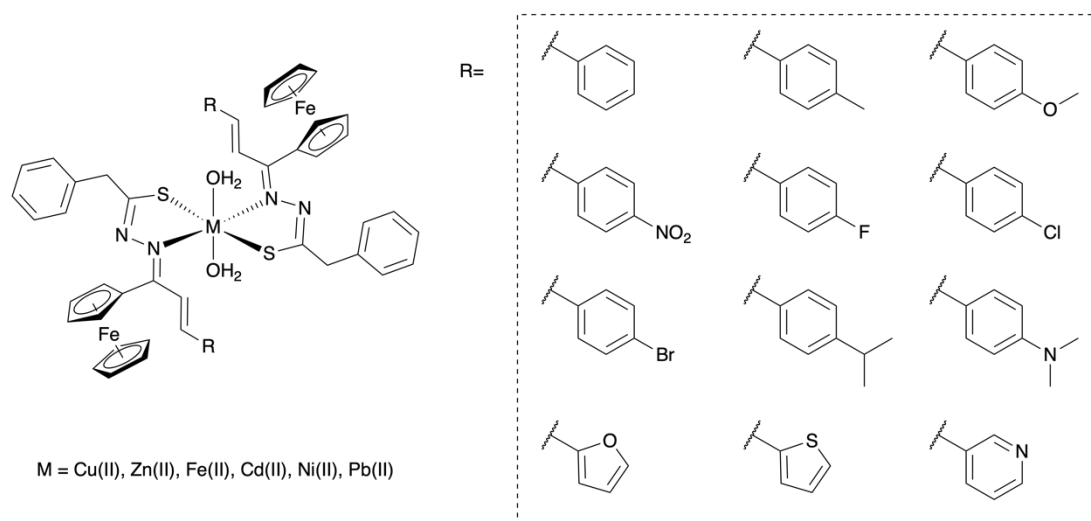


**Fig. 79:** Dithiocarbamate chalcones derivatised with ferrocene and a range of aromatic functional groups and complexed with various metal ions.

## 17. Conclusion

With the global rise of antifungal resistance to the commonly used drugs, there is an urgent demand for the discovery of new, effective, safe, and cheap drugs to be used as alternative treatments against multi-drug resistant pathogenic fungi. In this line of thinking, metal complexes based on bioactive ligands and known drugs hold great potential as broad-spectrum pathogenic fungicides. Varied physicochemical properties, such as redox activity, coordination geometry, biocompatibility and microbicidal activity are available across the Periodic Table. These metal ion properties, along with intrinsic bioactivities of the free ligand may yield improved antifungal activities via multiple modes of action, potentially bypassing rapid resistance of organisms. Despite a lot of research concerning metal-based antifungal agents being published recently, the rational design of molecular structures to yield antifungal activity is often still empirical. Mechanistic studies are limited to DNA interaction studies and in many cases not related to the specific targeting of fungi. More in-depth studies to understand the modes of action of metal-based antifungal agents are needed, in particular with respect to fungi-specific targets such as ergosterol, CYP51, yeast-to-hyphae transitions, antibiofilm formation, adhesion of fungal cells, metalloproteinases, morphological transitions and mutagenic potential. Standardisation of antifungal results relative to positive controls (appropriate for the fungal strains studied) would also further help to advance the field.

After complexation of organic molecules with metal ions, improvements in antifungal activities were often observed compared to the free ligand, but more than often not rationalized. Of the reported metal complexes, organometallic compounds such as ferrocene derivatives exhibited significant antifungal activities. Additionally, cationic species – e.g. cationic Ru-cyclopentadienyl complexes – were found to be more effective than their neutral counterparts on several instances. Complexes containing metal ions such as Cu(II), Zn(II), Mn(II) and Ni(II) and ligands that included triazole, phen, salicylaldehyde-/thiosemicarbazide-/thiocarbamate-based Schiff base moieties also exhibited significant antifungal activities.

Overall, we hope this review will help to inspire and direct researchers aiming to improve the clinical profiles of metal-based antifungal agents. Particularly regarding cytotoxicity and *in vivo* studies as the number of

articles reporting murine-based experiments are disappointingly scarce, and as without those the true efficacies of these compounds cannot be fully ascertained. Such highly needed experiments will allow for the accurate assessment of the potential of these metal-based compounds to help fighting the global societal and economic burdens of pathogenic fungal infections.

## **AUTHOR INFORMATION**

### **Corresponding Author**

\* e-mail: kevin.cariou@chimieparistech.psl.eu; gilles.gasser@chimieparistech.psl.eu

### **ORCID:**

Yan Lin: 0000-0001-7808-5444

Harley Betts: 0000-0002-1149-2675

Sarah Keller: 0000-0003-2667-9157

Kevin Cariou: 0000-0002-5854-9632

Gilles Gasser: 0000-0002-4244-5097

### **Funding Information**

This work was financially supported by the Swiss National Science Foundation (Grant Sinergia CRSII5\_173718, to G.G.), an ERC Consolidator Grant PhotoMedMet to G.G. (GA 681679) and has received support under the program *Investissements d'Avenir* launched by the French Government and implemented by the ANR with the reference ANR-10-IDEX-0001-02 PSL (G.G.). Y. L. thanks the China Scholarship Council for financial support. The work was further supported by a Feodor Lynen Research Fellowship from the Alexander von Humboldt Foundation (S.K.) as well as an Early Postdoc. Mobility Fellowship from the Swiss National Science Foundation (S.K., Grant P2 BSP2\_181760).

### **Acknowledgements**

The authors would like to acknowledge the artistic contribution of Marie Huynh who created the Graphical Abstract for this article.



## REFERENCES

- 1 M. Buckley, *Am. Soc. Microbiol.*, 2008, 48.
- 2 L. Romani, *Nat. Rev. Immunol.*, 2011, **11**, 275–288.
- 3 N. M. Martinez-Rossi, N. T. A. Peres and A. Rossi, *Mycopathologia*, 2008, **166**, 369–383.
- 4 G. D. Brown, D. W. Denning, N. A. R. Gow, S. M. Levitz, M. G. Netea and T. C. White, *Sci. Transl. Med.*, 2012, **4**, 165rv13.
- 5 J. Jampilek, *Expert Opin. Drug Discov.*, 2016, **11**, 1–9.
- 6 M. A. Garcia-Solache and A. Casadevall, *mBio*, 2010, **1**, e00061-10.
- 7 N. A. R. Gow, J.-P. Latge and C. A. Munro, in *The Fungal Kingdom*, American Society of Microbiology, 2017, 267–292.
- 8 Antifungal Pharmacology, <https://drfungus.org/knowledge-base/antifungal-pharmacology/>, (accessed April 17, 2021).
- 9 K. C. Howard, E. K. Dennis, D. S. Watt and S. Garneau-Tsodikova, *Chem. Soc. Rev.*, 2020, **49**, 2426–2480.
- 10 D. J. Sheehan, C. A. Hitchcock and C. M. Sibley, *Clin. Microbiol. Rev.*, 1999, **12**, 40–79.
- 11 N. H. Georgopapadakou and T. J. Walsh, *Antimicrob. Agents Chemother.*, 1996, **40**, 279–291.
- 12 T. C. White, K. A. Marr and R. A. Bowden, *Clin. Microbiol. Rev.*, 1998, **11**, 382–402.
- 13 D. W. Denning, *THE LANCET*, 2003, **362**, 10.
- 14 N. S. Ryder, *Br. J. Dermatol.*, 1992, **126**, 2–7.
- 15 A. B. Orth, M. J. Henry and H. D. Sisler, *Pestic. Biochem. Physiol.*, 1990, **37**, 182–191.
- 16 J. Berman and D. J. Krysan, *Nat. Rev. Microbiol.*, 2020, **18**, 319–331.
- 17 J. R. Perfect, *Nat Rev Drug Discov*, 2017, **16**, 603–616.
- 18 B. D. Alexander and M. A. Pfaller, *Clin. Infect. Dis.*, 2006, **43**, S15–S27.
- 19 M. A. Pfaller, *Am. J. Med.*, 2012, **125**, S3–S13.
- 20 S. Ghosh, *Bioorganic Chem.*, 2019, **88**, 102925.
- 21 P. C. Bruijninx and P. J. Sadler, *Curr. Opin. Chem. Biol.*, 2008, **12**, 197–206.
- 22 N. Graf and S. J. Lippard, *Adv. Drug Deliv. Rev.*, 2012, **64**, 993–1004.

- 23 S. Yasmeeen, S. H. Sumrra, M. S. Akram and Z. H. Chohan, *J. Enzyme Inhib. Med. Chem.*, 2017, **32**, 106–112.
- 24 J. E. Weder, C. T. Dillon, T. W. Hambley, B. J. Kennedy, P. A. Lay, J. R. Biffin, H. L. Regtop and N. M. Davies, *Coord. Chem. Rev.*, 2002, **232**, 95–126.
- 25 Y. C. Ong, S. Roy, P. C. Andrews and G. Gasser, *Chem. Rev.*, 2019, **119**, 730–796.
- 26 *Mini-Rev. Med. Chem.*, 2004, **4**, 23–30.
- 27 N. C. Lloyd, H. W. Morgan, B. K. Nicholson and R. S. Ronimus, *Angew. Chem. Int. Ed.*, 2005, **44**, 941–944.
- 28 D. W. Woolley, *J. Biol. Chem.*, 1944, **152**, 225–232.
- 29 R. A. Fromtling, *CLIN MICROBIOL REV*, 1988, **1**, 187–217.
- 30 A. Groll, S. Piscitelli and T. Walsh, *Adv. Pharmacol. San Diego Calif*, 1998, **44**, 343–500.
- 31 A. Pascual, T. Calandra, S. Bolay, T. Buclin, J. Bille and O. Marchetti, *Clin. Infect. Dis.*, 2008, **46**, 201–211.
- 32 D. Schiller and H. Fung, *Clin. Ther.*, 2007, **29**, 1862–1886.
- 33 J. H. Rex, M. G. Rinaldi and M. A. Pfaller, *Antimicrob. Agents Chemother.*, 1995, **39**, 1–8.
- 34 K. Venkateswarlu, M. Taylor, N. J. Manning, M. G. Rinaldi and S. L. Kelly, *Antimicrob. Agents Chemother.*, 1997, **41**, 748–751.
- 35 J. Wheat, P. Marichal, H. Vanden Bossche, A. Le Monte and P. Connolly, *Antimicrob. Agents Chemother.*, 1997, **41**, 410–414.
- 36 D. W. Denning, K. Venkateswarlu, K. L. Oakley, M. J. Anderson, N. J. Manning, D. A. Stevens, D. W. Warnock and S. L. Kelly, *Antimicrob. Agents Chemother.*, 1997, **41**, 1364–1368.
- 37 M. Misslinger, B. E. Lechner, K. Bacher and H. Haas, *Metallomics*, 2018, **10**, 1687–1700.
- 38 U. E. Schaible and S. H. E. Kaufmann, *Nat. Rev. Microbiol.*, 2004, **2**, 946–953.
- 39 A. Tripathi, E. Liverani, A. Y. Tsygankov and S. Puri, *J. Biol. Chem.*, 2020, **295**, 10032–10044.
- 40 D. R. van Staveren and N. Metzler-Nolte, *Chem. Rev.*, 2004, **104**, 5931–5986.
- 41 C. G. Hartinger, N. Metzler-Nolte and P. J. Dyson, *Organometallics*, 2012, **31**, 5677–5685.
- 42 M. Patra and G. Gasser, *Nat. Rev. Chem.*, 2017, **1**, 0066.
- 43 S. Top, J. Tang, A. Vessières, D. Carrez, C. Provot and G. Jaouen, *Chem Commun*, 1996, 955–956.
- 44 G. Jaouen, A. Vessières and S. Top, *Chem. Soc. Rev.*, 2015, **44**, 8802–8817.

- 45 C. Biot, G. Glorian, L. A. Maciejewski, J. S. Brocard, O. Domarle, G. Blampain, P. Millet, A. J. Georges, H. Abessolo, D. Dive and J. Lebibi, *J. Med. Chem.*, 1997, **40**, 3715–3718.
- 46 C. Biot and D. Poulain, *Bioorg Med Chem Lett*, 2000, **3**.
- 47 J.-X. Fang, Z. Jin, Z.-M. Li and W. Liu, *Appl. Organomet. Chem.*, 2003, **17**, 145–153.
- 48 Z. Jin, Y. Hu, A. Huo, W. Tao, L. Shao, J. Liu and J. Fang, *J. Organomet. Chem.*, 2006, **691**, 2340–2345.
- 49 J. Fang, Z. Jin, Y. Hu, W. Tao and L. Shao, *Appl. Organomet. Chem.*, 2006, **20**, 813–818.
- 50 J. Liu, T. Liu, H. Dai, Z. Jin and J. Fang, *Appl. Organomet. Chem.*, 2006, **20**, 610–614.
- 51 H. Yu, L. Shao and J. Fang, *J. Organomet. Chem.*, 2007, **692**, 991–996.
- 52 N. Chandak, P. Kumar, C. Sharma, K. R. Aneja and P. K. Sharma, *Lett. Drug Des. Discov.*, 2012, **9**, 63–68.
- 53 A. Pejović, A. Minić, J. Bugarinović, M. Pešić, I. Damljanović, D. Stevanović, V. Mihailović, J. Katanić and G. A. Bogdanović, *Polyhedron*, 2018, **155**, 382–389.
- 54 H. Walter, H. Tobler, D. Gribkov and C. Corsi, *Chim. Int. J. Chem.*, 2015, **69**, 425–434.
- 55 R. Rubbiani, O. Blacque and G. Gasser, *Dalton Trans.*, 2016, **45**, 6619–6626.
- 56 G. Singh, A. Arora, P. Kalra, I. K. Maurya, C. E. Ruizc, M. A. Estebanc, S. Sinha, K. Goyal and R. Sehgal, *Bioorg. Med. Chem.*, 2019, **27**, 188–195.
- 57 S. Yagnam, E. Rami Reddy, R. Trivedi, N. V. Krishna, L. Giribabu, B. Rathod, R. S. Prakasham and B. Sridhar, *Appl. Organomet. Chem.*, 2019, **33**, e4817.
- 58 M. Ge, J. Feng, H. Huang, X. Gou, C. Hua, B. Chen and J. Zhao, *J. Heterocycl. Chem.*, 2019, **56**, 3297–3302.
- 59 R. Rubbiani, T. Weil, N. Tocci, L. Mastrobuoni, S. Jeger, J. Ng, Y. Lin, J. Hess, S. Ferrari, A. Kaech, L. Young, A. L. Moore, K. Cariou, M. Borghi, R. Giorgia, L. Romani and G. Gasser, *ChemRxiv*, , DOI:<https://doi.org/10.26434/chemrxiv.12672794.v1>.
- 60 U. Pindur, M. Haber and K. Sattler, *J. Chem. Educ.*, 1993, **70**, 263–269.
- 61 A. W. Addison, M. Palaniandavar, W. L. Driessen, F. Paap and J. Reedijk, *Inorganica Chim. Acta*, 1988, **142**, 95–100.
- 62 B. Vinay Kumar, H. S. Bhojya Naik, D. Girija, N. Sharath, S. M. Pradeepa, H. Joy Hoskeri and M. C. Prabhakara, *Spectrochim. Acta. A. Mol. Biomol. Spectrosc.*, 2012, **94**, 192–199.
- 63 A. Martínez, T. Carreon, E. Iniguez, A. Anzellotti, A. Sánchez, M. Tyan, A. Sattler, L. Herrera, R. A. Maldonado and R. A. Sánchez-Delgado, *J. Med. Chem.*, 2012, **55**, 3867–3877.

- 64 M. Patra, T. Joshi, V. Pierroz, K. Ingram, M. Kaiser, S. Ferrari, B. Spingler, J. Keiser and G. Gasser, *Chem. - Eur. J.*, 2013, **19**, 14768–14772.
- 65 J. Kljun, A. J. Scott, T. Lanišnik Rižner, J. Keiser and I. Turel, *Organometallics*, 2014, **33**, 1594–1601.
- 66 M. Navarro, T. Lehmann, E. J. Cisneros-Fajardo, A. Fuentes, R. A. Sanchez-Delgado, P. Silva and J. A. Urbina, *Polyhedron*, 2000, 2319–2325.
- 67 M. Navarro, E. J. Cisneros-Fajardo, T. Lehmann, R. A. Sánchez-Delgado, R. Atencio, P. Silva, R. Lira and J. A. Urbina, *Inorg. Chem.*, 2001, **40**, 6879–6884.
- 68 R. A. Sánchez-Delgado, M. Navarro, K. Lazard, R. Atencio, M. Capparelli, F. Vargas and J. A. Urbina, *Inorg. Chem.*, 1998, **275–276**, 528–540.
- 69 T. Gagini, L. Colina-Vegas, W. Villarreal, L. P. Borba-Santos, C. de Souza Pereira, A. A. Batista, M. Kneip Fleury, W. de Souza, S. Rozental, L. A. S. Costa and M. Navarro, *New J. Chem.*, 2018, **42**, 13641–13650.
- 70 N. Lj. Stevanović, I. Aleksic, J. Kljun, S. Skaro Bogojevic, A. Veselinovic, J. Nikodinovic-Runic, I. Turel, M. I. Djuran and B. Đ. Glišić, *Pharmaceuticals*, 2020, **14**, 24.
- 71 J. A. de Azevedo-França, L. P. Borba-Santos, G. de Almeida Pimentel, C. H. J. Franco, C. Souza, J. de Almeida Celestino, E. F. de Menezes, N. P. dos Santos, E. G. Vieira, A. M. D. C. Ferreira, W. de Souza, S. Rozental and M. Navarro, *J. Inorg. Biochem.*, 2021, **219**, 111401.
- 72 G. Golbaghi, M. Groleau, Y. López de los Santos, N. Doucet, E. Déziel and A. Castonguay, *ChemBioChem*, 2020, **21**, 3112–3119.
- 73 W. W. Brandt, F. P. Dwyer and E. D. Gyarfas, *Chem. Rev.*, 1954, **54**, 959–1017.
- 74 R. A. MacLeod, *J. Biol. Chem.*, 1952, **197**, 751–761.
- 75 F. Dwyer, I. Reid, A. Shulman, G. Laycock and S. Dixon, *Aust. J. Exp. Biol. Med. Sci.*, 1969, **47**, 203–218.
- 76 M. McCann, M. Geraghty, M. Devereux, D. O’Shea, J. Mason and L. O’Sullivan, *Met.-Based Drugs*, 2000, **7**, 185–193.
- 77 B. Coyle, K. Kavanagh, M. McCann, M. Devereux and M. Geraghty, *BioMetals*, 2003, **16**, 321–329.
- 78 B. Coyle, P. Kinsella, M. McCann, M. Devereux, R. O’Connor, M. Clynes and K. Kavanagh, *Toxicol. In Vitro*, 2004, **18**, 63–70.
- 79 M. McCann, B. Coyle, S. McKay, P. McCormack, K. Kavanagh, M. Devereux, V. McKee, P. Kinsella, R. O’Connor and M. Clynes, *BioMetals*, 2004, **17**, 635–645.
- 80 M. Q. Granato, D. de S. Gonçalves, S. H. Seabra, M. McCann, M. Devereux, A. L. S. dos Santos and L. F. Kneipp, *Front. Microbiol.*, 2017, **8**, 76.

- 81 M. Q. Granato, T. P. Mello, R. S. Nascimento, M. D. Pereira, T. L. S. A. Rosa, M. C. V. Pessolani, M. McCann, M. Devereux, M. H. Branquinha, A. L. S. Santos and L. F. Kneipp, *Front. Microbiol.*, 2021, **12**, 941.
- 82 R. M. Gandra, P. Mc Carron, M. F. Fernandes, L. S. Ramos, T. P. Mello, A. C. Aor, M. H. Branquinha, M. McCann, M. Devereux and A. L. S. Santos, *Front. Microbiol.*, 2017, **8**, 1257.
- 83 R. M. Gandra, P. McCarron, L. Viganor, M. F. Fernandes, K. Kavanagh, M. McCann, M. H. Branquinha, A. L. S. Santos, O. Howe and M. Devereux, *Front. Microbiol.*, 2020, **11**, 470.
- 84 N. Raman and S. Sobha, *J. Serbian Chem. Soc.*, 2010, **75**, 773–788.
- 85 F. Gomes da Silva Dantas, A. Araújo de Almeida-Apolonio, R. Pires de Araújo, L. Regiane Vizolli Favarin, P. Fukuda de Castilho, F. de Oliveira Galvão, T. Inez Estivalet Svidzinski, G. Antônio Casagrande and K. Mari Pires de Oliveira, *Molecules*, 2018, **23**, 1856.
- 86 T. Dimitrijević, I. Novaković, D. Radanović, S. B. Novaković, M. V. Rodić, K. Anđelković and M. Šumar-Ristović, *J. Coord. Chem.*, 2020, **73**, 702–716.
- 87 E. H. Edinsha Gladis, K. Nagashri and J. Joseph, *Inorg. Chem. Commun.*, 2020, **122**, 108232.
- 88 T. P. Andrejević, I. Aleksic, M. Počkaj, J. Kljun, D. Milivojevic, N. Lj. Stevanović, J. Nikodinovic-Runic, I. Turel, M. I. Djuran and B. Đ. Glišić, *Dalton Trans.*, 2021, **50**, 2627–2638.
- 89 T. S. Lobana, S. Indoria, H. Sood, D. S. Arora, M. Kaur and J. P. Jasinski, *Dalton Trans.*, 2021, 10.1039.D1DT00657F.
- 90 Z. H. Chohan, M. Arif, M. A. Akhtar and C. T. Supuran, *Bioinorg. Chem. Appl.*, 2006, **2006**, 1–13.
- 91 R. Senthil Kumar and S. Arunachalam, *Polyhedron*, 2007, **26**, 3255–3262.
- 92 L. H. Abdel-Rahman, R. M. El-Khatib, L. A. E. Nassr, A. M. Abu-Dief, M. Ismael and A. A. Seleem, *Spectrochim. Acta. A. Mol. Biomol. Spectrosc.*, 2014, **117**, 366–378.
- 93 M. A. Raza, M. Amin, G. Muhammad, A. Rashid and A. Adnan, *Russ. J. Gen. Chem.*, 2017, **87**, 2678–2683.
- 94 M. Daniluk, W. Buchowicz, M. Koszytkowska-Stawińska, K. Jarzabek, K. N. Jarzemska, R. Kamiński, M. Piszcz, A. E. Laudy and S. Tyski, *ChemistrySelect*, 2019, **4**, 11130–11135.
- 95 M. Muthukumar, P. Viswanathamurthi and K. Natarajan, *Spectrochim. Acta. A. Mol. Biomol. Spectrosc.*, 2008, **70**, 1222–1226.
- 96 M. Muthukumar and P. Viswanathamurthi, *Spectrochim. Acta. A. Mol. Biomol. Spectrosc.*, 2009, **74**, 454–462.
- 97 J. Muškinja, A. Burmudžija, Z. Ratković, B. Ranković, M. Kosanić, G. A. Bogdanović and S. B. Novaković, *Med. Chem. Res.*, 2016, **25**, 1744–1753.

- 98 J. C. Ballin, *JAMA J. Am. Med. Assoc.*, 1974, **230**, 1184–1185.
- 99 Z. H. Chohan, A. U. Shaikh, M. M. Naseer and C. T. Supuran, *J. Enzyme Inhib. Med. Chem.*, 2006, **21**, 771–781.
- 100 Z. H. Chohan, *Transit. Met. Chem.*, 2009, **34**, 153–161.
- 101 Z. H. Chohan and M. M. Naseer, *Appl. Organomet. Chem.*, 2007, **21**, 728–738.
- 102 Z. H. Chohan, *J. Enzyme Inhib. Med. Chem.*, 2008, **23**, 120–130.
- 103 Z. H. Chohan, H. A. Shad, M. H. Youssoufi and T. Ben Hadda, *Eur. J. Med. Chem.*, 2010, **45**, 2893–2901.
- 104 Z. H. Chohan and H. A. Shad, *J. Enzyme Inhib. Med. Chem.*, 2012, **27**, 403–412.
- 105 Z. H. Chohan, A. U. Shaikh and M. M. Naseer, *Appl. Organomet. Chem.*, 2006, **20**, 729–739.
- 106 Z. H. Chohan, C. T. Supuran, T. Ben Hadda, F.-U.-H. Nasim and K. M. Khan, *J. Enzyme Inhib. Med. Chem.*, 2009, **24**, 859–870.
- 107 S. Rani, S. H. Sumrra and Z. H. Chohan, *Russ. J. Gen. Chem.*, 2017, **87**, 1834–1842.
- 108 A. Missner and P. Pohl, *ChemPhysChem*, 2009, **10**, 1405–1414.
- 109 Z. H. Chohan, M. Arif, Z. Shafiq, M. Yaqub and C. T. Supuran, *J. Enzyme Inhib. Med. Chem.*, 2006, **21**, 95–103.
- 110 Z. H. Chohan, *J. Enzyme Inhib. Med. Chem.*, 2009, **24**, 169–175.
- 111 S. Yavuz and H. Yıldırım, *J. Chem.*, 2013, **2013**, 149693.
- 112 U. N. Tripathi, G. Venubabu, Mohd. Safi Ahmad, S. S. Rao Kolisetty and A. K. Srivastava, *Appl. Organomet. Chem.*, 2006, **20**, 669–676.
- 113 T. W. Welch and H. H. Thorp, *J. Phys. Chem.*, 1996, **100**, 13829–13836.
- 114 F. Arjmand, B. Mohani and S. Ahmad, *Eur. J. Med. Chem.*, 2005, **40**, 1103–1110.
- 115 A. M. Mansour, *Eur. J. Inorg. Chem.*, 2018, **2018**, 852–860.
- 116 O. A. Dar, S. A. Lone, M. A. Malik, F. M. Aqlan, M. Y. Wani, A. A. Hashmi and A. Ahmad, *Heliyon*, 2019, **5**, e02055.
- 117 H. A. Özbek, P. S. Aktaş, J.-C. Daran, M. Oskay, F. Demirhan and B. Çetinkaya, *Inorganica Chim. Acta*, 2014, **423**, 435–442.
- 118 A. Burmudžija, Z. Ratković, J. Muškinja, N. Janković, B. Ranković, M. Kosanić and S. Đorđević, *RSC Adv.*, 2016, **6**, 91420–91430.

- 119 H. Parveen, R. A. S. Alatawi, N. H. El Sayed, S. Hasan, S. Mukhtar and A. U. Khan, *Arab. J. Chem.*, 2017, **10**, 1098–1106.
- 120 H. Parveen, R. A. S. Alatawi, M. A. Alsharif, M. I. Alahmdi, S. Mukhtar, S. A. Khan, S. Hasan and A. U. Khan, *Appl. Organomet. Chem.*, 2018, **32**, e4257.
- 121 J. P. Bugarinović, M. S. Pešić, A. Minić, J. Katanić, D. Ilić-Komatina, A. Pejović, V. Mihailović, D. Stevanović, B. Nastasijević and I. Damljanović, *J. Inorg. Biochem.*, 2018, **189**, 134–142.
- 122 A. Pejović, A. Minić, J. Jovanović, M. Pešić, D. I. Komatina, I. Damljanović, D. Stevanović, V. Mihailović, J. Katanić and G. A. Bogdanović, *J. Organomet. Chem.*, 2018, **869**, 1–10.
- 123 R. Lippert, S. Vojnovic, A. Mitrovic, N. Jux, I. Ivanović-Burmazović, B. Vasiljevic and N. Stankovic, *Bioorg. Med. Chem. Lett.*, 2014, **24**, 3506–3511.
- 124 R. Lippert, T. E. Shubina, S. Vojnovic, A. Pavic, J. Veselinovic, J. Nikodinovic-Runic, N. Stankovic and I. Ivanović-Burmazović, *J. Inorg. Biochem.*, 2017, **171**, 76–89.
- 125 R. Karvembu, C. Jayabalakrishnan and K. Natarajan, *Transit. Met. Chem.*, 2002, **27**, 574–579.
- 126 N. P. Priya, S. V. Arunachalam, N. Sathya, V. Chinnusamy and C. Jayabalakrishnan, *Transit. Met. Chem.*, 2009, **34**, 437–445.
- 127 Z. H. Chohan, *Appl. Organomet. Chem.*, 2006, **20**, 112–116.
- 128 L. Dkhar, M. Sawkmie, A. L. Ka-Ot, S. R. Joshi, W. Kaminsky and M. R. Kollipara, *J. Organomet. Chem.*, 2020, **923**, 121418.
- 129 M. Allison, P. Caramés-Méndez, C. M. Pask, R. M. Phillips, R. M. Lord and P. C. McGowan, *Chem. – Eur. J.*, 2021, **27**, 3737–3744.
- 130 R. Gul, M. K. Rauf, A. Badshah, S. S. Azam, M. N. Tahir and A. Khan, *Eur. J. Med. Chem.*, 2014, **85**, 438–449.
- 131 F. Chen, J. Moat, D. McFeely, G. Clarkson, I. J. Hands-Portman, J. P. Furner-Pardoe, F. Harrison, C. G. Dowson and P. J. Sadler, *J. Med. Chem.*, 2018, **61**, 7330–7344.
- 132 A. Okumus, Z. Kilic and T. Hokelek, *New J. Chem.*, 2016, **40**, 5588–5603.
- 133 G. Elmas, A. Okumuş, R. Cemaloğlu, Z. Kılıç, S. P. Çelik, L. Açıık, B. Ç. Tunalı, M. Türk, N. A. Çerçi, R. Güzel and T. Hökelek, *J. Organomet. Chem.*, 2017, **853**, 93–106.
- 134 S. Ali, G. Yasin, Z. Zuhra, Z. Wu, I. S. Butler, A. Badshah and I. ud Din, *Bioinorg. Chem. Appl.*, 2015, **2015**, 386587.
- 135 F. Asghar, A. Badshah, B. Lal, I. S. Butler, S. Tabassum and M. N. Tahir, *Inorganica Chim. Acta*, 2016, **439**, 82–91.

- 136 R. A. Hussain, A. Badshah, M. N. Tahir, T.- Hassan and A. Bano, *J. Biochem. Mol. Toxicol.*, 2014, **28**, 60–68.
- 137 Z. H. Chohan, K. M. Khan and C. T. Supuran, *Appl. Organomet. Chem.*, 2004, **18**, 305–310.
- 138 K. Naresh Kumar, R. Ramesh and Y. Liu, *J. Inorg. Biochem.*, 2006, **100**, 18–26.
- 139 M. Al-Noaimi, A. Nafady, I. Warad, R. Alshwafy, A. Husein, W. H. Talib and T. B. Hadda, *Spectrochim. Acta. A. Mol. Biomol. Spectrosc.*, 2014, **122**, 273–282.
- 140 Z. Yuan, X. Shen and J. Huang, *RSC Adv.*, 2015, **5**, 10521–10528.
- 141 P. A. Khalaf-Alla, *Appl. Organomet. Chem.*, 2020, **34**, e5628.
- 142 Z. H. Chohan, M. Arif and M. Sarfraz, *Appl. Organomet. Chem.*, 2007, **21**, 294–302.
- 143 S. H. Sumrra, F. Mushtaq, M. Khalid, M. A. Raza, M. F. Nazar, B. Ali and A. A. C. Braga, *Spectrochim. Acta. A. Mol. Biomol. Spectrosc.*, 2018, **190**, 197–207.
- 144 K. Singh, Y. Kumar, P. Puri, C. Sharma and K. R. Aneja, *Bioinorg. Chem. Appl.*, 2011, **2011**, 901716.
- 145 Z. H. Chohan, S. H. Sumrra, M. H. Youssoufi and T. B. Hadda, *Eur. J. Med. Chem.*, 2010, **45**, 2739–2747.
- 146 S. H. Sumrra and Z. H. Chohan, *Spectrochim. Acta. A. Mol. Biomol. Spectrosc.*, 2012, **98**, 53–61.
- 147 M. Hanif and Z. H. Chohan, *Appl. Organomet. Chem.*, 2013, **27**, 36–44.
- 148 S. H. Sumrra, S. Kausar, M. A. Raza, M. Zubair, M. N. Zafar, M. A. Nadeem, E. U. Mughal, Z. H. Chohan, F. Mushtaq and U. Rashid, *J. Mol. Struct.*, 2018, **1168**, 202–211.
- 149 Z. H. Chohan and M. Hanif, *J. Enzyme Inhib. Med. Chem.*, 2013, **28**, 944–953.
- 150 R. Jayarajan, G. Vasuki and P. S. Rao, *Org. Chem. Int.*, 2010, **2010**, 648589.
- 151 J. Joseph and G. A. B. Rani, *Spectrosc. Lett.*, 2014, **47**, 86–100.
- 152 K. R. Surati, *Spectrochim. Acta. A. Mol. Biomol. Spectrosc.*, 2011, **79**, 272–277.
- 153 R. Karvembu, C. Jayabalakrishnan, N. Dharmaraj, S. V. Renukadevi and K. Natarajan, *Transit. Met. Chem.*, 2002, **27**, 631–638.
- 154 N. Dharmaraj, P. Viswanathamurthi and K. Natarajan, *Transit. Met. Chem.*, 2001, **26**, 105–109.
- 155 R. Ramesh and S. Maheswaran, *J. Inorg. Biochem.*, 2003, **96**, 457–462.
- 156 K. Nagaraj, S. Sakthinathan and S. Arunachalam, *J. Fluoresc.*, 2014, **24**, 589–598.



- 157 N. Raman, R. Mahalakshmi, T. Arun, S. Packianathan and R. Rajkumar, *J. Photochem. Photobiol. B*, 2014, **138**, 211–222.
- 158 T. Mangamamba, M. C. Ganorkar and G. Swarnabala, *Int. J. Inorg. Chem.*, 2014, **2014**, 1–22.
- 159 S. Shujah, Zia-ur-Rehman, N. Muhammad, S. Ali, N. Khalid and M. N. Tahir, *J. Organomet. Chem.*, 2011, **696**, 2772–2781.
- 160 L. Logu, K. Raja Kamatchi, H. Rajmohan, S. Manohar, R. Gurusamy and E. Deivanayagam, *Appl. Organomet. Chem.*, 2015, **29**, 90–95.
- 161 S. Arunachalam, N. Padma Priya, K. Boopathi, C. Jayabalakrishnan and V. Chinnusamy, *Appl. Organomet. Chem.*, 2010, **24**, 491–498.
- 162 R. de A. Cordeiro, D. J. Astete-Medrano, F. J. de F. Marques, H. T. L. Andrade, L. V. Perdigão Neto, J. L. Tavares, R. A. C. de Lima, K. K. N. R. Patoilo, A. J. Monteiro, R. S. N. Brilhante, M. F. G. Rocha, Z. P. de Camargo and J. J. C. Sidrim, *Mem. Inst. Oswaldo Cruz*, 2011, **106**, 1045–1048.
- 163 V. K. Sharma, A. Srivastava and S. Srivastava, *J. Serbian Chem. Soc.*, 2006, **71**, 917–928.
- 164 M. R. Karekal, V. Biradar and M. Bennikallu Hire Mathada, *Bioinorg. Chem. Appl.*, 2013, **2013**, 315972.
- 165 M. Patra and G. Gasser, *Nat. Rev. Chem.*, 2017, **1**, 0066.
- 166 W. H. Mahmoud, R. G. Deghadi, M. M. I. El Dessouky and G. G. Mohamed, *Appl. Organomet. Chem.*, 2019, **33**, e4556.
- 167 W. H. Mahmoud, N. F. Mahmoud and G. G. Mohamed, *J. Organomet. Chem.*, 2017, **848**, 288–301.
- 168 A. A. Abou-Hussein and W. Linert, *Spectrochim. Acta. A. Mol. Biomol. Spectrosc.*, 2014, **117**, 763–771.
- 169 W. H. Mahmoud, N. F. Mahmoud and G. G. Mohamed, *J. Chin. Chem. Soc.*, 2019, **66**, 945–959.
- 170 Z. H. Chohan and C. T. Supuran, *Appl. Organomet. Chem.*, 2005, **19**, 1207–1214.
- 171 S. U. Rehman, Z. H. Chohan, F. Gulnaz and C. T. Supuran, *J. Enzyme Inhib. Med. Chem.*, 2005, **20**, 333–340.
- 172 P. Viswanathamurthi and K. Natarajan, *India J. Chem.*, 1999, **38**, 797–801.
- 173 N. E. A. El-Gamel, *Monatshefte Für Chem. - Chem. Mon.*, 2013, **144**, 1627–1634.
- 174 S. Yasmeen, S. H. Sumrra, M. S. Akram and Z. H. Chohan, *J. Enzyme Inhib. Med. Chem.*, 2017, **32**, 106–112.

- 175 N. Raman, A. Selvan and S. Sudharsan, *Spectrochim. Acta. A. Mol. Biomol. Spectrosc.*, 2011, **79**, 873–883.
- 176 M. Amjad, S. H. Sumrra, M. S. Akram and Z. H. Chohan, *J. Enzyme Inhib. Med. Chem.*, 2016, **31**, 88–97.
- 177 V. V. Dhayabaran and T. D. Prakash, *Luminescence*, 2017, **32**, 1339–1348.
- 178 N. Raman, K. Pothiraj and T. Baskaran, *J. Mol. Struct.*, 2011, **1000**, 135–144.
- 179 A. Kumar, V. K. Vashistha, P. Tevatia and R. Singh, *Spectrochim. Acta. A. Mol. Biomol. Spectrosc.*, 2017, **176**, 123–133.
- 180 K. Shanker, R. Rohini, V. Ravinder, P. M. Reddy and Y.-P. Ho, *Spectrochim. Acta. A. Mol. Biomol. Spectrosc.*, 2009, **73**, 205–211.
- 181 P. P. Netalkar, S. P. Netalkar and V. K. Revankar, *Polyhedron*, 2015, **100**, 215–222.
- 182 T. Rosu, E. Pahontu, S. Pasculescu, R. Georgescu, N. Stanica, A. Curaj, A. Popescu and M. Leabu, *Eur. J. Med. Chem.*, 2010, **45**, 1627–1634.
- 183 A. A. Al-Amiery, A. A. H. Kadhum and A. B. Mohamad, *Bioinorg. Chem. Appl.*, 2012, **2012**, 795812.
- 184 E. Pahontu, F. Julea, T. Rosu, V. Purcarea, Y. Chumakov, P. Petrenco and A. Gulea, *J. Cell. Mol. Med.*, 2015, **19**, 865–878.
- 185 A. K. El-Sawaf, *Sci. J. Chem.*, 2014, **2**, 17–26.
- 186 Z. H. Chohan, H. Pervez, K. M. Khan and C. T. Supuran, *J. Enzyme Inhib. Med. Chem.*, 2005, **20**, 81–89.
- 187 E. Pahontu, V. Fala, A. Gulea, D. Poirier, V. Tapcov and T. Rosu, *Molecules*, 2013, **18**, 8812–8836.
- 188 I. Babahan, F. Eyduran, E. P. Coban, N. Orhan, D. Kazar and H. Biyik, *Spectrochim. Acta. A. Mol. Biomol. Spectrosc.*, 2014, **121**, 205–215.
- 189 S. S. Anchuri, S. Thota, R. N. Bongoni, R. Yerra, R. N. Reddy and S. Dhulipala, *J. Chin. Chem. Soc.*, 2013, **60**, 153–159.
- 190 M. Aljahdali and A. A. EL-Sherif, *Inorganica Chim. Acta*, 2013, **407**, 58–68.
- 191 D. Singh and R. V. Singh, *J. Inorg. Biochem.*, 1993, **50**, 227–234.
- 192 A. S. Kumbhar, S. B. Padhye, A. P. Saraf, H. B. Mahajan, B. A. Chopade and D. X. West, *Biol. Met.*, 1991, **4**, 141–143.
- 193 G. L. Parrilha, J. G. da Silva, L. F. Gouveia, A. K. Gasparoto, R. P. Dias, W. R. Rocha, D. A. Santos, N. L. Speziali and H. Beraldo, *Eur. J. Med. Chem.*, 2011, **46**, 1473–1482.

- 194 U. El-Ayaan, *J. Coord. Chem.*, 2012, **65**, 629–642.
- 195 S. Kannan, M. Sivagamasundari, R. Ramesh and Y. Liu, *J. Organomet. Chem.*, 2008, **693**, 2251–2257.
- 196 H. Yildirim, E. Guler, M. Yavuz, N. Ozturk, P. Kose Yaman, E. Subasi, E. Sahin and S. Timur, *Mater. Sci. Eng. C*, 2014, **44**, 1–8.
- 197 N. V. Kulkarni, G. S. Hegde, G. S. Kurdekar, S. Budagumpi, M. P. Sathisha and V. K. Revankar, *Spectrosc. Lett.*, 2010, **43**, 235–246.
- 198 K. Alomar, A. Landreau, M. Allain, G. Bouet and G. Larcher, *J. Inorg. Biochem.*, 2013, **126**, 76–83.
- 199 E. A. Bakr, G. B. Al-Hefnawy, M. K. Awad, H. H. Abd-Elatty and M. S. Youssef, *Appl. Organomet. Chem.*, 2018, **32**, e4104.
- 200 R. C. Maurya and S. Rajput, *J. Mol. Struct.*, 2007, **833**, 133–144.
- 201 P. Jain and V. Singh, *Asian J. Pharm.*, 2016, **10**, 612–622.
- 202 J. Singh and P. Singh, *Bioinorg. Chem. Appl.*, 2012, **2012**, 104549.
- 203 S. A. Khan, K. Rizwan, S. Shahid, M. A. Noamaan, T. Rasheed and H. Amjad, *Appl. Organomet. Chem.*, 2020, **34**, e5444.
- 204 K. Deepa and K. K. Aravindakshan, *Synth. React. Inorg. Met.-Org. Nano-Met. Chem.*, 2005, **35**, 409–416.
- 205 H. S. Patel and K. K. Oza, *E-J. Chem.*, 2009, **6**, 371–376.
- 206 S. H. Sumrra, A. Suleman, Z. H. Chohan, M. N. Zafar, M. A. Raza and T. Iqbal, *Russ. J. Gen. Chem.*, 2017, **87**, 1281–1287.
- 207 C. R. Madzivire, P. Caramés-Méndez, C. M. Pask, R. M. Phillips, R. M. Lord and P. C. McGowan, *Inorganica Chim. Acta*, 2019, **498**, 119025.
- 208 N. V. Loginova, T. V. Koval'chuk, N. P. Osipovich, G. I. Polozov, V. L. Sorokin, A. A. Chernyavskaya and O. I. Shadyro, *Polyhedron*, 2008, **27**, 985–991.
- 209 M. Hanif, Z. H. Chohan, J.-Y. Winum and J. Akhtar, *J. Enzyme Inhib. Med. Chem.*, 2014, **29**, 517–526.
- 210 S. H. Sumrra, M. Hanif, Z. H. Chohan, M. S. Akram, J. Akhtar and S. M. Al-Shehri, *J. Enzyme Inhib. Med. Chem.*, 2016, **31**, 590–598.
- 211 D. Kwiatek, M. Kubicki, J. Belter, R. Jastrzab, H. Wiśniewska, S. Lis and Z. Hnatejko, *Polyhedron*, 2017, **133**, 187–194.
- 212 M. H. Soliman, G. G. Mohamed and G. H. Elgemeie, *J. Therm. Anal. Calorim.*, 2016, **123**, 583–594.

- 213 S. Chandra, Vandana and S. Kumar, *Spectrochim. Acta. A. Mol. Biomol. Spectrosc.*, 2015, **135**, 356–363.
- 214 L. F. O. Bomfim Filho, M. R. L. Oliveira, L. D. L. Miranda, A. E. C. Vidigal, S. Guilardi, R. A. C. Souza, J. Ellena, J. D. Ardisson, L. Zambolim and M. M. M. Rubinger, *J. Mol. Struct.*, 2017, **1129**, 60–67.
- 215 L. C. Dias, M. M. M. Rubinger, J. P. Barolli, J. D. Ardisson, I. C. Mendes, G. M. de Lima, L. Zambolim and M. R. L. Oliveira, *Polyhedron*, 2012, **47**, 30–36.
- 216 D. C. Menezes, F. T. Vieira, G. M. de Lima, A. O. Porto, M. E. Cortés, J. D. Ardisson and T. E. Albrecht-Schmitt, *Eur. J. Med. Chem.*, 2005, **40**, 1277–1282.
- 217 D. C. Menezes, F. T. Vieira, G. M. de Lima, J. L. Wardell, M. E. Cortés, M. P. Ferreira, M. A. Soares and A. Vilas Boas, *Appl. Organomet. Chem.*, 2008, **22**, 221–226.
- 218 S. K. Verma and V. K. Singh, *J. Organomet. Chem.*, 2015, **791**, 214–224.
- 219 L. J. Nogueira, M. A. de Resende, S. R. Oliveira, M. H. de Araújo, T. F. F. Magalhães, M. B. de Oliveira, C. V. B. Martins, M. T. P. Lopes, A. C. Araújo e Silva and C. L. Donnici, *Mycoses*, 2011, **54**, e323–e329.
- 220 C. Donnici, L. Nogueira, M. Araujo, S. Oliveira, T. Magalhães, M. Lopes, A. Silva, A. Ferreira, C. Martins and M. de Resende Stoianoff, *Molecules*, 2014, **19**, 5402–5420.
- 221 Y. Liu, L. Yang, D. Yin, Y. Dang, L. Yang, Q. Zou, J. Li and J. Sun, *J. Organomet. Chem.*, 2019, **899**, 120903.
- 222 Y.-T. Liu, G.-D. Lian, D.-W. Yin and B.-J. Su, *Spectrochim. Acta. A. Mol. Biomol. Spectrosc.*, 2013, **100**, 131–137.
- 223 Y.-T. Liu, G.-D. Lian, D.-W. Yin and B.-J. Su, *Res. Chem. Intermed.*, 2012, **38**, 1043–1053.

## Graphical Abstract

